Labile Ligand Variation in Polyazine-Bridged Ruthenium/Rhodium Supramolecular Complexes Providing New Insight into Solar Hydrogen Production from Water

Hannah Mallalieu Rogers

Dissertation submitted to the faculty of the Virginia Polytechnic Institute and State University in partial fulfillment of the requirements for the degree of

Doctor of Philosophy

In

Chemistry

J. M. Tanko, Chair

Karen J. Brewer, Co-Chair

Shamindri M. Arachchige

Amanda J. Morris

Brian E. Hanson

December 3, 2015

Blacksburg, Virginia

Keywords: inorganic chemistry, supramolecular complexes, photochemical molecular devices, electrochemistry, photophysics, photochemistry, ruthenium, rhodium, halides, hydroxide, ion pairing, photocatalysis, solar fuels, hydrogen production

Labile Ligand Variation in Polyazine-Bridged Ruthenium/Rhodium Supramolecular Complexes Providing New Insight into Solar Hydrogen Production from Water

Hannah Mallalieu Rogers

Abstract

Mixed-metal supramolecular complexes containing one or two Ru^{II} light absorbing subunits coupled through polyazine bridging ligands to a Rh^{III} reactive metal center were prepared for use as photocatalysts for the production of solar H_2 fuel from H_2O. The electrochemical, photophysical, and photochemical properties upon variation of the monodentate, labile ligands coordinated to the Rh reactive metal center were investigated.

Bimetallic complexes $[(Ph_2phen)_2Ru(dpp)RhX_2(Ph_2phen)]^{3+}$ (Ph_2phen = 4,10-diphenyl-1,10-phenanthroline; dpp = 2,3-bis(2-pyridyl)pyrazine; X = Br^- or Cl^-) were prepared using a building block approach, allowing for selective component choice. The identity of the halide coordinated to Rh did not impact the light absorbing or excited state properties of the structural motif. However, the σ-donating ability of the halides modulated the Rh-based cathodic electrochemistry and required the use of multiple pathways to explain the reduction of Rh by two electrons. Regardless of halide identity, the bimetallic complex possessed a Ru-based HOMO (highest occupied molecular orbital) and Rh-based LUMO (lowest unoccupied molecular orbital) important for photoinitiated electron collection at Rh. As a photocatalyst for H_2 evolution, the X = Br^- complex produced nearly 30% more H_2 than the X = Cl^- analogue. H_2 production experiments with added halide suggested that ion pairing with halides played a major

role in catalyst deactivation, which provided evidence for the importance of component selection for photocatalyst design.

New trimetallic complex $[\{(bpy)_2Ru(dpp)\}_2Ru(OH)_2](PF_6)_5$ (bpy = 2,2′-bipyridine) was prepared for comparison to halide analogues $[\{(bpy)_2Ru(dpp)\}_2RhX_2](PF_6)_5$ ($X = Br^-$ or Cl^-). The synthesis of a halide-free supramolecule containing OH^- ligands afforded an ideal system to further examine the impact of the ligands at the reactive metal center on H_2 photocatalysis. Electrochemistry results revealed that while the identity of the ligands at Rh did modulate the Rh-based reduction potential, all three complexes possessed a Ru-based HOMO and Rh-based LUMO. The light absorbing properties were not impacted by the identity of the monodentate ligands at Rh; however, the excited state properties did vary upon changing the ligands at Rh. The hydroxo trimetallic complex functioned as a photocatalyst for H_2 production in organic solvent, producing nearly double the amount of H_2 as the highest performing Br^- trimetallic complex in DMF solvent. Interestingly, H_2 production studies in high dielectric aqueous solvent revealed no discrepancies in H_2 evolution upon variation of the ligands at Rh, which further supported the ion pairing phenomenon realized for the bimetallic motif.

Variation of the labile ligands coordinated to the Rh reactive metal center in $Ru^{II}Rh^{III}$ multimetallic supramolecules provided important insight about the large impact of small structural variation on H_2 photocatalysis. Electrochemical, photophysical, and photochemical studies of new $Ru^{II}Rh^{III}$ complexes afforded a deeper understanding of the molecular processes important for the design of new complexes applicable to solar fuel production schemes.

Acknowledgements

First, I wish to thank the late Prof. Karen J. Brewer, my graduate advisor. From a nervous freshman in your general chemistry for majors course in 2007 to three years (2011 – 2014) as your graduate student mentee, I am immensely grateful for all I've learned from you – from chemistry, to a love for community outreach, to so many tokens of wisdom and lessons about life. Thank you for believing in me and instilling in me the confidence I needed to succeed. Your keen insight on chemistry and life in general will always remain with me. I owe much appreciation to my committee member, Dr. Shamindri M. Arachchige. Your friendship, guidance, and support, particularly over the last year, have been a tremendously positive influence. When I was feeling down about graduate school, a quick meeting with you always lifted my spirits and gave me the encouragement to move forward. I thank Prof. J. M. Tanko for stepping in as my advisor during my final year of graduate school. Thank you for being a dependable, encouraging mentor, and thank you for reviewing my manuscripts and dissertation drafts. I thank Prof. Amanda J. Morris and Prof. Brian E. Hanson for serving as my committee members and for providing input during committee meetings and milestone assignments. I thank Prof. Joseph S. Merola for serving as my undergraduate advisor and for introducing me to research in inorganic chemistry. A conversation we had late in my senior year of college led me to stay at Virginia Tech for graduate school, and I will forever be grateful for this encouragement. From the Virginia Tech Department of Chemistry, I thank Mr. William Bebout, Dr. Mehdi Ashraf-Khorassani, Mr. John Burleson, Mr. Larry Jackson, Mr. Donald Neel, and Mr. Tom Wertalik for providing analytical and technical support throughout my graduate studies. Thank you to the Chemical Sciences, Geosciences and Biosciences Division, Office of Basic Energy Sciences, Office of Sciences, U.S. Department of Energy (DE FG02-05ER15751) for

providing generous financial support of my research, including several semesters of Research Assistantship support. To past and present members of the Brewer research group, I owe a tremendous amount of appreciation for providing me with a graduate experience from which I've learned much more than science. To Dr. Travis A. White and Dr. Jessica Knoll White, thank you for taking me "under your wing" as a young graduate student. Your friendship and support saw me though the highs and lows of graduate school, and I'm so grateful to call you both friends. Specials thanks are also given to Dr. Samantha L. Hopkins, Dr. Jing Wang, Dr. Rongwei Zhou, Ms. Elise M. Naughton, Dr. Alec T. Wagner, Mrs. Hannah J. Sayre, Mr. Theodore R. Canterbury, Dr. Gilbert K. Kosgei, and Ms. Kristen M. Felice. I owe an enormous amount gratitude to my chemistry teacher at Luray High School, Mr. Kevin Carini, for inspiring me to choose chemistry as my college major. Your enthusiasm for teaching chemistry and including as many in-class demos as you could muster lit the spark in me to further explore this fascinating field of science.

I thank my big, wonderful family for their never-ending love and support. In particular, I thank my parents, Mark and Beth Mallalieu. I feel exceptionally fortunate to have your continuous guidance and love. Thank you for your encouragement and "tough love" approach on days when I thought I wouldn't make it through graduate school, and thank you for always being a phone call away to enthusiastically celebrate my achievements along the way. I also wish to thank my brothers Richard, Ben, and Thomas for all of their support. I'm the luckiest sister to count you three as siblings and friends. Lastly, I thank my dear husband, Andrew Rogers, for always believing in me and encouraging me to be my best. I can imagine no greater joy than sharing my life with you.

Table of Contents

Abstract ii
Acknowledgements iv
Table of Contents vi
List of Abbreviations ix
Attributions xi
Thesis Statement 1
List of Publications 1
1. Introduction 2
1.1. Need for Alternative Energy Sources 2
1.2. Solar-to-Chemical Energy Conversion 2
1.3. H_2O Splitting 4
1.4. H_2 as a Fuel Source 5
1.5. Photocatalytic Reduction of H_2O to H_2 5
1.6. Supramolecular Complexes 8
1.7. Supramolecular Components 9
1.7.1. Redox Properties 9
1.7.1.1. Ru^{II} Monometallic Complexes 11
1.7.1.2. Rh^{III} Monometallic Complexes 15
1.7.2. Light Absorbing Properties 17
1.7.2.1. Ru^{II} Monometallic Complexes 21
1.7.2.2. Rh^{III} Monometallic Complexes 23
1.7.3. Excited State Properties 24
1.7.3.1. Ru^{II} Monometallic Complexes 24
1.7.3.2. Rh^{III} Monometallic Complexes 29
1.8. Photochemical Molecular Devices 30
1.8.1. Photoinitiated Electron Collectors 30
1.9. Supramolecular Complexes for Solar H_2 Production 33
1.9.1. Photocatalysts using Pd, Pt, or Co as the Reactive Metal Center 34
1.9.2. Photocatalysts using Rh as the Reactive Metal Center 37
1.9.3. Impact of Labile Ligand Selection at the Reactive Metal Center 40
1.10. Project Description 43
1.11. References 44
2. Mechanistic Insight into the Electronic Influences Imposed by Substituent Variation in Polyazine-Bridged Ruthenium(II)/Rhodium(III) Supramolecules .. 51
2.1. Abstract 51
2.2. Introduction 51
2.3. Results and Discussion 54
2.4. Acknowledgements 61
2.5. Supplemental Information 61

2.5.1. Experimental Procedures 61
2.5.1.1. Materials 61
2.5.1.2. Synthesis of $[(Ph_2phen)_2Ru(dpp)RhCl_2(^tBu_2bpy)](PF_6)_3$ 62
2.5.1.3. Electrochemistry 62
2.5.2. Supplemental Figures and Tables 63
2.6. References 66
3. Nonchromophoric Halide Ligand Variation in Polyazine-Bridged Ru(II),Rh(III) Bimetallic Supramolecules Offering New Insight into Photocatalytic Hydrogen Production from Water 70
3.1. Abstract 70
3.2. Introduction 71
3.3. Experimental Section 74
3.3.1. Materials 74
3.3.2. Synthesis 75
3.3.3. Mass Spectrometry 76
3.3.4. Electrochemistry 76
3.3.5. Electronic Absorption Spectroscopy 77
3.3.6. Steady-State and Time-Resolved Emission Spectroscopy 77
3.3.7. Photolysis Experiments 78
3.4. Results and Discussion 79
3.4.1. Synthesis 79
3.4.2. Electrochemistry 80
3.4.3. Electronic Absorption Spectroscopy 83
3.4.4. Steady-State and Time-Resolved Emission Spectroscopy 85
3.4.5. Photocatalytic H_2 Production 87
3.5. Conclusions 90
3.6. Acknowledgement 91
3.7. References 91
4. Enhancement of Solar Fuel Production Schemes by Using a Supramolecular Photocatalyst Containing Hydroxide Labile Ligands 96
4.1. Abstract 96
4.2. Introduction 96
4.3. Results and Discussion 100
4.3.1. Synthesis and Characterization 100
4.3.2. Photocatalytic H_2 Production Studies 105
4.4. Conclusions 110
4.5. Experimental Section 112
4.5.1. Materials 112
4.5.2. Synthesis of $[Rh(H_2O)_6](CF_3SO_3)_3$ 112
4.5.3. Synthesis of $[\{(bpy)_2Ru(dpp)\}_2Rh(OH)_2](PF_6)_5$ (**1-OH**) 113

4.6. Acknowledgements 114
4.7. Supplemental Information 114
4.7.1. Methods 114
4.7.1.1. Mass Spectrometry 114
4.7.1.2. Electrochemistry 114
4.7.1.3. Electronic Absorption Spectroscopy 115
4.7.1.4. Steady-State Luminescence Spectroscopy 115
4.7.1.5. Time-Resolved Luminescence Spectroscopy 115
4.7.1.6. H_2 Photolysis Experiments 116
4.7.2. Supplemental Figures 117
4.8. References 119
5. Conclusions 124

List of Abbreviations

A = absorbance in Beer's law
BL = bridging ligand
Bu_4NBr = tetra-*n*-butylammonium bromide
Bu_4NCl = tetra-*n*-butylammonium chloride
Bu_4NPF_6 = tetra-*n*-butylammonium hexafluorophosphate
c = species concentration in Beer's law
C = chemical reaction step; electrochemical term
CT = charge transfer
bpy = 2,2′-bipyridine
CV = cyclic voltammetry
dpb = 2,3-bis(2-pyridyl)benzoquinoxaline
DMA = *N*,*N*-dimethylaniline
DMF = *N*,*N*-dimethylformamide
$dmgBF_2$ = (difluoroboryl)dimethylglyoximate
dpp = 2,3-bid(2-pyridyl)pyrazine
dpq = 2,3-bis(2-pyridyl)quinoxaline
E = electron transfer step; electrochemical term
$E_{1/2}$ = half wave potential
ED = electron donor
EDTA = ethylenediaminetetraacetic acid
E_f = final potential
E_i = initial potential
E_p = peak potential
ES = excited state
ER = electron relay
Fc = ferrocene ($Fe(C_5H_5)_2$)
GS = ground state
HOMO = highest occupied molecular orbital
hv = photoexcitation
IL = intraligand
i_p = peak current
l = path length in Beer's law
k = rate constant value
L1 = 1,2-bis[4-(4′-methyl-2,2′-bipyridinyl)ethane
LA = light absorber
LF = ligand field
LL = bidentate polypyridyl ligand
LMCT = ligand-to-metal charge transfer
L-pyr = (4-pyridine)oxazolo[4,5-f]phenanthroline
LUMO = lowest unoccupied molecular orbital
MLCT = metal-to-ligand charge transfer
MMCT = metal-to-metal charge transfer

n = number of electrons transferred in electrochemical event
NAD = nicotinamide adenine dinucleotide
NHE = normal hydrogen electrode
pbn = 2-(2-pyridyl)benzo[*b*]-1,5-napthyridine
PEC = photoinitiated electron collector
phen = 1,10-phenanthroline
Ph_2phen = 4,7-diphenyl-1,10-phenanthroline
PMD = photochemical molecular device
ppy = 2-phenylpyridine
RT = room temperature
^{t}Bu$_2$bpy = 4,4′-di-*tert*-butyl-2,2′-bipyridine
tatpp = 9,11,20,22-tetraazatetrapyrido[3,2-*a*:2′3′-*c*:3′′,2′′-1:2′′′,3′′′-*n*]pentacene
tatpq = 9,11,20,22-tetraazatetrapyrido[3,2-*a*:2′3′-*c*:3′′,2′′-1:2′′′,3′′′-*n*]pentacene-10,21-quinone
TEA = triethylamine
TEOA = triethanolamine
TL = terminal ligand
TON = turnover number
tpphz = tetrapyrido[3,2-a:2′,3′-c:3′′,2′′-h:2′′′,3′′′-j]phenazine
UV = ultraviolet
v/v = volume/volume percent

ΔE_p = electrochemical potential separation
ε = extinction coefficient; dielectric constant
λ = wavelength
τ = excited state lifetime
Φ = quantum yield

Attributions

Chapters 2, 3, and 4 of this dissertation were written using published manuscripts to which the author, Hannah Mallalieu Rogers (H.M.R.), majorly contributed. The contributions of the co-authors to the publications are as follows:

Chapter 2. Travis A. White, former Ph.D. student at Virginia Tech, began the study of the $Ru^{II}Rh^{III}$ bimetallic complexes for application as photocatalysts for solar H_2 production, synthesized the $^{t}Bu_2$bpy/chloride and Ph_2phen/chloride bimetallic complexes and performed the corresponding electrochemical studies, and assisted with manuscript writing and editing. H.M.R. (formerly Hannah E. Mallalieu) synthesized the Ph_2phen/bromide bimetallic complex and performed the corresponding electrochemical studies, wrote the majority of the manuscript, edited the manuscript following comments from reviewers, and produced the cover art for the issue. Jing Wang, former Ph.D. student at Virginia Tech, studied analogous $Ru^{II}Rh^{III}$ bimetallic complexes and assisted with mechanistic assignment. Karen J. Brewer, principle investigator, supervised the research project and provided technical insight during experimentation, writing, and editing.

Chapter 3. H.M.R. performed all syntheses, characterizations, and photocatalytic H_2 production studies, wrote and submitted the manuscript, and responded to comments from reviewers. Travis A. White provided guidance to H.M.R. in the early stages of this research project. Brittany N. Stone was an undergraduate researcher working with H.M.R. during the early stages of this research project. Shamindri M. Arachchige, General Chemistry instructor and advisory committee member, provided

guidance and writing support to H.M.R. during the late stages of manuscript preparation. Karen J. Brewer supervised the research project and provided technical insight during experimentation.

Chapter 4. H.M.R. performed all syntheses, characterizations, and photocatalytic H_2 production studies, wrote and submitted the manuscript, and responded to comments from reviewers. Shamindri M. Arachchige provided guidance and support during the preparation, submission, and review period of this manuscript. Karen J. Brewer supervised the research project and provided technical insight during experimentation.

Thesis Statement

The goal of this research is to develop new $Ru^{II}Rh^{III}$ supramolecular complexes with varied monodentate ligands coordinated at Rh to examine the impact of labile ligand identity on the electrochemical, photophysical, and photochemical properties related to photocatalytic solar H_2 production schemes.

List of Publications

Rogers, H. M.; Arachchige, S. M.; Brewer, K. J. "Enhancement of Solar Fuel Production Schemes by Using a Ru,Rh,Ru Supramolecular Photocatalyst Containing Hydroxide Labile Ligands." *Chemistry – A European Journal* **2015**, *21*, 16948–16954.
This publication was selected as a "Hot Paper".

Rogers, H. M.; White, T. A.; Stone, B. N.; Arachchige, S. M.; Brewer, K. J. "Nonchromophoric Halide Ligand Variation in Polyazine-Bridged Ru(II),Rh(III) Bimetallic Supramolecules Offering New Insight into Photocatalytic Hydrogen Production from Water." *Inorganic Chemistry* **2015**, *54*, 3545–3551.

Rogers, H. M.; Arachchige, S. M.; Brewer, K. J.; Swavey, S. "Polyatomic Bridging Ligands." **2014**, In: Reedijk, J. (Ed.) Elsevier Reference Module in *Chemistry, Molecular Sciences and Chemical Engineering*. Waltham, MA: Elsevier. doi: 10.1016/B978-0-12-409547-2.11313-9.

White, T. A.; Mallalieu, H. E.; Wang, J.; Brewer, K. J. "Mechanistic Insight into the Electronic Influences Imposed by Substituent Variation in Polyazine-Bridged Ruthenium(II)/Rhodium(III) Supramolecules." *Chemistry – A European Journal* **2014**, *20*, 8265–8268.
This publication was featured on the front cover art for the issue.

1. Introduction

1.1. Need for Alternative Energy Sources

As the supply and availability of fossil fuels dwindle, the need for alternative energy sources becomes increasingly important to sustain a growing population.[1] Fossil fuels provide energy though combustion of coal, oil, and natural gas; yet, their use is environmentally detrimental due to the destruction of natural habitats often required to obtain the fuel and due to CO_2 emissions formed by combustion of the fuel. Current, more sustainable energy sources include solar panels and energy created using wind and hydroelectric methods; however, energy in the form of electricity is created by these methods, posing problematic transportation and storage issues.[2] The sun offers a nearly inexhaustible energy source, and storing solar energy in the form of chemical bonds could alleviate fossil fuel dependence and help to power the planet's future.

1.2. Solar-to-Chemical Energy Conversion

The sun provides a vast, globally available energy source that is a leading alternative energy contender. Currently, energy is consumed globally at a rate of 15 TW, yet solar energy reaches the earth at a rate of 120,000 TW.[3-4] However, due to the transient nature of sunlight, solar energy must be stored in an accessible form to satisfy long-term energy needs. Nature provides the ultimate example of solar energy storage through photosynthesis, the process by which solar energy is stored in the form of chemical bonds. To successfully mimic natural processes, systems must be created that are capable of powering uphill chemical reactions using sunlight.

The solar irradiance spectrum (**Figure 1.1**) displays the amount of energy reaching a 1 m^2 area at the surface of the earth as a function of wavelength.

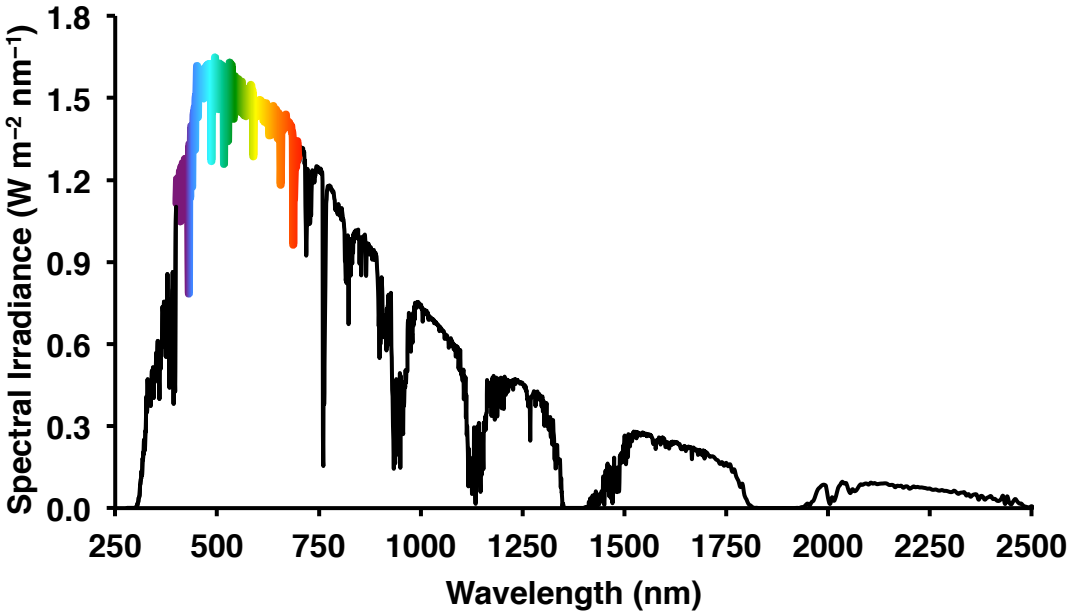

Figure 1.1. Solar spectrum representing spectral irradiance (solar power density) as a function of wavelength (nm). Figure adapted from reference 5.

Solar photons with wavelengths from 280 nm (4.4 eV) to 2500 nm (0.5 eV) reach the surface of the earth, yet the highest photon intensity occurs in the visible region of the electromagnetic spectrum (400 – 700 nm).[5-6] Conversion of energy from the sun to a useable fuel is a desirable and promising alternative energy source. An ideal artificial photosynthetic system will absorb light from the sun to create a potential gradient as a result of directional electron transfer. In the presence of an appropriate catalyst, the reservoir of excited electrons will be funneled to a cheap, readily available feedstock capable of being reduced to a functional, energy-dense fuel (**Figure 1.2**).[7] In the context of this dissertation, H_2O will be the feedstock examined for production of solar fuels.

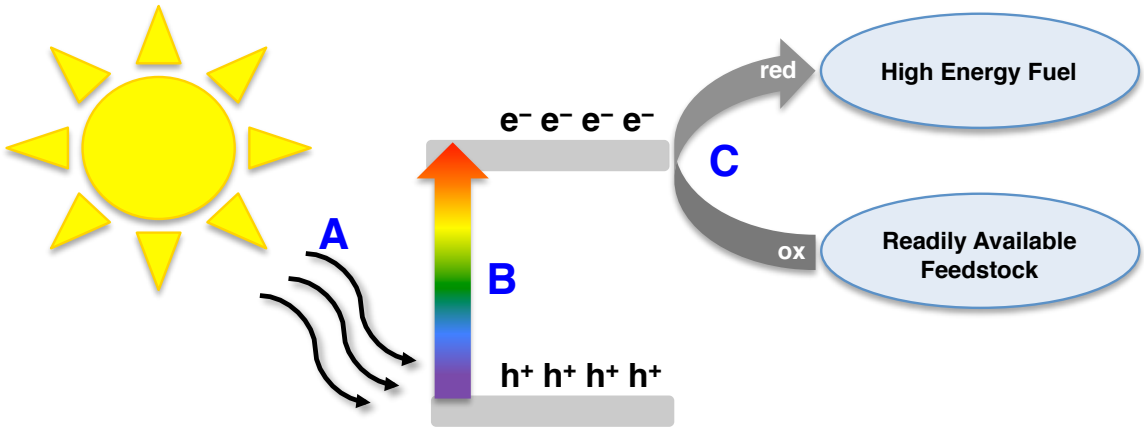

Figure 1.2. Schematic representation of the steps required to harness energy from the sun for conversion to a fuel. **A** = light harvesting; **B** = electron transfer to create potential gradient; **C** = catalytic reduction of a feedstock to a fuel; red = reduced; ox = oxidized.

1.3. H_2O Splitting

The separation of H_2O into its molecular components H_2 and O_2 is shown in **Equation 1.1**.

$$2\ H_2O\ (l) \rightarrow 2\ H_2\ (g) + O_2\ (g) \qquad E = -1.23\ V \qquad (1.1)$$

$$2\ H_2O\ (l) \rightarrow 4\ H^+\ (aq) + O_2\ (g) + 4\ e^- \qquad E = -0.82\ V \qquad (1.2)$$

$$4\ H^+\ (aq) + 4\ e^- \rightarrow 2\ H_2\ (g) \qquad E = -0.41\ V \qquad (1.3)$$

The oxidative and reductive half reactions are shown in **Equations 1.2** and **1.3**, respectively. Each half reaction is pH- and temperature-dependent, provided above at pH = 7 and 298 K.[8] The least energy intensive H_2O splitting process requires 1.23 V per electron vs. the normal hydrogen electrode (NHE), corresponding to wavelengths shorter than 1000 nm, and occurs via a multi-electron process. The single-electron process of H_2O splitting requires nearly 5 V of energy, corresponding to high-energy wavelengths shorter than 250 nm. In the hopes of using visible light from the sun to drive the energetically demanding process of H_2O splitting, systems examined herein

will be capable of delivering multiple reducing equivalents. Ideally, H_2O splitting will be carried out using electrons produced through H_2O oxidation for the reduction of protons to H_2 fuel.[8-9] However, the design and application of a functional system that undergoes complete H_2O splitting has proven difficult, thus research in the field often focuses on either the reductive or oxidative half reaction and uses a sacrificial chemical species to accept or donate electrons.[10-11] The oxidative half reaction of H_2O splitting is an active research arena,[2, 12-14] but this dissertation will focus on the reduction of H_2O to H_2 fuel.

1.4. H_2 as a Fuel Source

H_2 gas shows considerable promise as a carbon neutral fuel of the future. As a fuel source, H_2 has the highest power density (kilowatt hours per kilogram) of any non-nuclear-based fuel source.[10] When combusted in O_2, H_2 gives up both of its available electrons and oxidizes to form H_2O, regenerating the fuel feedstock and providing an exemplary cyclic system.[11] Hydrogen is the most abundant element in the universe; however, most of the accessible hydrogen is bound to oxygen in the form of H_2O, and elemental hydrogen (H_2) is not present in substantial quantities on earth.[15] For H_2 gas to serve as a viable fuel source, it needs to be produced in large quantities. Photocatalytic H_2 fuel production via solar H_2O reduction is a promising alternative fuel production method.

1.5 Photocatalytic Reduction of H_2O to H_2

To store solar energy in the form of chemical bonds as H_2 fuel, the field of inorganic chemistry has received much attention for the design and preparation of metal complexes capable of carrying out demanding tasks. Early systems used multiple

components, each responsible for a given task, to perform a complex feat such as H_2O reduction. Lehn and Sauvage reported a multi-component system in the late 1970s comprised of a $[Ru(bpy)_3]^{2+}$ (bpy = 2,2′-bipyridine) as the light absorber (LA), a Rh-bpy complex formed *in situ* from a $RhCl_3$ salt and excess bpy ligand as the electron relay (ER), triethylamine (TEA) as the sacrifical electron donor (ED), and K_2PtCl_6 as the catalyst. When combined in a neutral aqueous solution and irradiated with visible light, H_2 gas was photocatalytically generated over a period of 2 h.[16] This system was further studied, substituting $[Rh(bpy)_3]^{3+}$ as the ER, triethanolamine (TEOA) as the ED, and colloidal Pt^0 as the catalyst.[8] Several Rh intermediates were proposed during the cycle for H_2 production including $[Rh^{I}(bpy)_2]^{+}$ and $[Rh^{III}(bpy)_2L_2]^{n+}$ ($L = OH^-$; n = 1 or $L = H_2O$; n = 3). Creutz, Sutin, and coworkers examined an analogous multi-component system for photocatalytic H_2 production and proposed a mechanism (**Figure 1.3**).[17-18] Upon excitation of $[Ru(bpy)_3]^{2+}$ with visible light (450 ± 20 nm), an excited chromophore $*[Ru(bpy)_3]^{2+}$ was generated and subsequently oxidized by $[Rh(bpy)_3]^{2+}$ to form $[Ru(bpy)_3]^{3+}$ and $[Rh(bpy)_3]^{2+}$. The TEOA ED prevented detrimental back electron transfer and reduced $[Ru(bpy)_3]^{3+}$ to $[Ru(bpy)_3]^{2+}$, regenerating the LA. $[Rh(bpy)_3]^{2+}$ disproportionated to form $[Rh(bpy)_3]^{3+}$ and $[Rh(bpy)_2]^{+}$. In the presence of the colloidal Pt^0 catalyst, H_2 was generated. Each electron transfer process occurred twice to achieve multi-electron collection required to carry out H_2O reduction.

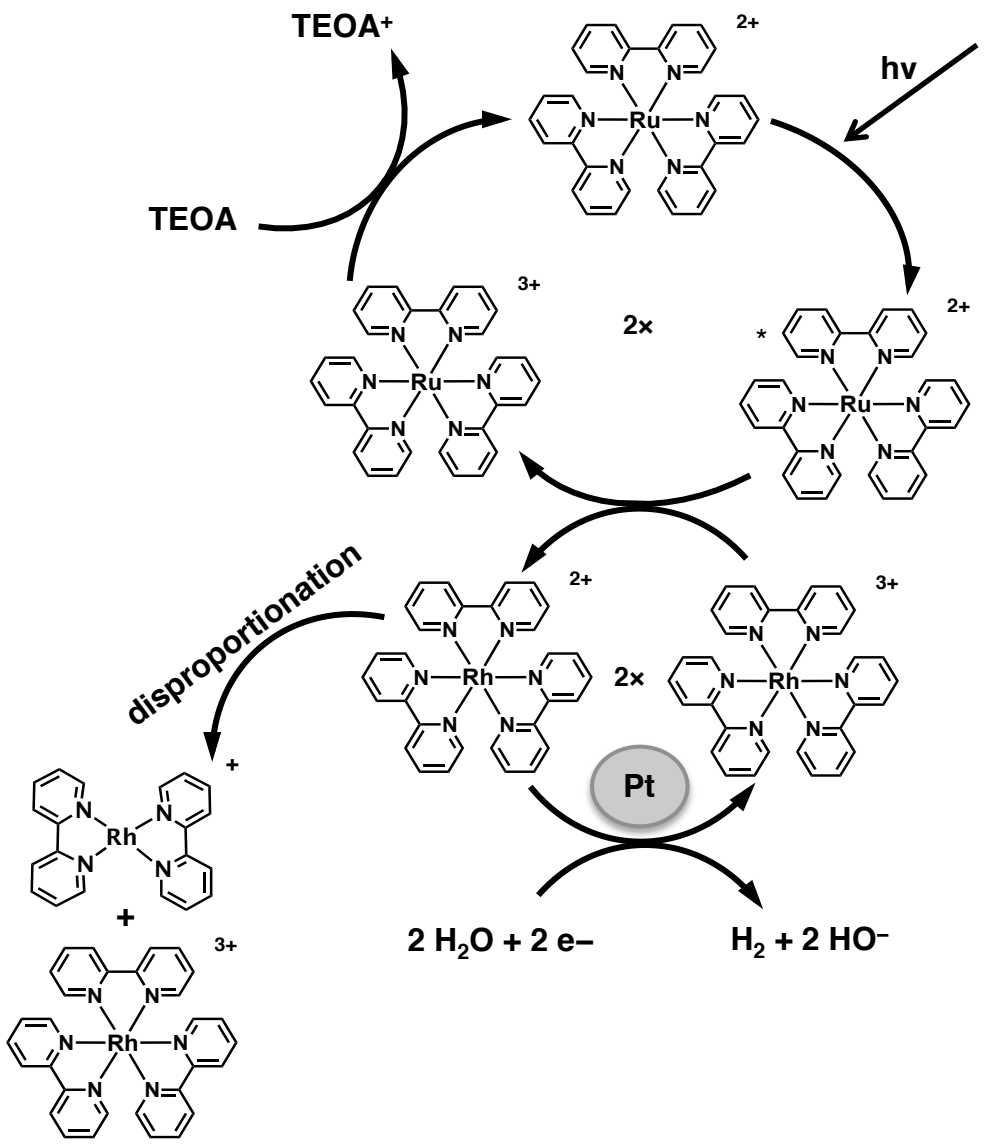

Figure 1.3. Mechanism for photocatalytic H_2 production employing a multi-component system comprised of a $[Ru(bpy)_3]^{2+}$ light absorber, TEOA electron donor, $[Rh(bpy)_3]^{3+}$ electron relay, and Pt catalyst. hv = photoexcitation; bpy = 2,2′-bipyridine; TEOA = triethanolamine. Figure generated using information from reference 17.

Photocatalytic H_2 generation using a multicomponent system continues to serve as an important area of research as new catalyst components are explored. Recent reports discussed the use of multi-component systems capable of photochemical H_2 evolution employing first row transition metal complexes as catalytically active metals.[19-

[21] The use of first-row transition metals in catalysis is an important step towards the use of more abundant catalytic materials; however, achieving the long-term stability and high H_2 yields possible with catalytically active metals such as Rh remains a challenge.

While the study of multi-component photocatalytic systems for H_2 production has advanced fundamental knowledge about mechanistic processes, several significant limitations exist for these systems. All components of the system must collide in solution on a suitable timescale to carry out the appropriate electron transfers needed to collect multiple reducing equivalents for active photocatalysis. In the case of the systems involving the $[Rh(bpy)_3]^{3+}$ ER, the four-coordinate $[Rh^{I}(bpy)_2]^{+}$ postulated to form during the catalytic cycle was susceptible was Rh^{I}-Rh^{I} dimerization, which prohibited further catalytic iterations. For the systems involving colloidal metal catalysts, H_2 evolution was limited by the number of surface sites available on the solid metal catalyst, a notable disadvantage when using expensive metals such at Pt. If key components such as the LA, ER, and catalyst could be covalently coupled in one molecule, disadvantages associated with multi-component systems would be alleviated.

1.6. Supramolecular Complexes

In lieu of studying molecular components as separate species, the field of supramolecular chemistry emphasizes the importance of molecular components collaborating in a bound species. A supramolecular complex, as defined by Balzani, consists of covalently linked molecular subunits each capable of carrying out a specific function that contribute to an overall task.[22-24] Often comprised of a complex network of multiple metal centers and organic ligands, inorganic supramolecules provide the

necessary architectures to carry out complex intramolecular processes needed for the discovery of alternative energy sources.

1.7. Supramolecular Components

While the overall goal of a supramolecular complex is to carry out a complicated task, understanding the contributions of individual components helps to achieve more capable systems. In the context of this dissertation, studied complexes will involve Rh as the catalytic metal and Ru as the light absorber metal bound together by polypyridyl and polyazine ligands. When designing supramolecular architectures, particular significance is given to the relative orbital energetics and redox properties of metal centers in the molecule, the light absorbing properties of the chromophoric subunits, and the excited state dynamics of intramolecular processes.

1.7.1. Redox Properties

Examination of the reductive and oxidative behavior of supramolecular systems comprised of redox-active metals and ligands provides insight about the relative orbital energetics crucial for light-induced processes such as photocatalytic H_2 generation from H_2O. In addition to providing knowledge about the relative orbital energetics, electrochemical experiments afford an understanding of the stability of a molecule following redox events, thus providing insight about the composition of the supramolecule during catalytic processes.

Cyclic voltammetry (CV) is the primary electrochemical technique used to examine complexes included in this dissertation. CV is a potential sweep method where the potential is varied over time and the current response is measured (**Figure 1.4A**).[25]

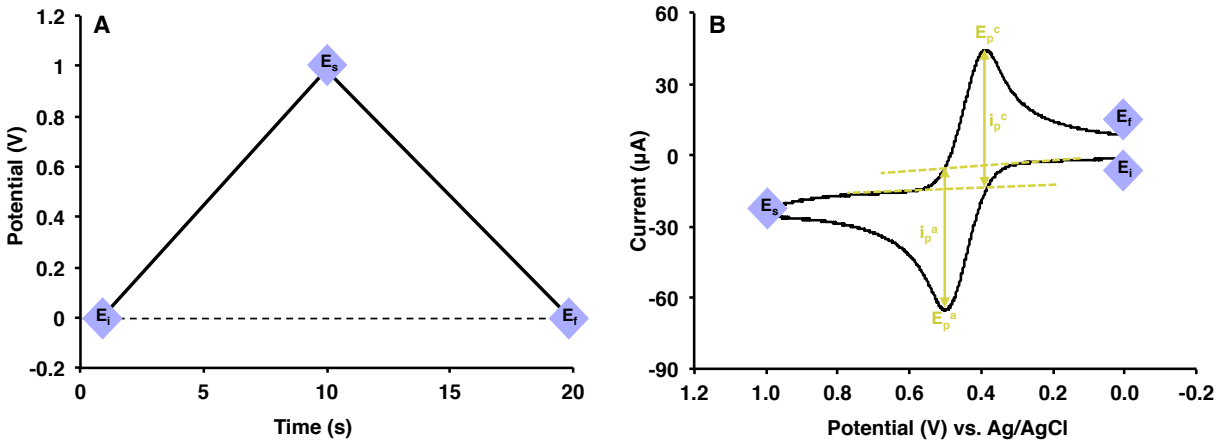

Figure 1.4. (**A**) Potential waveform with potential (V) plotted versus time (s) and (**B**) cyclic voltammogram for ferrocene with current (µA) plotted versus potential (V). E_i = initial potential; E_s = switching potential; E_f = final resting potential; E_p^a = anodic peak potential; E_p^a = cathodic peak potential; i_p^a = anodic peak current; i_p^c = cathodic peak current.

Using the well-studied complex ferrocene ($Fe^{II}(C_5H_5)_2$ (Fc)) as an example (**Figure 1.4B**), the CV experiment begins at an initial potential (E_i) of 0 V. First, with a scan rate of 0.1 V/s, the potential is increased to 1.0 V over a period of 10 s. Upon reaching 1.0 V, the potential is switched (E_s) in the opposite direction and decreased over a period of 10 s to the final potential (E_f) of 0 V. The initial scan from E_i to E_s, oxidizing Fc to Fc^+, is called an anodic scan, and the second scan direction from E_s to E_f, reducing Fc^+ to back to Fc, is called a cathodic scan. Because the anodic peak current (i_p^a) is equal in magnitude to the cathodic peak current (i_p^c), the Fc/Fc^+ redox couple is considered reversible, a property that holds true when $i_p^a/i_p^c = 1$ and does not change with variation of the scan rate. Furthermore, a redox couple is considered reversible when the potential separation (ΔE_p) between the anodic peak potential (E_p^a) and the cathodic peak potential (E_p^c) is 0.59 V per electron transferred (*n*), according to **Equation 1.4**:

$$\Delta E_p = E_p^c - E_p^a = \frac{0.59\ V}{n} \quad (1.4)$$

For a reversible redox event such as the oxidation of Fc, the potential is reported as the half wave potential ($E_{1/2}$) (**Equation 1.5**):

$$E_{1/2} = \frac{E_p^c + E_p^a}{2} \quad (1.5)$$

The $E_{1/2}$ of the Fc/Fc^+ redox couple occurs at +0.46 V vs. Ag/AgCl (3 M NaCl).[26] However, systems exist that do not follow the criteria outlined for reversible redox events. When $i_p^a/i_p^c \neq 1$ and/or varies as a function of scan rate or when $\Delta E_p \neq 0.59$ V per electron transferred, the couple is considered quasi-reversible. When no current response is detected for either i_p^a or i_p^a, the couple is considered irreversible.[25] For this dissertation, Ru^{II} complexes typically have reversible or quasi-reversible redox couples and Rh^{III} complexes typically have quasi-reversible or irreversible redox couples.

1.7.1.1. Ru^{II} Monometallic Complexes

Ru^{II} complexes have long been studied as important light-absorbing species, with $[Ru(bpy)_3]^{2+}$ as the prototypical inorganic light absorber.[27-29] In photocatalytic systems, excitation of the LA subunit promotes electron transfer to lower lying states needed to achieve active catalysis. The CV of $[Ru(bpy)_3]^{2+}$ provides insight about the frontier orbital energetics of this fundamental LA (**Figure 1.5**).

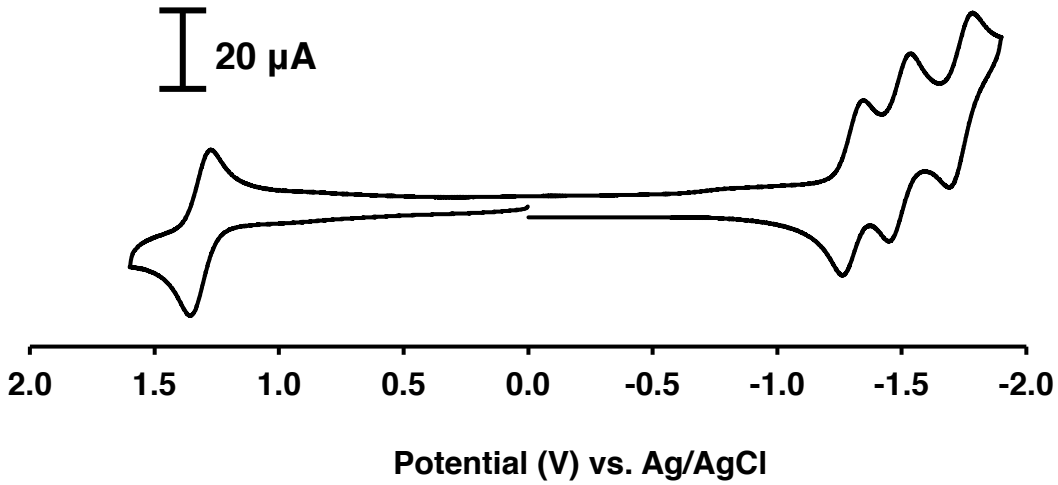

Figure 1.5. Cyclic voltammogram of $[Ru(bpy)_3]^{2+}$. The experiment was performed in 0.1 M Bu_4NPF_6 electrolyte in CH_3CN using a glassy carbon disc working electrode, a platinum wire auxiliary electrode, and a Ag/AgCl reference electrode. The obtained voltammogram agrees with reported values. bpy = 2,2′-bipyridine.

Anodically, a one-electron reversible couple is assigned as $Ru^{II/III}$ at +1.31 V vs. Ag/AgCl, and cathodically, three one-electron couples are assigned to successive $bpy^{0/-}$ reductions at –1.30 V, –1.49 V, and –1.76 V. The electrochemical analysis of $[Ru(bpy)_3]^{2+}$ provides evidence for a Ru-based HOMO and bpy-based lowest unoccupied molecular orbital (LUMO). Analogous systems exist where bpy is replaced with a different bidentate polypyridyl ligand (LL) to prepare complexes of the form $[Ru(LL)_3]^{2+}$.[28, 30] In addition to bpy (**Figure 1.6A**), 4,7-diphenyl-1,10-phenanthroline (Ph_2phen) will be examined in the context of this dissertation (**Figure 1.6B**). When LL = Ph_2phen, the redox properties are not greatly perturbed compared to bpy, with a $Ru^{II/III}$ couple at +1.29 V and an initial $Ph_2phen^{0/-}$ couple at –1.27 V.[31]

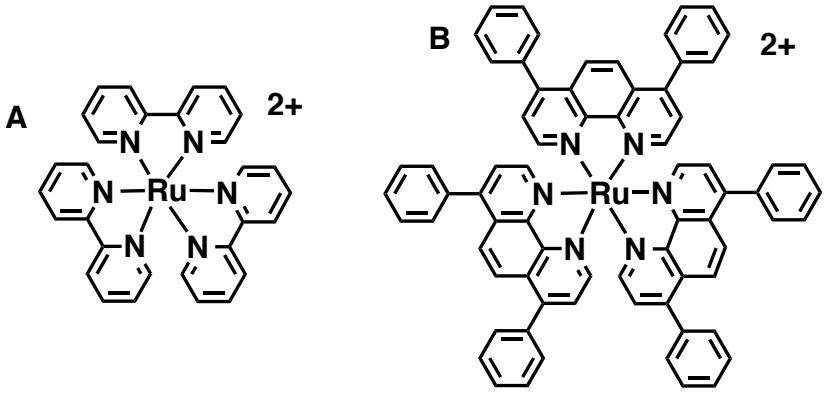

Figure 1.6. Structures of two Ru-polypyridyl complexes bearing terminal ligands that possess no open coordination sites. (**A**) $[Ru(bpy)_3]^{2+}$ and (**B**) $[Ru(Ph_2phen)_3]^{2+}$. bpy = 2,2′-bipyridine; Ph_2phen = 4,7-diphenyl-1,10-phenanthroline.

The inclusion of bidentate polypyridyl ligands with no remaining coordination sites, often referred to as terminal ligands (TL), limits supramolecular expansion by incorporation of additional metal centers. Therefore, the use of polyazine bridging ligands (BL) containing open coordination sites is desirable to create expanded supramolecular architectures. A polyazine, bis-bidentate bridging ligand, 2,3-bis(2-pyridyl)pyrazine (dpp), is explored herein for supramolecular motifs. When one polypyridyl TL in $[Ru(TL)_3]^{2+}$ is substituted with a dpp BL, a heteroleptic Ru(II) complex bearing an open coordination site results (**Figure 1.7A–B**).[31-34]

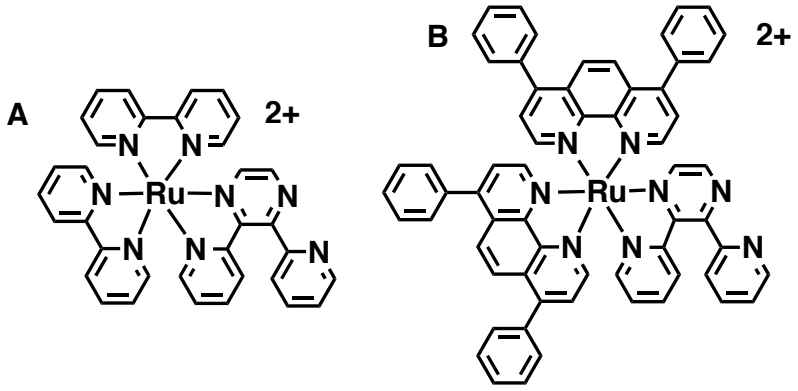

Figure 1.7. Structures of two Ru-polypyridyl complexes bearing terminal ligands and bridging ligands. (**A**) $[(dpp)Ru(bpy)_3]^{2+}$ and (**B**) $[(dpp)Ru(Ph_2phen)_3]^{2+}$. bpy = 2,2′-bipyridine; Ph_2phen = 4,7-diphenyl-1,10-phenanthroline; dpp = 2,3-bis(2-pyridyl)pyrazine.

Similar to $[Ru(TL)_3]^{2+}$ complexes (TL = bpy or Ph_2phen), anodic scans for $[(TL)_2Ru(dpp)]^{2+}$ display a reversible, one-electron $Ru^{II/III}$ couple at +1.38 V for TL = bpy and +1.39 V for TL = Ph_2phen. However, metal-based redox events are impacted by the surrounding ligand environment, and the $Ru^{II/III}$ oxidation shifts upon inclusion of a BL.[33] The $E_{1/2}$ value for the Ru-based oxidation is positively shifted due to the presence of the more electron-withdrawing dpp ligand causing stabilization of the Ru(dπ) orbitals. Cathodically, $[(TL)_2Ru(dpp)]^{2+}$ complexes display a $dpp^{0/-}$ couple at −1.01 V when TL = bpy and −1.04 V when TL = Ph_2phen. Two sequential TL reductions follow the BL reduction. Similar to the Ru homoleptic analogues, $[(TL)_2Ru(dpp)]^{2+}$ complexes possess a Ru(dπ)-based HOMO and a ligand-based LUMO (**Figure 1.8** for TL = bpy); yet, for the heteroleptic complexes, the LUMO lies on the BL rather than a TL. The energy difference between the Ru-based HOMO and the BL-based LUMO plays a large role in the light absorption and excited state properties for supramolecular complexes (*vide infra*).

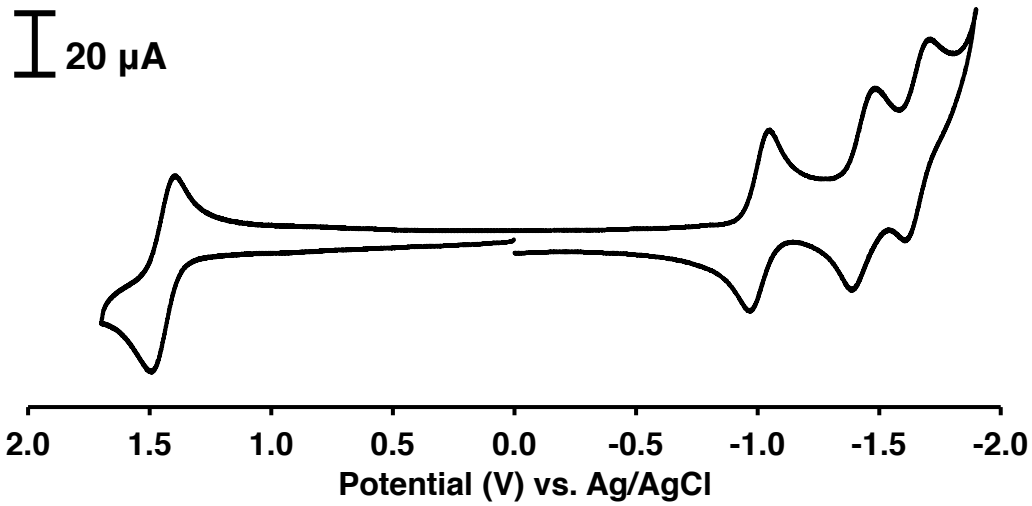

Figure 1.8. Cyclic voltammogram of $[(bpy)_2Ru(dpp)]^{2+}$. The experiment was performed in 0.1 M Bu_4NPF_6 electrolyte in CH_3CN using a glassy carbon disc working electrode, a platinum wire auxiliary electrode, and a Ag/AgCl reference electrode. The obtained voltammogram agrees with reported values. bpy = 2,2′-bipyridine.

1.7.1.2. Rh^{III} Monometallic Complexes

Examination of the redox properties of Rh-polypyridyl complexes provides great insight about the multi-electron collection required to carry out active photocatalytic H_2 evolution. Monometallic Rh^{III} complexes of the form $[Rh(LL)_2X_2]^+$ (LL = TL or BL; X = halide) served as early models for electrochemistry related to the construction of supramolecular complexes employing Rh as both the electron collector and catalytically active metal. Cathodic scans at 0.2 V/s of complex $[Rh(bpy)_2Cl_2]^+$ show overlapping, irreversible, two-electron $Rh^{III/II/I}$ reductions at –0.89 V vs. Ag/AgCl followed by $bpy^{0/-}$ ligand reductions at –1.32 and –1.62 V.[35-36] The CV results provide evidence for a Rh(dσ*)-based LUMO and higher lying ligand-based orbitals. Exhaustive scan rate variation studies were carried out to better understand the cathodic electrochemistry, and a mechanism was proposed by DeArmond and coworkers for the reduction of

$[Rh(LL)_2X_2]^+$ (LL = bpy or 1,10-phenanthroline (phen); X = Cl^-) (**Figure 1.9A**).[36-37] Starting with the initial species $[Rh^{III}(LL)_2X_2]^+$ (**Figure 1.9B**), electron transfer occurred to produce the one-electron reduced species $[Rh^{II}(LL)_2X_2]^+$. Rapid halide loss occurred next to produce species $[Rh^{II}(LL)_2X]^+$. The sequential process of an electron transfer (E) followed by a chemical reaction (C), such as halide loss, is called an EC process and is typical for Rh(III)-polypyridyl complexes.[35-36, 38]

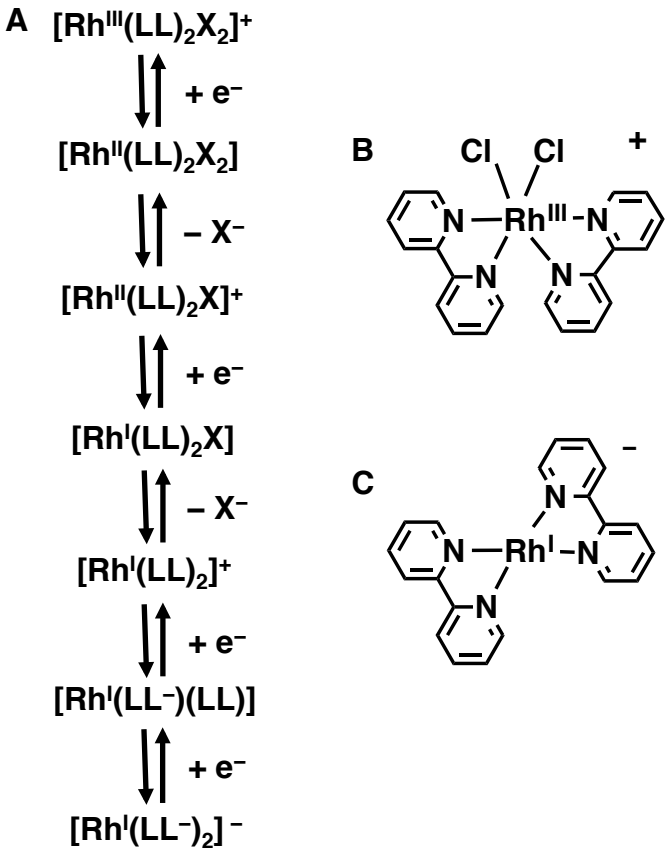

Figure 1.9. (**A**) Electrochemical mechanism for the reduction of a Rh-polypyridyl complex of the form $[Rh^{III}(LL)_2X_2]^+$ (LL = polypyridyl ligand; X = halide) as proposed by DeArmond and coworkers in Reference 36. (**B**) Example of the initial species in the proposed pathway, $[Rh^{III}(bpy)_2Cl_2]^+$. (**C**) Example of the final species in the proposed pathway, $[Rh^{I}(bpy^-)_2]^-$. bpy = 2,2′-bipyridine.

A second EC process occurred to produce a square-planar, four-coordinate Rh^I species bearing no halide ligands, $[Rh^I(LL)_2]^+$. Lastly, two more electron transfers reduced each

LL ligand, producing the final species $[Rh^{I}(LL^{-})_2]^{-}$ (**Figure 1.9C**). The $Rh^{III/II/I}$ reductions in $[Rh(LL)_2X_2]^{+}$ complexes are irreversible redox events due to a chemical reaction (halide loss) occurring after the electron transfer, causing an irreversible chemical change in the initial species examined.

As with Ru^{II} complexes, the ligand set coordinated to the Rh^{III} metal center influences the orbital energetics and the redox properties.[35-39] When the more electron-donating 4,4′-di-*tert*-butyl-2,2′-bipyridine ($^{t}Bu_2bpy$) polypyridyl ligand is used as LL in $[Rh(LL)_2Cl_2]^{+}$ complexes, the Rh center becomes more difficult to reduce relative to LL = bpy complexes and shifts the $Rh^{III/II/I}$ reduction to a more negative potential (E_p^{c} = –0.96 V).[35] When the halides at Rh are varied from Cl^{-} to weaker σ-donating Br^{-} ligands to produce complex $[Rh(bpy)_2Br_2]^{+}$, the Rh center becomes easier reduce relative to $[Rh(bpy)_2Cl_2]^{+}$ and the $Rh^{III/II/I}$ reduction is shifted to a less negative potential (E_p^{c} = –0.79 V). When bidentate ligands with less electron-donating character, such as the dpp BL, are used to produce complex $[Rh(dpp)_2Br_2]^{+}$, the reduction potential shifts to a less negative potential (E_p^{c} = –0.60 V).[38] The ability to finely tune the LUMO by ligand variation in $[Rh(LL)_2X_2]^{+}$ complexes is a key aspect in the design of supramolecular complexes attempting to achieve electron collection at a catalytically active metal.

1.7.2. Light Absorbing Properties

Efficient light absorption by a supramolecular complex is critical to photocatalytic H_2 production from H_2O. Electronic excitation occurs when a chromophore absorbs a photon of visible light (hv), promoting the molecule from the ground state to an electronic excited state. Excited state molecules display photochemical and

photophysical properties that are often vastly different from their ground state counterparts.[40-41] Electronic absorption spectroscopy is used to study light absorption by photoactive species and to better understand their unique properties.

The intensity of an electronic transition between two different states is based on the overlap of the ground state and excited state wave functions and on adherence to the symmetry and spin selection rules.[40-41] Electronic transition strength is mathematically defined by f, where ε is the extinction coefficient at a given energy value (v) (**Equation 1.6**):

$$f = 4.32 \times 10^{-9} \int_{-v}^{v} \varepsilon(v) dv \tag{1.6}$$

Fully allowed transitions have a value of f ≈ 1. The intensity of an electronic transition is related through f to ε, and the Beer-Lambert law relates ε to absorbance intensity in electronic absorption spectroscopy, where A_λ = absorbance at a given wavelength (λ), ε_λ = the extinction coefficient at λ, c = species concentration, and l = the absorbance path length (**Equation 1.7**):

$$A_\lambda = \varepsilon_\lambda c l \tag{1.7}$$

The symmetry selection rules dictate that electronic transitions in a centrosymmetric molecule are forbidden between states of the same parity (gerade to gerade; ungerade to ungerade).[42] The spin selection rules dictate that a transition is spin-allowed if the spin state of an electron does not change upon transitioning from one state to another (**Figure 1.10A**), and conversely, a transition is spin-forbidden if the electronic spin state does change (**Figure 1.10B**).

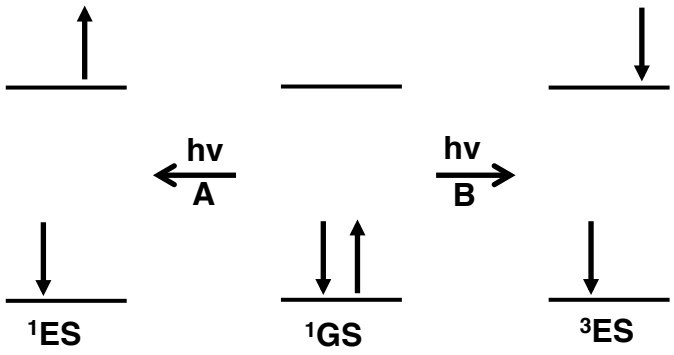

Figure 1.10. The electron configuration of a singlet ground state (^{1}GS) and subsequent photoexcitation (hv) to (**A**) a spin-allowed singlet excited state (^{1}ES) and to (**B**) a spin-forbidden triplet excited state (^{3}ES).

Spin- and symmetry-allowed electron transitions have the highest ε values between 10^2 and 10^6 $M^{-1}cm^{-1}$. Spin-forbidden but symmetry-allowed transitions are often still observable in electronic absorption spectroscopy with somewhat lower ε values between 1 and 10^2 $M^{-1}cm^{-1}$, and complexes that contain heavier second and third row transition metals tend to have ε values at the top of that range near 10^2 $M^{-1}cm^{-1}$. Such formally spin-forbidden transitions maintain modest ε values due to relaxation of the spin-selection rules arising from spin-orbit coupling, which is prone to occur in complexes containing heavy metals such as Ru.[40]

In transition metal photochemistry, many types of electronic transitions are possible.[27, 40-41] **Figure 1.11** depicts a block-style molecular orbital (MO) diagram for a six-coordinate, octahedral d^6 metal complex (ML_6). The MO configuration of the pseudooctahedral complex $[Ru(bpy)_3]^{2+}$ can be approximated using this diagram. While the block orbitals are labeled in a localized manner based on the dominant contribution of each unit, metal (M) or ligand (L), the orbitals are largely delocalized.

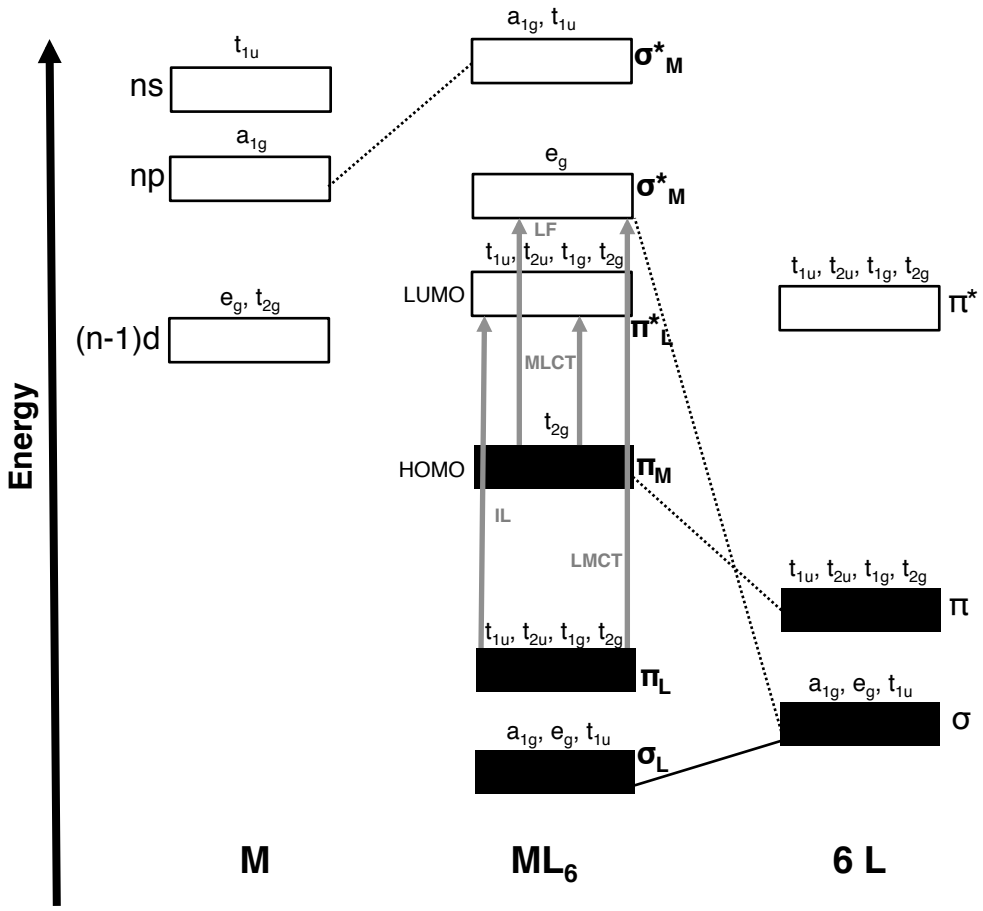

Figure 1.11. Block-style molecular orbital diagram for electronic transitions occurring in a d^6 metal complex (ML_6). Bonding orbitals are designated without an asterisk and anti-bonding orbitals with an asterisk. Filled black boxes indicate filled or partially filled orbitals and empty black boxes indicate unfilled orbitals. HOMO = highest occupied molecular orbital; LUMO = lowest unoccupied molecular orbital; IL = intraligand transition; LF = ligand field transitions; LMCT = ligand-to-metal charge transfer transition; MLCT = metal-to-ligand charge transfer transition. Figure adapted from reference 40.

Intraligand (IL) transitions occur when an electron is promoted from a ligand-based orbital to another ligand-based orbital belonging to the same ligand set. Ligand field (LF) transitions occur when an electron is promoted from a metal-based orbital to another metal-based orbital belonging to the same metal. A special type of transition called a charge transfer (CT) transition occurs when an electron is promoted from an orbital primarily of one character to an orbital primarily of another character. CT transitions are

particularly important in transition metals complexes that carry out photochemical reactions. Metal-to-ligand CT (MLCT) transitions and ligand-to-metal CT (LMCT) transitions occur for d^6 octahedral metal complexes. Careful ligand selection in Ru and Rh complexes is important to achieve optimal light absorption.

1.7.2.1. Ru^{II} Monometallic Complexes

The properties of $[Ru(bpy)_3]^{2+}$ are well studied and provide an exemplary LA model for photocatalytic H_2 evolution.[28-29, 43-44] The electronic absorption spectra for $[Ru(bpy)_3]^{2+}$ contains multiple electronic transitions, notably a set of lowest energy ^{1}MLCT transitions (**Figure 1.12**).

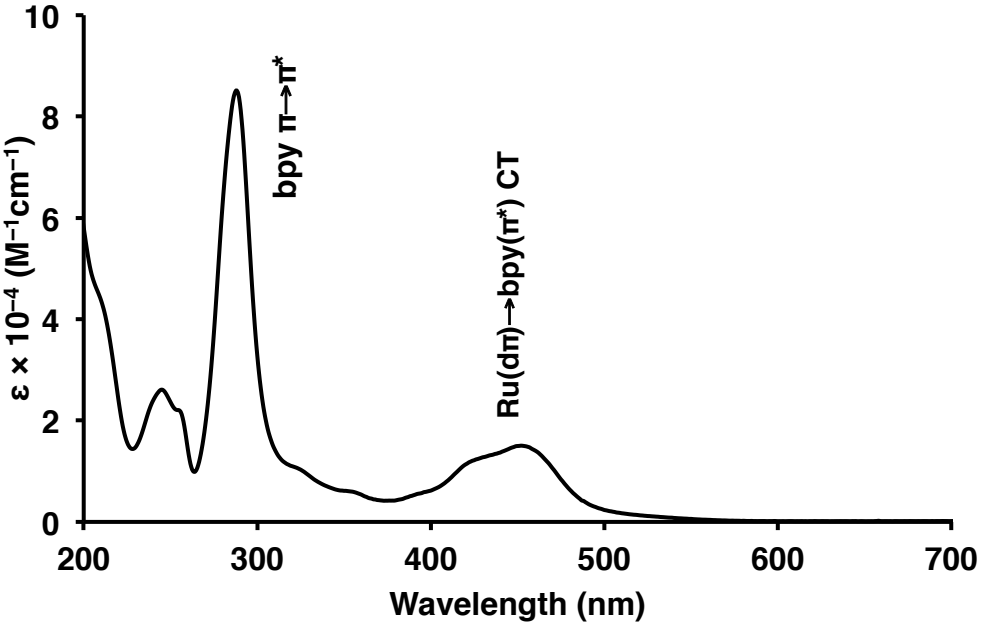

Figure 1.12. Electronic absorption spectrum for $[Ru(bpy)_3]^{2+}$ obtained in CH_3CN in a 1 cm quartz cuvette. bpy = 2,2′-bipyridine; CT = charge transfer. The obtained spectrum agrees with reported values.

In the UV, bpy π→π* IL transitions occur at λ_{max}^{abs} = 286 nm (ε = 8.7 × 10^4 $M^{-1}cm^{-1}$). In the visible, CT transfer transitions dominate with Ru(dπ)→bpy(π*) ^{1}MLCT transitions at

λ_{max}^{abs} = 449 nm (ε = 1.5 × 10^4 $M^{-1}cm^{-1}$). When bpy TLs are substituted for Ph_2phen, complex $[Ru(Ph_2phen)_3]^{2+}$ demonstrates enhanced light absorption capabilities in addition to a slight shift to lower energy for Ru(dπ)→Ph_2phen(π^*) ^{1}MLCT transitions, λ_{max}^{abs} = 460 nm (ε = 2.9 × 10^4 $M^{-1}cm^{-1}$).[45] While both $[Ru(TL)_3]^{2+}$ complexes (TL = bpy or Ph_2phen) are efficient LA subunits, increased absorption in the visible region by TL = Ph_2phen complexes may be useful to exploit in the development of photocatalysts for solar H_2 production.

Substituting one TL in $[Ru(TL)_3]^{2+}$ complexes for a BL produces heteroleptic complexes $[(TL)_2Ru(BL)]^{2+}$ (TL = bpy or Ph_2phen; BL = dpp) that contain an open coordination site important for the construction of multimetallic architectures. The light absorbing properties of $[(TL)_2Ru(BL)]^{2+}$ are shifted compared to the $[Ru(TL)_3]^{2+}$ analogues due to the incorporation of the more electron-withdrawing dpp BL. Similar to the electrochemical potential shifts observed, $[(bpy)_2Ru(dpp)]^{2+}$ possesses higher energy Ru(dπ)→bpy(π^*) ^{1}MLCT transitions at λ_{max}^{abs} = 434 nm (ε = 1.2 × 10^4 $M^{-1}cm^{-1}$) due to stabilization of the Ru(dπ) orbitals.[33, 46] The lowest energy ^{1}MLCT transitions result from Ru(dπ)→dpp(π^*) transitions at λ_{max}^{abs} = 468 nm (ε = 1.1 × 10^4 $M^{-1}cm^{-1}$) (**Figure 1.13**).

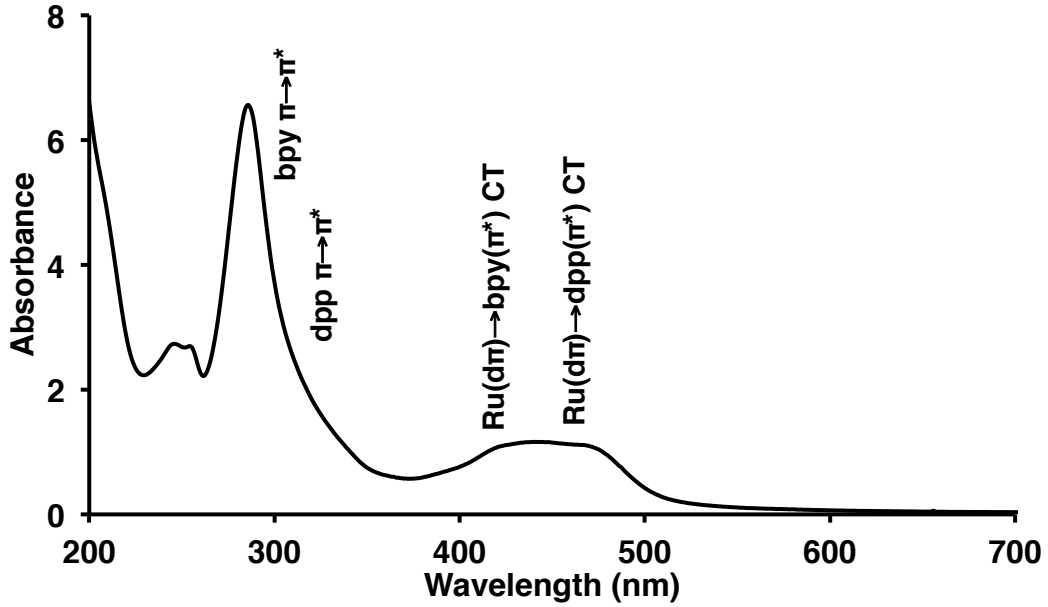

Figure 1.13. Electronic absorption spectrum for $[(bpy)_2Ru(dpp)]^{2+}$ obtained in CH_3CN in a 1 cm quartz cuvette. bpy = 2,2′-bipyridine; dpp = 2,3-bis(2-pyridyl)pyrazine. The obtained spectrum agrees with reported values.

The TL = Ph_2phen Ru(II) complex containing a dpp BL possesses Ru(dπ)→Ph_2phen(π*) ^{1}MLCT transitions at λ_{max}^{abs} = 424 nm (ε = 1.8 × 10^4 $M^{-1}cm^{-1}$) and a lowest-energy Ru(dπ)→dpp(π*) ^{1}MLCT transitions at λ_{max}^{abs} = 474 nm (ε = 1.5 × 10^4 $M^{-1}cm^{-1}$).[32] Monometallic Ru^{II} polypyridyl and polyazine complexes possess notable light absorbing abilities and hold promise for use in supramolecular architectures for solar energy conversion.

1.7.2.2. Rh^{III} Monometallic Complexes

Rh-polypyridyl and polyzazine complexes are capable of light absorption and transitions typically occur in the UV region. Complexes of the form $[Rh(LL)_2X_2]^+$ (LL = TL or BL; X = halide) possess high energy IL π→π* transitions attributed to the polypyridyl ligands. Electronic transition energies are not greatly affected by variation of the halide in $[Rh(bpy)_2Cl_2]^+$ (λ_{max}^{abs} = 302 and 310 nm) to $[Rh(bpy)_2Br_2]^+$ (λ_{max}^{abs} = 302 and 311

nm).[40] The negligible change in λ_{max} upon halide variation suggests that the nonchromophoric halide ligands do not significantly impact light absorbing properties. Substitution of the more electron-withdrawing dpp ligands for bpy ligands to produce $[Rh(dpp)_2Br_2]^+$ (λ_{max}^{abs} = 280 and 328 nm) shifts the IL transitions and further demonstrates the impact ligand variation can have on the electronic properties of metal complexes.[38] When studied in conjunction with strongly absorbing Ru-polypyridyl complexes, the light absorbing properties of Rh-polypyridyl complexes are often obscured by electronic transitions from Ru species with comparatively larger ε values.

1.7.3. Excited State Properties

Metal complexes, upon photon absorption, can populate excited states required to carry out energetically demanding chemical reactions. While the stability of Ru^{II} and Rh^{III} d^6 metal complexes can make syntheses involving ligand exchange difficult, the coordinative stability of these complexes is essential for the study of excited state electron transfer interactions.[27] When excited state deactivation occurs by a radiative process, the energy of the excited state can be quantified using luminescence spectroscopy. Both steady-state and time-resolved luminescence spectroscopy are used to examine metal-polypyridyl complexes of interest for photochemical H_2O reduction to produce H_2 fuel.

1.7.3.1. Ru^{II} Monometallic Complexes

Complicated excited state processes are responsible for the complex excited state behavior of Ru-polypyridyl species such as $[Ru(bpy)_3]^{2+}$.[44] Morse potential energy

surface diagrams are used to model transitions and state populations following excitation with light (**Figure 1.14**).[40]

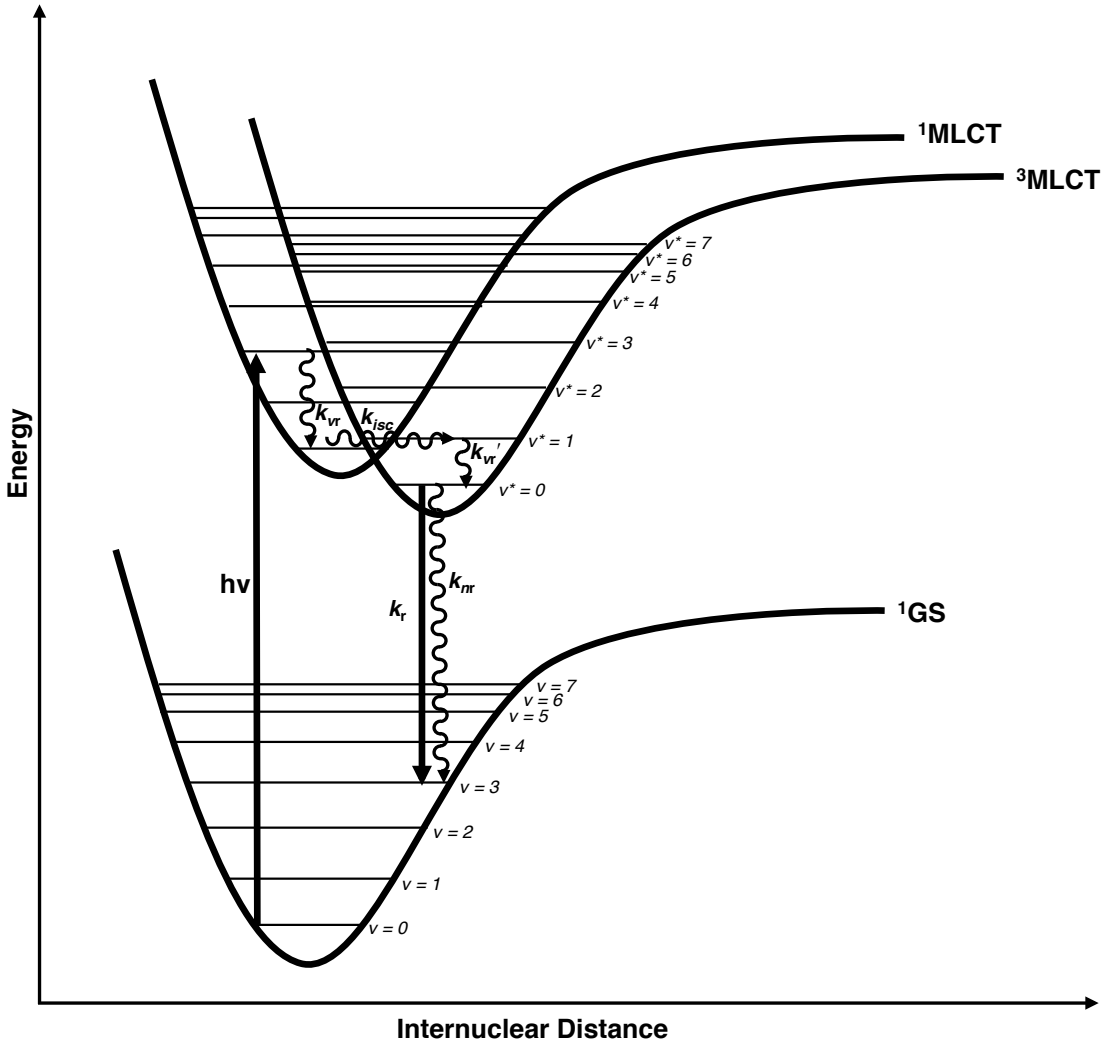

Figure 1.14. Morse potential energy surface diagram for an octahedral $[Ru(TL)_3]^{2+}$ metal complex. Straight arrows represent radiative processes and wavy arrows represent non-radiative processes. TL = terminal ligand; hv = photoexcitation; k_{vr} = rate of vibrational relaxation; k_{isc} = rate of intersystem crossing; k_{nr} = rate of nonradiative decay; k_r = rate of radiative decay; MLCT = metal-to-ligand charge transfer; GS = ground state; v = vibrational energy level.

Upon absorption of a photon of light (hv) of the appropriate energy, a $[Ru(TL)_3]^{2+}$ complex undergoes excitation from a ^{1}GS to populate a ^{1}MLCT excited state. The molecule initially occupies a Frank-Condon state but vibrationally relaxes (k_{vr}) to the

thermally equilibrated excited state (thexi state). From the ^{1}MLCT excited state, the molecule undergoes intersystem crossing (k_{isc}) to populate the low-energy ^{3}MLCT excited state from where emission occurs, following Kasha's rule that states emission occurs from the lowest energy excited state regardless of excitation energy.[42] This spin-forbidden (^{1}MLCT→^{3}MLCT) transition becomes allowed due to spin-orbit coupling that occurs in Ru^{II} complexes.[44] Radiative decay (k_r) from the ^{3}MLCT excited state provides a probe to study the excited state dynamics and excited state reactions in Ru-polypyridyl complexes. Nonradiative decay (k_{nr}) is another deactivation pathway from the ^{3}MLCT excited state and occurs through vibrational relaxation. Dynamic excited state processes are often represented as the more-simplified Jablonski-type diagram (**Figure 1.15A**), which can be further simplified to include diagonal arrows for the vector sum of vertical and subsequent horizontal state transfer processes (**Figure 1.15B**).

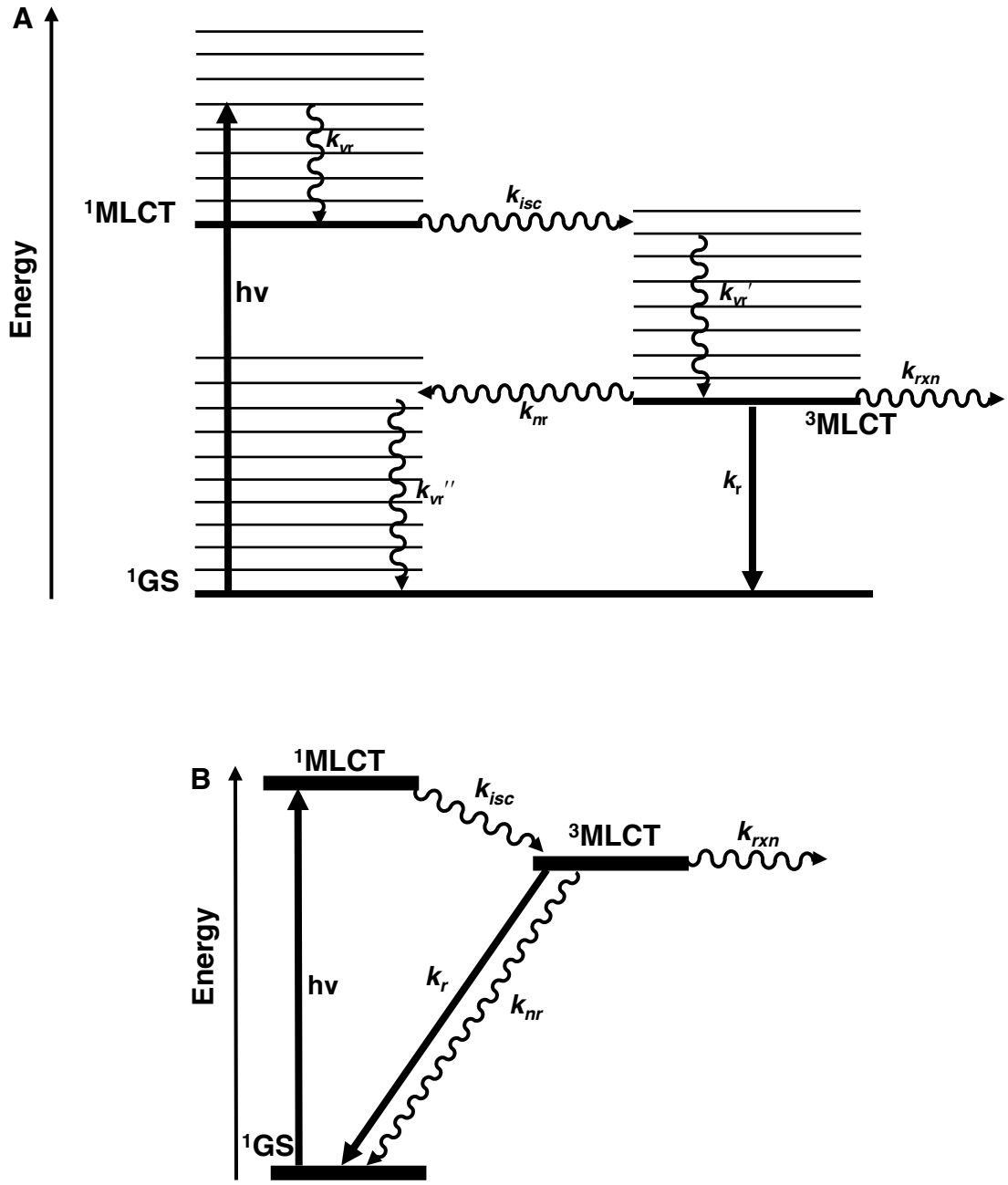

Figure 1.15. Jablonski-type diagram for the excited state processes for an octahedral $[Ru(TL)_3]^{2+}$ metal complex. (**A**) State diagram representing all vibrational relaxation processes and (**B**) simplified state diagram where vertical and subsequent horizontal processes are shown as the diagonal vector sum. Solid arrows represent radiative processes and wavy arrows represent non-radiative processes. TL = terminal ligand; hv = photoexcitation; k_{vr} = rate of vibrational relaxation; k_{isc} = rate of intersystem crossing; k_{nr} = rate of nonradiative decay; k_r = rate of radiative decay; k_{rxn} = rate of follow-up chemical reaction; MLCT = metal-to-ligand charge transfer; GS = ground state.

The emissive nature of the ^{3}MLCT excited state in Ru-polypyridyl complexes allows examination of the excited state dynamics.[47] The quantum yield of emission (Φ^{em}) and the lifetime of the excited state (τ) are useful for quantifying the deactivation rates of electronic excited states.[40] For $[(Ru(TL)_3]^{2+}$ (TL = bpy or Ph_2phen) complexes having no follow-up chemical reaction (k_{rxn}), the τ is equal to the inverse sum of the deactivating rate constants (k_r and k_{nr}) (**Equation 1.8**):

$$\tau = \frac{1}{k_r + k_{nr}} \tag{1.8}$$

The Φ^{em} gives a measure of the efficiency of radiative decay as a ratio of the light emitted over the light absorbed (**Equation 1.9**):

$$\Phi^{em} = \frac{total\ photons\ emitted}{total\ photons\ absorbed} \tag{1.9}$$

The Φ^{em} can also be related through the rate constants for deactivation from the excited state (**Equation 1.10)**:

$$\Phi^{em} = \Phi^{pop}\frac{k_r}{k_r + k_{nr}} \tag{1.10}$$

The quantum yield of population (Φ^{pop}) is a measure of efficiency of population of the excited state. In the case of the ^{3}MLCT excited state for a $[(Ru(TL)_3]^{2+}$ complex, $\Phi^{pop} = 1$ based on the assumption that intersystem crossing occurs with unit efficiency from the ^{1}MLCT excited state, consistent with Kasha's rule.[42] When **Equation 1.8** and **1.10** are combined, **Equation 1.11** results:

$$\Phi^{em} = k_r\tau \tag{1.11}$$

Upon determination of the Φ^{em} and the τ, both k_r and k_{nr} can be calculated. When examining supramolecular complexes for photocatalytic H_2 production, a deep

understanding of the excited state processes associated with photocatalyst components allows for mechanistic insight in the area of inorganic photochemistry.

The excited state dynamics of $[Ru(bpy)_3]^{2+}$ are probed following population of the emissive lowest-energy excited state. Radiative decay occurs from the Ru(dπ)→bpy(π*) ^{3}MLCT excited state with λ_{max}^{em} = 603 nm, Φ^{em} = 0.07, and τ = 850 ns in 298 K deoxygenated CH_3CN.[30, 33] By contrast, $[Ru(Ph_2phen)_3]^{2+}$ has an emissive Ru(dπ)→Ph_2phen(π*) ^{3}MLCT excited state with a slightly lower energy emission band (λ_{max}^{em} = 618 nm) but greatly increased Φ^{em} (0.37) and τ (6400 ns) in 293 K deoxygenated 4:1 ethanol/methanol solution.[48] The extended lifetime in $[Ru(Ph_2phen)_3]^{2+}$ provides more time for excited state reactions, a useful feature to exploit for the design of photocatalysts for H_2 production. Examination of the dpp BL substituted species $[(TL)_2Ru(dpp)]^{2+}$ (TL = bpy or Ph_2phen) further demonstrates the impact of ligand variation on photophysical properties. Both $[(TL)_2Ru(dpp)]^{2+}$ complexes possess a similar emissive Ru(dπ)→dpp(π*) ^{3}MLCT excited state. $[(bpy)_2Ru(dpp)]^{2+}$ has λ_{max}^{em} = 691 nm, Φ^{em} = 0.023, and τ = 380 ns and $[(Ph_2phen)_2Ru(dpp)]^{2+}$ has λ_{max}^{em} = 664 nm, Φ^{em} = 0.035, and τ = 820 ns in 298 K deoxygenated CH_3CN.[32, 47] The noted differences in λ_{max}^{em} and lifetime of the formally Ru(dπ)→dpp(π*) ^{3}MLCT excited state for both TL = bpy and Ph_2phen species suggest the choice of TL continues to influence the excited state properties by tuning the electronics of the Ru metal center.

1.7.3.2. Rh^{III} Monometallic Complexes

Examination of the excited state properties of $[Rh(LL)_2X_2]^+$ (LL = TL or BL; X = halide) complexes reveals low energy emissions arising from LF excited states.[38, 40, 49]

Emission from $[Rh(LL)_2X_2]^+$ complexes occurs at low temperatures (77 K) and is localized on the Rh metal because spin-orbit coupling facilitates emission from the LF excited state. Complex $[Rh(bpy)_2Br_2]^+$ displays an emission band centered at λ_{max}^{em} = 660 nm in an ethanol/methanol glass matrix at 77 K. Upon variation of bpy to the dpp BL, $[Rh(dpp)_2Br_2]^+$ displays an emission band centered at 707 nm.[38] The low energy emission shift upon inclusion of dpp BLs is expected due to the electron-withdrawing character of dpp relative to bpy. Luminescence spectroscopy provides further evidence for the modulation of the electronics of Rh-polypyridyl complexes by variation of the ligand set.

1.8. Photochemical Molecular Devices

Developing an understanding of individual molecular components is important for the design of supramolecular complexes where each subunit works together to carry out a complicated task such as photocatalytic H_2 evolution from H_2O. Photochemical molecular devices (PMDs) are a subclass of supramolecular complexes possessing definite individual components that work together to achieve demanding photoinitiated processes though careful component selection.[22, 24, 50] Transition metal complexes comprised of several metal centers linked through one or more BLs are exemplary PMD candidates. When a PMD is capable of collecting two or more reducing equivalents by a light-induced process, it is termed a photoinitiated electron collector (PEC).[51]

1.8.1. Photoinitiated Electron Collectors

Early PECs exist that collect multiple redox equivalents at low-lying ligand-based (π^*) orbitals (**Figure 1.16**).[52-57]

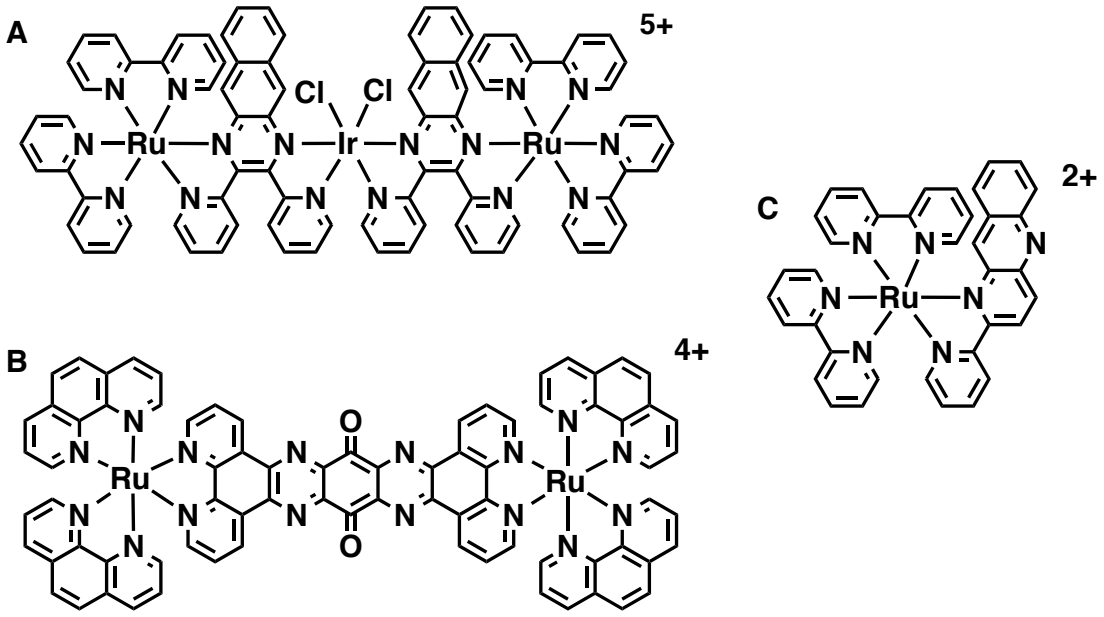

Figure 1.16. Molecular structures for photoinitiated electron collectors that collect multiple redox equivalents on ligand-based orbitals. (**A**) $[\{(bpy)_2Ru(dpb)\}_2IrCl_2]^{5+}$; (**B**) $[(phen)_2Ru(tatpq)Ru(phen)_2]^{4+}$; (**C**) $[(bpy)_2Ru(pbn)]^{2+}$. bpy = 2,2′-bipyridine; dpb = 2,3-bis(2-pyridyl)benzoquinoxaline; phen = 1,10-phenanthroline; tatpq = 9,11,20,22-tetraazatetrapyridol[3,2-*a*:2′3′-*c*:3″,2″-1:2‴,3‴-*n*]pentacene-10,21-quinone; pbn = 2-(2-pyridyl)benzo[*b*]-1,5-napthyridine.

The first reported PMD to serve as a PEC was $[\{(bpy)_2Ru(dpb)\}_2IrCl_2]^{5+}$ (dpb = 2,3-bis(2-pyridyl)benzoquinoxaline).[56] This trimetallic complex covalently coupled two Ru^{II} chromophores through dpb BLs to an Ir^{III} metal center. Upon photolysis in the presence of *N,N*-dimethylaniline (DMA) electron donor, $[\{(bpy)_2Ru(dpb)\}_2IrCl_2]^{5+}$ collected two electrons to produce $[\{(bpy)_2Ru(dpb^{-})\}_2IrCl_2]^{3+}$, while higher lying Ir-based acceptor orbitals prevented electron collection at the metal center. The DMA electron donor prevented rapid back electron transfer from the excited chromophore and was necessary for intramolecular electron transfer to the BL-based LUMO. Bimetallic complexes $[(phen)_2Ru(tatpp)Ru(phen)_2]^{4+}$ and $[(phen)_2Ru(tatpq)Ru(phen)_2]^{4+}$ (tatpp = 9,11,20,22-tetraazatetrapyrido[3,2-*a*:2′3′-*c*:3″,2″-1:2‴,3‴-*n*]pentacene; tatpq =

9,11,20,22-tetraazatetrapyrido[3,2-*a*:2′3′-*c*:3′′,2′′-1:2′′′,3′′′-*n*]pentacene-10,21-quinone) were also reported as PECs. When irradiated with visible light in the presence of TEA electron donor, electron collection occurred at the large, planar BLs, with two electrons stored on the complex with a tatpp BL and up to four electrons stored on the complex with a tatpq BL.[54-55] Complex $[(bpy)_2Ru(pbn)]^{2+}$ (pbn = 2-(2-pyridyl)benzo[*b*]-1,5-napthyridine) collected multiple electrons on the pbn π* ligand system. Modeled after the NAD^+/NADH (NAD = nicotinamide adenine dinucleotide) redox mediator important in a variety of biological systems, the Ru monometallic complex was reported to undergo proton-coupled electron transfer in the presence of a sacrificial reductant whereby protonation maintained the charge of the complex following the collection of two electrons on the pbn ligand to produce $[(bpy)_2Ru(pbnHH)]^{2+}$.[52-53, 57]

The study of ligand-centered PECs led to the design of systems capable of collecting multiple electrons at metal-based centers important for H_2 photocatalysis. Complex $[\{(bpy)_2Ru(dpp)\}_2RhCl_2]^{5+}$ was the first PEC for the photocatalytic reduction of H_2O to H_2 fuel (**Figure 1.17**).[58-59]

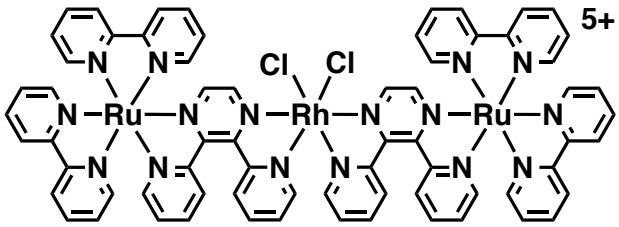

Figure 1.17. The first reported photoinitated electron collector for the reduction of H_2O to H_2 fuel, $[\{(bpy)_2Ru(dpp)\}_2RhCl_2]^{5+}$. bpy = 2,2′-bipyridine; dpp = 2,3-bis(2-pyridyl)pyrazine.

Two Ru^{II} chromophores were covalently linked though dpp BLs to a catalytically active Rh^{III} *cis*-dichloro center. In the presence of DMA sacrificial electron donor,

$[\{(bpy)_2Ru(dpp)\}_2Rh^{III}Cl_2]^{5+}$ underwent photointiated electron collection at Rh to produce the two-electron reduced species $[\{(bpy)_2Ru(dpp)\}_2Rh^{I}]^{5+}$.[59] Unlike the first PEC $[\{(bpy)_2Ru(dpb)\}_2IrCl_2]^{5+}$ that possessed a ligand-based LUMO, $[\{(bpy)_2Ru(dpp)\}_2RhCl_2]^{5+}$ possessed a metal-based LUMO at Rh to facilitate metal-based multi-electron collection. The octahedral, six-coordinate Rh^{III} loses two chlorides to produce the four-coordinate, square planar Rh^{I} species that was proposed as the catalytically active form for H_2 production. Notably, the Ru,Rh,Ru trimetallic complex remained intact even following the conformational changes associated with photoinitiated electron collection and halide loss, allowing the active catalyst to cycle from $Rh^{III/II/I}$ to achieve H_2 evolution in the presence of H_2O in organic solvent under visible light irradiation.[58] The Ru,Rh,Ru trimetallic complex produced 22 TON (6.0 μmol of H_2) following 2 h photolysis at λ = 470 nm in CH_3CN solvent with DMA ED H_2 (TON = mol of H_2 produced/mol of catalyst).[60-61] This early Ru,Rh,Ru PEC supports the significance of careful component selection to properly tune the molecular electronics to achieve catalytically active supramolecular complexes.

1.9. Supramolecular Complexes for Solar H_2 Production

Obtaining an understanding of the interactions between the LA(s), the electron relay BL(s), and the catalytically active metal center is critical for the development of photocatalysts for solar energy conversion. Supramolecular H_2 photocatalysts often contain two or more metal centers that must perform specific tasks, such as light absorption or electron collection, to achieve an overall goal such as H_2 production.[60, 62-66] While the focus of this dissertation is on systems containing Ru LAs and Rh catalytic

centers, supramolecular complexes containing different reactive metal centers are also reported to serve as PECs for H_2 photocatalysis.

1.9.1. Photocatalysts using Pd, Pt, or Co as the Reactive Metal Center

Multimetallic supramolecular complexes containing Pd, Pt, or Co reactive metal centers are active photocatalysts for H_2 evolution.[62-66]

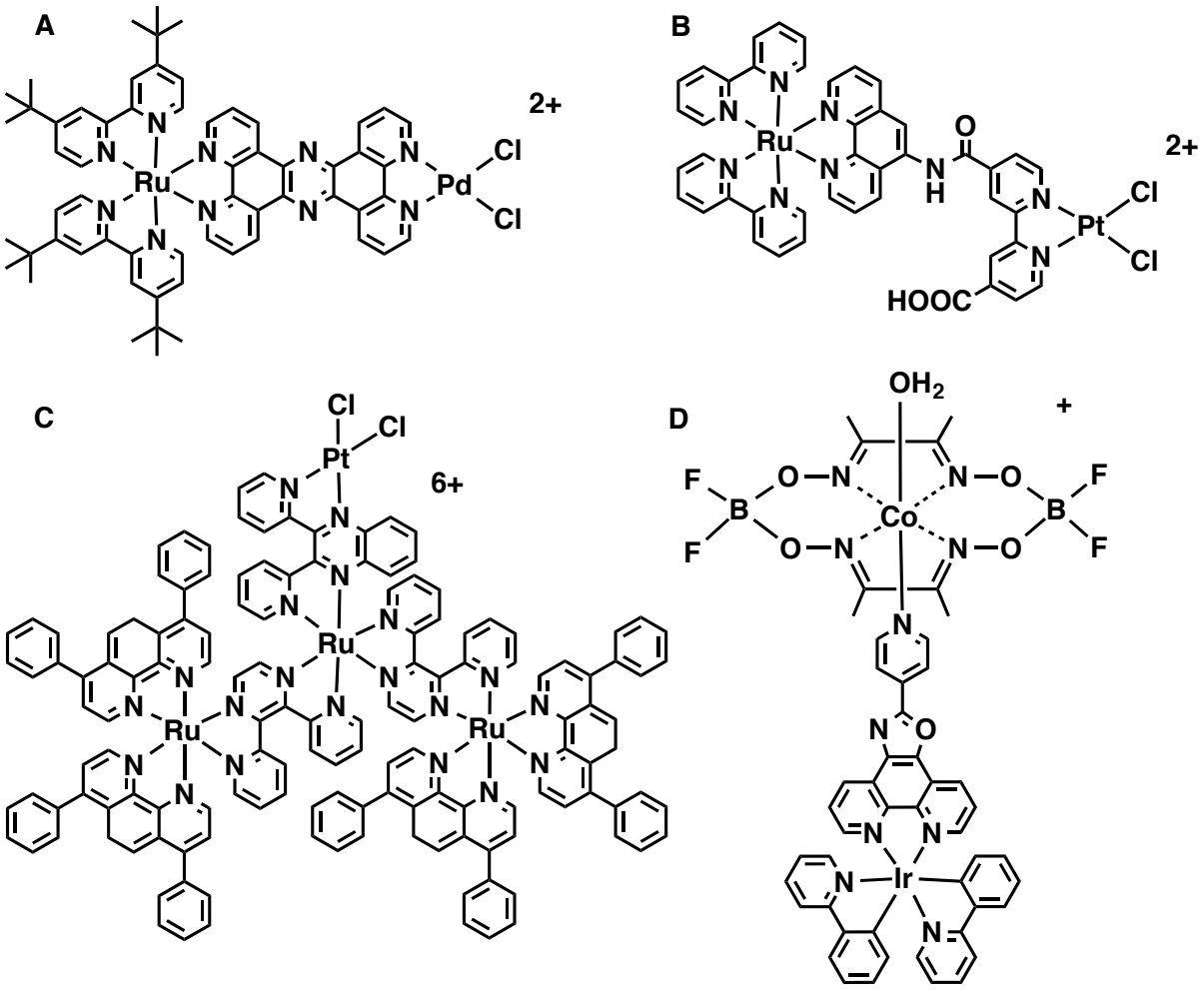

Figure 1.18. Structures of supramolecular photocatalysts for H_2 production. (**A**) $[Ru(^tBu_2bpy)_2(tpphz)PdCl_2]^{2+}$; (**B**) $[Ru(bpy)_2(phen\text{-}NHCO\text{-}bpy)PtCl_2]^{2+}$; (**C**) $[\{(Ph_2phen)_2Ru(dpp)\}_2Ru(dpq)PtCl_2]^{6+}$; (**D**) $[(ppy)_2Ir(L\text{-}pyr)Co(dmgBF_2)_2(OH_2)]^{+}$. $^tBu_2bpy$ = 4,4′-di-*tert*-butyl-2,2′-bipyridine; tpphz = tetrapyrido[3,2-a:2′,3′-c:3″,2″-h:2‴,3‴-j]phenazine; bpy = 2,2′-bipyridine; phen = 1,10-phenanthroline; Ph_2phen = 4,7-diphenyl-1,10-phenanthroline; dpp = 2,3-bis(2-pyridyl)pyrazine; dpq = 2,3-bis(2-pyridyl)quinoxaline; ppy = 2-phenylpyridine; L-pyr = (4-pyridine)oxazolo[4,5-f]phenanthroline; $dmgBF_2$ = (difluoroboryl)dimethylglyoximate.

Complex $[Ru(^tBu_2bpy)_2(tpphz)PdCl_2]^{2+}$ (tpphz = tetrapyrido[3,2-a:2′,3′-c:3″,2″-h:2‴,3‴-j]phenazine) (**Figure 1.18A**), with a Ru LA bound through a tpphz BL to a Pd reactive metal center, performed as a photocatalyst for H_2 production.[65] Upon irradiation with visible light (λ = 470 nm) in the presence of TEA sacrificial reductant in CH_3CN solvent,

the Ru,Pd bimetallic complex produced 56 TON. Complex $[Ru(bpy)_2(phen\text{-}NHCO\text{-}bpy)PtCl_2]^{2+}$ (**Figure 1.18B**) functioned as a H_2 production photocatalyst employing a Ru^{II} LA bound though a BL to a Pt^{II} catalyst.[63, 66] The supramolecule produced H_2 fuel from H_2O when irradiated with visible light ($390 < \lambda < 490$ nm) using ethylenediaminetetraacetic acid (EDTA) as a sacrificial reductant in acetate buffer solution, achieving 4.8 TON (2.4 μmol of H_2) following 10 h photolysis. Interestingly, no H_2 evolution was observed when the photocatalytic experiment was performed using Ru and Pt complexes as separate components, providing evidence for the benefits of using covalently bound components to achieve H_2O reduction. Complex $[\{(Ph_2phen)_2Ru(dpp)\}_2Ru(dpq)PtCl_2]^{6+}$ (dpq = 2,3-bis(2-pyridyl)quinoxaline) (**Figure 1.18C**) covalently coupled three Ru^{II} LA subunits to a Pt^{II} reactive metal center for the photocatalytic production of H_2 fuel from H_2O. The tetrametallic complex produced 94 TON (21 μmol of H_2) following 10 h photolysis with visible light (λ = 470 nm) in the presence of DMA sacrificial reductant in CH_3CN solvent.[62] Complex $[(ppy)_2Ir(L\text{-}pyr)Co(dmgBF_2)_2(OH_2)]^{+}$ (ppy = 2-phenylpyridine; L-pyr = (4-pyridine)oxazolo[4,5-f]phenanthroline; $dmgBF_2$ = (difluoroboryl)dimethylglyoximate) (**Figure 1.18D**) coupled a cyclometalated Ir LA to a Co-based reactive metal center. The bimetallic Ir,Co complex produced 210 TON following 15 h photolysis ($\lambda > 380$ nm) in a TEA/acetone solvent mixture.[64] The achievement of H_2 photocatalysis using complexes containing Pd, Pt, or Co reactive metal centers provides useful insight about component choice for catalyst design.

1.9.2. Photocatalysts using Rh as the Reactive Metal Center

Component variation within architectures possessing Rh as the reactive metal center affords an understanding of the long-term stability of Rh-based photocatalysts for H_2 evolution. TL variation within the original $[\{(bpy)_2Ru(dpp)\}_2RhCl_2]^{5+}$ architecture produces trimetallic complexes $[\{(TL)_2Ru(dpp)\}_2RhCl_2]^{5+}$ (TL = phen or Ph_2phen) that are reported as active photocatalysts for H_2 fuel production (**Figure 1.19A**).[60, 67] The TL = Ph_2phen complex is a superior H_2 photocatalyst (150 TON; 44 μmol of H_2; 20 h photolysis) in CH_3CN solvent using DMA sacrificial reductant when photolyzed with visible light (λ = 470 nm) relative to the TL = phen analogue (20 TON; 5.4 μmol of H_2; 2 h photolysis), and the increase in catalytic activity for the Ph_2phen species was attributed to several factors, notably an enhanced excited state lifetime (52 ns for Ph_2phen; 35 ns for phen) and greater steric bulk about the Rh center for the complex with bulkier Ph_2phen ligands.[67] Complex $[\{(bpy)_2Ru(L1)\}_2RhCl_2]^{5+}$ (L1 = 1,2-bis[4-(4′-methyl-2,2′-bipyridinyl)ethane) (**Figure 1.19B**) used a similar molecular architecture to earlier Ru,Rh,Ru supramolecular photocatalysts, but a non-conjugated BL was used to link the two Ru LA subunits to the Rh reactive metal center. The complex served as a photocatalyst for H_2 evolution in aqueous solution employing ascorbate buffer as the sacrificial reductant, producing 430 TON following 12 h photolysis with visible light (λ = 400-700 nm).[68] The steric bulk of the two Ru-polypyridyl LA subunits on either side of the Rh moiety likely serve to protect the reactive metal center from interfering ions that may prevent photocatalytic H_2 production.

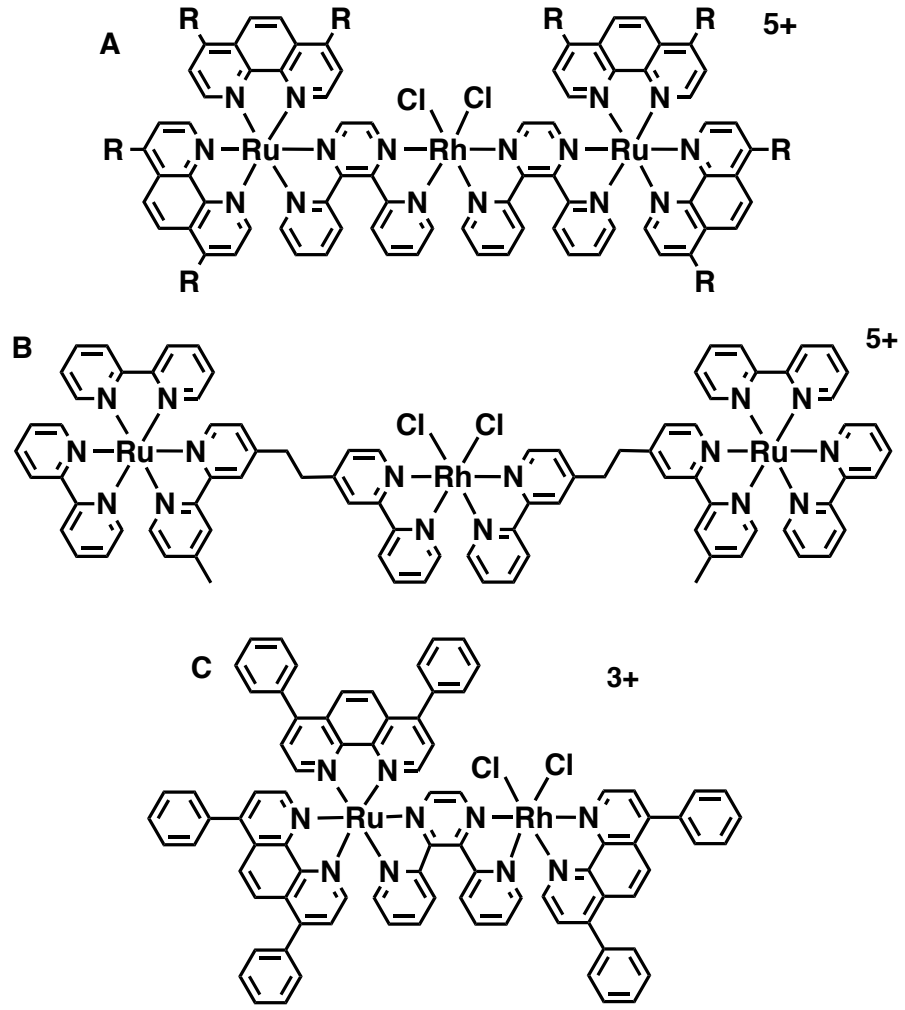

Figure 1.19. Structures of supramolecular photocatalysts for H_2 production that use Rh reactive metal centers. (**A**) $[\{(phen)_2Ru(dpp)\}_2RhCl_2]^{5+}$ for R = H; $[\{(Ph_2phen)_2Ru(dpp)\}_2RhCl_2]^{5+}$ for R = phenyl; (**B**) $[\{(bpy)_2Ru(L1)\}_2RhCl_2]^{5+}$; (**C**) $[(Ph_2phen)_2Ru(dpp)RhCl_2(Ph_2phen)]^{3+}$. dpp = 2,3-bis(2-pyridyl)pyrazine; phen = 1,10-phenanthroline; Ph_2phen = 4,7-diphenyl-1,10-phenanthroline; bpy = 2,2-bipyridine; L1 = 1,2-bis[4-(4′-methyl-2,2′-bipyridinyl)ethane.

When the number of Ru LA subunits in the trimetallic architecture was decreased from two to one, Ru,Rh bimetallic architectures of the form $[(TL)_2Ru(dpp)RhCl_2(TL')]^{3+}$ (TL = Ru terminal ligands; TL′ = Rh terminal ligand) resulted. Complex $[(phen)_2Ru(dpp)RhCl_2(bpy)]^{3+}$ achieved photoinitiated electron collection at Rh; however, the lack of steric protection around the Rh center facilitated formation of Rh^{I}-

Rh^{I} dimers upon PEC, inhibiting interaction of the H_2O substrate with the catalytically active metal center and resulting in no detectable H_2 production.[51] Complex $[(bpy)_2Ru(dpp)RhCl_2(^tBu_2bpy)]^{3+}$ was synthesized in an attempt to increase the steric protection around Rh by using a bulkier polypyridyl ligand at Rh (TL′ = $^tBu_2bpy$). However, this complex showed no H_2 production because electron collection occurred at lowest-lying dpp BL-based π* orbitals rather than at Rh.[69] The electron-donating nature of the $^tBu_2bpy$ TL′ destabilized the Rh-based acceptor orbitals, which afforded a dpp BL-based LUMO. The appropriate steric and electronic requirements for H_2 photocatalysis were realized with complex $[(Ph_2phen)_2Ru(dpp)RhCl_2(Ph_2phen)]^{3+}$ (**Figure 1.19C**).[69] The bulky TL′ = Ph_2phen provided the necessary steric protection for the catalytically active Rh center, and the relatively electron-withdrawing nature of Ph_2phen provided for a Rh(dσ*)-based LUMO and permitted multi-electon collection at Rh. The bimetallic complex produced 70 TON (0.48 mL of H_2) following 20 h of visible light (λ = 470) photolysis in CH_3CN solvent using DMA ED. Relative to the trimetallic analogue $[\{(Ph_2phen)_2Ru(dpp)\}_2RhCl_2]^{5+}$, bimetallic complex $[(Ph_2phen)_2Ru(dpp)RhCl_2(Ph_2phen)]^{3+}$ bearing one Ru LA produced roughly half the amount of H2 (70 TON vs. 150 TON), which correlated with the complex being absorbing about half as much light in the visible region. Active photocatalysis by a Ru,Rh bimetallic complex provided a simplified structural motif that allows a closer examination of Rh-based supramolecular photocatalysts for H_2 production.

1.9.3. Impact of Labile Ligand Selection at the Reactive Metal Center

TL and BL variations in supramolecular photocatalysts for H_2 production modulate the molecular orbital energetics and influence the electrochemical, photophysical, and photochemical properties that ultimately govern photocatalytic reactivity. Further variation of the ligands coordinated to the reactive metal center, often halides, also tunes the reactivity of the supramolecular motif. Halide variation in complexes $[\{(bpy)_2Ru(dpp)\}_2RhX_2]^{5+}$ (X = Cl^- or Br^-) provided for photocatalysts capable of H_2 evolution from H_2O.[60, 70] Upon photoinitiated electron collection at Rh in the presence of a sacrificial reductant to produce $[\{(bpy)_2Ru(dpp)\}_2Rh^{I}]^{5+}$, two halides were lost to form the square planar complex proposed as the active catalyst species (**Figure 1.20** for X = Br^-).[60] Interestingly, the X = Br^- species outperformed the X = Cl^- analogue as a H_2 production photocatalyst (38 TON for X = Br^-; 30 TON for X = Cl^-) when photolyzed for 4 h with visible light (λ = 470 nm) in CH_3CN solvent in the presence of DMA ED.[70]

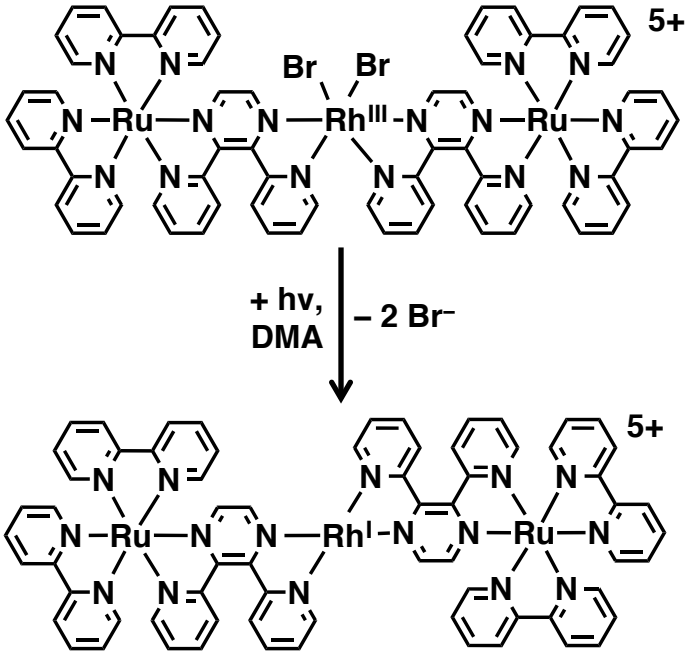

Figure 1.20. Photoinitiated electron collection for complex $[\{(bpy)_2Ru(dpp)\}_2RhBr_2]^{5+}$ to produce complex $[\{(bpy)_2Ru(dpp)\}_2Rh^{I}]^{5+}$ that is proposed as the active photocatalyst form for H_2 production from H_2O. bpy = 2,2′-bipyridine; dpp = 2,3-bis(2-pyridyl)pyrazine; hv = photoexcitation; DMA = *N*,*N*-dimethylaniline (sacrificial electron donor).

A similar increase in H_2 production by Br^- compared to Cl^- analogues of $[\{(TL)_2Ru(dpp)\}_2RhX_2]^{5+}$ (TL = phen or Ph_2phen) was also observed when the complex was photolyzed with λ = 470 nm light in a CH_3CN/DMA solvent system (TL = phen (2 h): 24 TON for X = Br^-; 20 TON for X = Cl^- and TL = Ph_2phen (20 h): 200 TON for X = Br^-; 150 TON for X = Cl^-).[61, 67] The identity of the halides coordinated to Rh impacted the observed H_2 production, despite halide loss to generate the catalytically active species. Electrochemistry results established that the halide identity modulated the electronics at the Rh center by shifting the potential of the $Rh^{III/II/I}$ reduction to a less negative potential for the complexes containing less σ-donating Br^- halides compared to Cl^-, consistent with results observed for the Rh monometallic complexes $[Rh(bpy)_2X_2]^+$ (X = Cl^- or Br^-).[35, 38, 60-61, 67] Earlier studies postulated that the leaving ability of the halide may

account for differences in observed H_2 photocatalysis. Furthermore, slight differences in the excited state properties upon halide variation in the $[\{(TL)_2Ru(dpp)\}_2RhX_2]^{5+}$ motifs led to different rate values of intramolecular electron transfer (k_{et}) to populate the lowest-lying excited state responsible for active photocatalysis, a value also proposed to account for discrepancies in H_2 production.[60, 67] While electrochemical and photophysical results provide a plausible argument for enhanced photocatalytic abilities for Ru,Rh,Ru photocatalysts bearing Br^- halides, this series of complexes would benefit from an in-depth analysis of the role of the labile halide ligands during photocatalytic H_2 production from H_2O.

The identity of the ligands coordinated to the reactive metal center also impacted H_2 evolution in a photocatalyst architecture with a Pt reactive metal center. Complexes $[Ru(^tBu_2bpy)_2(tpphz)PtX_2]^{2+}$ (X = I^- or Cl^-) were studied for their ability to photochemically reduce H_2O to H_2, and the I^- species produced nearly 40 times the amount of H_2 as the Cl^- analogue (276 TON for X = I^-; 7 TON for X = Cl^-).[71] Both experiments were carried out in CH_3CN solvent with TEA sacrificial reductant under visible light irradiation (λ = 470 nm) for 45 h. Unlike the Rh photocatalysts where the halides dissociated upon photoinitiated electron collection, the halides at Pt were found to remain coordinated during catalysis. In fact, excess I^- or Cl^- was added to the respective photocatalyst bearing that halide, and no change in H_2 production was observed, unlike the Ru,Rh,Ru systems where HCl addition inhibited catalysis.[58] After observing no noticeable differences in photophysical properties upon halide variation in the $[Ru(^tBu_2bpy)_2(tpphz)PtX_2]^{2+}$ system, the differences in electron density for the

complex bearing I^- versus Cl^- halides were used to describe the differences in H_2 production. Ligand variation at the reactive metal center in photocatalysts capable of H_2 evolution from H_2O is relatively unexplored and provides a means to optimize solar fuel production schemes.

1.10. Project Description

The purpose of the research is to obtain a better understanding of the photochemical reduction of H_2O to H_2 fuel employing Ru^{II},Rh^{III} bimetallic and trimetallic supramolecular photocatalysts. Notably, this research focuses on the impact of the identity of the labile ligands coordinated to the catalytically active Rh center. The new bimetallic photocatalyst $[(Ph_2phen)_2Ru(dpp)RhBr_2(Ph_2phen)]^{3+}$ is examined relative to established complex $[(Ph_2phen)_2Ru(dpp)RhCl_2(Ph_2phen)]^{3+}$ to gain an understanding of the electrochemical, photophysical, and photochemical properties upon halide variation in this architecture. As halide variation was shown to impact H_2 photocatalysis in Ru,Rh,Ru architectures, variation of the ligands at Rh in Ru,Rh bimetallic complexes and the resulting impact on photocatalysis is unexplored. To better understand the role of the halide ligands coordinated to Rh, synthesizing a photocatalyst bearing ligands other than halides at the Rh reaction metal center could provide important insight. Therefore, new trimetallic complex $[\{(bpy)_2Ru(dpp)\}_2Rh(OH)_2]^{5+}$ is prepared for analysis relative to halide analogues $[\{(bpy)_2Ru(dpp)\}_2RhX_2]^{5+}$ (X = Cl^- or Br^-). Removing the halides from the system with the hydroxo trimetallic complex affords an ideal system to explore the impact of the labile halides during H_2 photocatalysis. Systematic component

variation provides an excellent forum to gain insight on the importance of judicious ligand selection for the design for superior H_2O reduction photocatalysts (**Figure 1.21**).

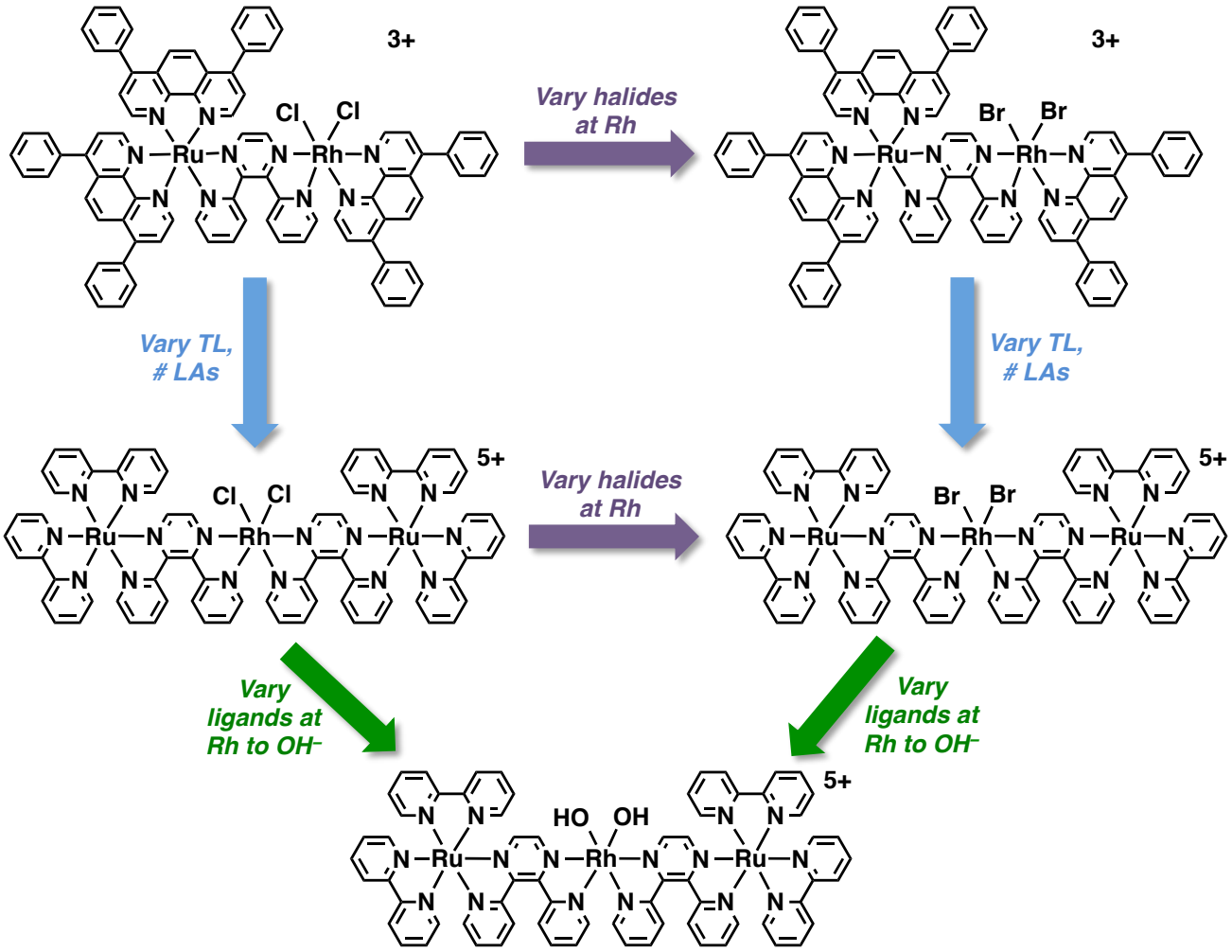

Figure 1.21. Component variation in Ru(II),Rh(III) supramolecular bimetallic and trimetallic architectures. TL = terminal ligand, LA = light absorber.

1.11. References

1. Balzani, V.; Credi, A.; Venturi, M., "Photochemical conversion of solar energy." *ChemSusChem* **2008,** *1* (1-2), 26-58.
2. Berardi, S.; Drouet, S.; Francas, L.; Gimbert-Surinach, C.; Guttentag, M.; Richmond, C.; Stoll, T.; Llobet, A., "Molecular artificial photosynthesis." *Chemical Society Reviews* **2014,** *43* (22), 7501-7519.
3. Blankenship, R. E.; Tiede, D. M.; Barber, J.; Brudvig, G. W.; Fleming, G.; Ghirardi, M.; Gunner, M. R.; Junge, W.; Kramer, D. M.; Melis, A.; Moore, T. A.; Moser,

C. C.; Nocera, D. G.; Nozik, A. J.; Ort, D. R.; Parson, W. W.; Prince, R. C.; Sayre, R. T., "Comparing Photosynthetic and Photovoltaic Efficiencies and Recognizing the Potential for Improvement." *Science* **2011,** *332* (6031), 805-809.
4. Barber, J., "Photosynthetic energy conversion: natural and artificial." *Chemical Society Reviews* **2009,** *38* (1), 185-196.
5. National Renewable Energy Laboratory. "Reference Solar Spectral Irradiance: ASTM G-173." http://rredc.nrel.gov/solar/spectra/am1.5/ASTMG173/ASTMG173.html.
6. Lewis, N. S.; Crabtree, G. *Basic Research Needs for Solar Energy Utilization*; Washington, D.C., 2005.
7. Hammarstrom, L., "Accumulative Charge Separation for Solar Fuels Production: Coupling Light-Induced Single Electron Transfer to Multielectron Catalysis." *Accounts of Chemical Research* **2015,** *48* (3), 840-850.
8. Kirch, M.; Lehn, J. M.; Sauvage, J. P., "Hydrogen generation by visible-light irradiation of aqueous-solutions of metal-complexes - approach to the photo-chemical conversion and storage of solar-energy " *Helvetica Chimica Acta* **1979,** *62* (4), 1345-1384.
9. Meyer, G. J., "Antenna molecule drives solar hydrogen generation." *Proceedings of the National Academy of Sciences* **2015,** *112* (30), 9146-9147.
10. McDaniel, N. D.; Bernhard, S., "Solar fuels: thermodynamics, candidates, tactics, and figures of merit." *Dalton Transactions* **2010,** *39* (42), 10021-10030.
11. Bard, A. J.; Fox, M. A., "Artificial photosynthesis: Solar splitting of water to hydrogen and oxygen." *Accounts of Chemical Research* **1995,** *28* (3), 141-145.
12. Neudeck, S.; Maji, S.; Lopez, I.; Meyer, S.; Meyer, F.; Llobet, A., "New Powerful and Oxidatively Rugged Dinuclear Ru Water Oxidation Catalyst: Control of Mechanistic Pathways by Tailored Ligand Design." *Journal of the American Chemical Society* **2014,** *136* (1), 24-27.
13. Chen, Z. F.; Concepcion, J. J.; Song, N.; Meyer, T. J., "Chloride-assisted catalytic water oxidation." *Chemical Communications* **2014,** *50* (59), 8053-8056.
14. Duan, L. L.; Bozoglian, F.; Mandal, S.; Stewart, B.; Privalov, T.; Llobet, A.; Sun, L. C., "A molecular ruthenium catalyst with water-oxidation activity comparable to that of photosystem II." *Nature Chemistry* **2012,** *4* (5), 418-423.
15. Soman, S., "Molecular Systems for Solar H_2: Path to a Renewable Future." *Comments on Inorganic Chemistry* **2015,** *35* (2), 82-120.
16. Lehn, J. M.; Sauvage, J. P., "Chemical storage of light energy - catalytic generation of hydrogen by visible light or sunlight - irradiation of neutral aqueous-solutions " *Nouveau Journal De Chimie-New Journal of Chemistry* **1977,** *1* (6), 449-451.
17. Chan, S. F.; Chou, M.; Creutz, C.; Matsubara, T.; Sutin, N., "Mechanism of the formation of dihydrogen from the photoinduced reactions of poly(pyridine)ruthenium(II) and poly(pyridine)rhodium(III) complexes " *Journal of the American Chemical Society* **1981,** *103* (2), 369-379.
18. Brown, G. M.; Chan, S. F.; Creutz, C.; Schwarz, H. A.; Sutin, N., "Mechanism of the formation of dihydrogen from the photoinduced reactions of tris(bipyridine)ruthenium(II) and tris(bipyridine)rhodium(III)." *Journal of the American Chemical Society* **1979,** *101* (25), 7638-7640.

19. Shan, B.; Baine, T.; Ma, X. A. N.; Zhao, X.; Schmehl, R. H., "Mechanistic Details for Cobalt Catalyzed Photochemical Hydrogen Production in Aqueous Solution: Efficiencies of the Photochemical and Non-Photochemical Steps." *Inorganic Chemistry* **2013,** *52* (9), 4853-4859.
20. Deponti, E.; Luisa, A.; Natali, M.; Iengo, E.; Scandola, F., "Photoinduced hydrogen evolution by a pentapyridine cobalt complex: elucidating some mechanistic aspects." *Dalton Transactions* **2014,** *43* (43), 16345-16353.
21. Das, A.; Han, Z.; Brennessel, W. W.; Holland, P. L.; Eisenberg, R., "Nickel Complexes for Robust Light-Driven and Electrocatalytic Hydrogen Production from Water." *ACS Catalysis* **2015,** *5* (3), 1397-1406.
22. Balzani, V.; Moggi, L.; Scandola, F., Towards a Supramolecular Photochemistry: Assembly of Molecular Components to Obtain Photochemical Molecular Devices. In *Supramolecular Photochemistry*, Balzani, V., Ed. NATO ASI Series 214, Reidel, Dordrecht: The Netherlands: 1987; pp 1-28.
23. Balzani, V.; Juris, A.; Venturi, M.; Campagna, S.; Serroni, S., "Luminescent and redox-active polynuclear transition metal complexes." *Chemical Reviews* **1996,** *96* (2), 759-833.
24. Balzani, V.; Bergamini, G.; Campagna, S.; Puntoriero, F., Photochemistry and photophysics of coordination compounds: Overview and general concepts. In *Photochemistry and Photophysics of Coordination Compounds I*, Balzani, V.; Campagna, S., Eds. 2007; Vol. 280, pp 1-36.
25. Elvington, M.; Brewer, K. J., Electrochemistry. In *Applications of Physical Methods to Inorganic and Bioiniorganic Chemistry*, Scott, R. A.; Lukehart, C. M., Eds. John Wiley & Sons: 2007; pp 17-38.
26. Gennett, T.; Milner, D. F.; Weaver, M. J., "Role of solvent reorganization dynamics in electron-transfer processes. Theory-experiment comparisons for electrochemical and homogeneous electron exchange involving metallocene redox couples." *Journal of Physical Chemistry* **1985,** *89* (13), 2787-2794.
27. Thompson, D. W.; Ito, A.; Meyer, T. J., "[Ru (bpy) 3] 2+* and other remarkable metal-to-ligand charge transfer (MLCT) excited states." *Pure and Applied Chemistry* **2013,** *85* (7), 1257-1305.
28. Kalyanasundaram, K., "Photophysics, photochemistry and solar energy conversion with tris(bipyridyl)ruthenium(II) and its analogues." *Coordination Chemistry Reviews* **1982,** *46*, 159-244.
29. Van Houten, J.; Watts, R., "Photochemistry of tris (2, 2'-bipyridyl) ruthenium (II) in aqueous solutions." *Inorganic Chemistry* **1978,** *17* (12), 3381-3385.
30. Kawanishi, Y.; Kitamura, N.; Tazuke, S., "Dependence of spectroscopic, electrochemical, and excited-state properties of tris chelate ruthenium(II) complexes on ligand structure " *Inorganic Chemistry* **1989,** *28* (15), 2968-2975.
31. Mongelli, M. T.; Brewer, K. J., "Synthesis and study of the light absorbing, redox and photophysical properties of Ru(II) and Os(II) complexes of 4,7-diphenyl-1,10-phenanthroline containing the polyazine bridging ligand 2,3-bis(2-pyridyl)pyrazine." *Inorganic Chemistry Communications* **2006,** *9* (9), 877-881.

32. Higgins, S. L. H.; White, T. A.; Winkel, B. S. J.; Brewer, K. J., "Redox, spectroscopic, and photophysical properties of Ru-Pt mixed-metal complexes incorporating 4,7-diphenyl-1,10-phenanthroline as efficient DNA binding and photocleaving agents." *Inorganic Chemistry* **2011,** *50* (2), 463-470.
33. Wallace, A. W.; Murphy, W. R.; Petersen, J. D., "Electrochemical and photophysical properties of monometallic and bimetallic ruthenium(II) complexes " *Inorganica Chimica Acta* **1989,** *166* (1), 47-54.
34. Braunstein, C. H.; Baker, A. D.; Strekas, T. C.; Gafney, H. D., "Spectroscopic and electrochemical properties of the dimer tetrakis(2,2'-bipyridine)(μ-2,3-bis(2-pyridyl)pyrazine)diruthenium(II) and its monomeric analog." *Inorganic Chemistry* **1984,** *23* (7), 857-864.
35. Bolinger, C. M.; Story, N.; Sullivan, B. P.; Meyer, T. J., "Electrocatalytic reduction of carbon dioxide by 2,2'-bipyridine complexes of rhodium and iridium." *Inorganic Chemistry* **1988,** *27* (25), 4582-4587.
36. Kew, G.; DeArmond, K.; Hanck, K., "Electrochemistry of rhodium-dipyridyl complexes." *Journal of Physical Chemistry* **1974,** *78* (7), 727-734.
37. Kew, G.; Hanck, K.; Dearmond, K., "Voltammetry of rhodium-1,10-phenanthroline complexes." *Journal of Physical Chemistry* **1975,** *79* (17), 1828-1835.
38. Rasmussen, S. C.; Richter, M. M.; Yi, E.; Place, H.; Brewer, K. J., "Synthesis and characterization of a series of novel rhodium and iridium complexes containing polypyridyl bridging ligands: potential uses in the development of multimetal catalysts for carbon dioxide reduction." *Inorganic Chemistry* **1990,** *29* (20), 3926-3932.
39. Amarante, D.; Cherian, C.; Ernmel, C.; Chen, H. Y.; Dayal, S.; Koshy, M.; Megehee, E. G., "Improved synthetic routes to rhodium bipyridine complexes: Comparison of microwave vs. conventional synthesis." *Inorganica Chimica Acta* **2005,** *358* (7), 2231-2238.
40. Kalyanasundaram, K., *Photochemistry of Polypyridine and Porphyrin Complexes*. Academic Press: London, 1992.
41. Roundhill, D. M., *Photochemistry and Photophysics of Metal Complexes*. Plenum Press: New York City, 1994.
42. Wagenknecht, P. S.; Ford, P. C., "Metal centered ligand field excited states: their roles in the design and performance of transition metal based photochemical molecular devices." *Coordination Chemistry Reviews* **2011,** *255* (5), 591-616.
43. Meyer, T. J., "Chemical approaches to artificial photosynthesis." *Accounts of Chemical Research* **1989,** *22* (5), 163-170.
44. Durham, B.; Caspar, J. V.; Nagle, J. K.; Meyer, T. J., "Photochemistry of $Ru(bpy)_3^{2+}$." *Journal of the American Chemical Society* **1982,** *104* (18), 4803-4810.
45. Lin, C. T.; Bottcher, W.; Chou, M.; Creutz, C.; Sutin, N., "Mechanism of quenching of emission of substituted polypyridineruthenium(II) complexes by iron(III), chromium(III), and europium(III) ions." *Journal of the American Chemical Society* **1976,** *98* (21), 6536-6544.
46. Kalyanasundaram, K.; Nazeeruddin, M. K., "Photophysics and photoredox reactions of ligand-bridged binuclear polypyridyl complexes of ruthenium(II) and of their monomeric analogs " *Inorganic Chemistry* **1990,** *29* (10), 1888-1897.

47. Denti, G.; Campagna, S.; Sabatino, L.; Serrni, S.; Ciano, M.; Balzani, V., "Luminescent and redox-reactive building blocks for the design of photochemical molecular devices: Mono-, di-, tri-, and tetranuclear ruthenium(II) polypyridine complexes." *Inorganic Chemistry* **1990,** *29* (23), 4750-4758.
48. Alford, P. C.; Cook, M. J.; Lewis, A. P.; McAuliffe, G. S. G.; Skarda, V.; Thomson, A. J.; Glasper, J. L.; Robbins, D. J., "Luminescent metal complexes. Part 5. Luminescent properties of ring-substituted 1,10-phenanthroline tris-complexes of ruthenium(II)." *Journal of the Chemical Society-Perkin Transactions 2* **1985,** (5), 705-709.
49. DeArmond, M. K.; Hillis, J. E., "Luminescence of transition metal d^6 chelates." *The Journal of Chemical Physics* **1971,** *54* (3), 2247-2253.
50. Schulz, M.; Karnahl, M.; Schwalbe, M.; Vos, J. G., "The role of the bridging ligand in photocatalytic supramolecular assemblies for the reduction of protons and carbon dioxide." *Coordination Chemistry Reviews* **2012,** *256* (15-16), 1682-1705.
51. Wang, J.; White, T. A.; Arachchige, S. M.; Brewer, K. J., "A new structural motif for photoinitiated electron collection: Ru,Rh bimetallics providing insight into H_2 production via photocatalysis of water reduction by Ru,Rh,Ru supramolecules." *Chemical Communications* **2011,** *47* (15), 4451-4453.
52. Fukushima, T.; Fujita, E.; Muckerman, J. T.; Polyansky, D. E.; Wada, T.; Tanaka, K., "Photochemical Stereospecific Hydrogenation of a Ru Complex with an NAD(+)/NADH-Type Ligand." *Inorganic Chemistry* **2009,** *48* (24), 11510-11512.
53. Polyansky, D. E.; Cabelli, D.; Muckerman, J. T.; Fukushima, T.; Tanaka, K.; Fujita, E., "Mechanism of hydride donor generation using a Ru(II) complex containing an NAD(+) model ligand: Pulse and steady-state radiolysis studies." *Inorganic Chemistry* **2008,** *47* (10), 3958-3968.
54. Konduri, R.; Ye, H. W.; MacDonnell, F. M.; Serroni, S.; Campagna, S.; Rajeshwar, K., "Ruthenium photocatalysts capable of reversibly storing up to four electrons in a single acceptor ligand: A step closer to artificial photosynthesis." *Angewandte Chemie-International Edition* **2002,** *41* (17), 3185-3187.
55. Kim, M. J.; Konduri, R.; Ye, H. W.; MacDonnell, F. M.; Puntoriero, F.; Serroni, S.; Campagna, S.; Holder, T.; Kinsel, G.; Rajeshwar, K., "Dinuclear ruthenium(II) polypyridyl complexes containing large, redox-active, aromatic bridging ligands: Synthesis, characterization, and intramolecular quenching of MLCT excited states." *Inorganic Chemistry* **2002,** *41* (9), 2471-2476.
56. Molnar, S. M.; Nallas, G.; Bridgewater, J. S.; Brewer, K. J., "Photoinitiated electron collection in a mixed-metal trimetallic complex of the form $[\{(bpy)_2Ru(dpb)\}_2IrCl_2](PF_6)_5$ (bpy = 2,2'-bipyridine and dpb = 2,3-bis(2-pyridyl)benzoquinoxaline)." *Journal of the American Chemical Society* **1994,** *116* (12), 5206-5210.
57. Polyansky, D.; Cabelli, D.; Muckerman, J. T.; Fujita, E.; Koizumi, T.; Fukushima, T.; Wada, T.; Tanaka, K., "Photochemical and radiolytic production of an organic hydride donor with a Ru-II complex containing an NAD(+) model ligand." *Angewandte Chemie-International Edition* **2007,** *46* (22), 4169-4172.

58. Elvington, M.; Brown, J.; Arachchige, S. M.; Brewer, K. J., "Photocatalytic hydrogen production from water employing a Ru, Rh, Ru molecular device for photoinitiated electron collection." *Journal of the American Chemical Society* **2007,** *129* (35), 10644-10645.
59. Elvington, M.; Brewer, K. J., "Photoinitiated electron collection at a metal in a rhodium-centered mixed-metal supramolecular complex." *Inorganic Chemistry* **2006,** *45* (14), 5242-5244.
60. Arachchige, S. M.; Brown, J. R.; Chang, E.; Jain, A.; Zigler, D. F.; Rangan, K.; Brewer, K. J., "Design considerations for a system for photocatalytic hydrogen production from water employing mixed-metal photochemical molecular devices for photoinitiated electron collection." *Inorganic Chemistry* **2009,** *48* (5), 1989-2000.
61. White, T. A.; Rangan, K.; Brewer, K. J., "Synthesis, characterization, and study of the photophysics and photocatalytic properties of the photoinitiated electron collector $[\{(phen)_2Ru(dpp)\}_2RhBr_2](PF_6)_5$." *Journal of Photochemistry and Photobiology A: Chemistry* **2010,** *209* (2-3), 203-209.
62. Knoll, J. D.; Higgins, S. H.; White, T. A.; Brewer, K. J., "Subunit Variation to Uncover Properties of Polyazine-Bridged Ru(II), Pt(II) Supramolecules with Low Lying Charge Separated States Providing Insight into the Functioning as H_2O Reduction Photocatalysts to Produce H_2." *Inorganic Chemistry* **2013,** *52* (17), 9749-9760.
63. Ozawa, H.; Sakai, K., "Photo-hydrogen-evolving molecular devices driving visible-light-induced water reduction into molecular hydrogen: structure-activity relationship and reaction mechanism." *Chemical Communications* **2011,** *47* (8), 2227-2242.
64. Fihri, A.; Artero, V.; Pereira, A.; Fontecave, M., "Efficient H_2-producing photocatalytic systems based on cyclometalated iridium- and tricarbonylrhenium-diimine photosensitizers and cobaloxime catalysts." *Dalton Transactions* **2008,** (41), 5567-5569.
65. Rau, S.; Schafer, B.; Gleich, D.; Anders, E.; Rudolph, M.; Friedrich, M.; Gorls, H.; Henry, W.; Vos, J. G., "A supramolecular photocatalyst for the production of hydrogen and the selective hydrogenation of tolane." *Angewandte Chemie-International Edition* **2006,** *45* (37), 6215-6218.
66. Ozawa, H.; Haga, M. A.; Sakai, K., "A photo-hydrogen-evolving molecular device driving visible-light-induced EDTA-reduction of water into molecular hydrogen." *Journal of the American Chemical Society* **2006,** *128* (15), 4926-4927.
67. White, T. A.; Higgins, S. L. H.; Arachchige, S. M.; Brewer, K. J., "Efficient photocatalytic hydrogen production in a single-component system using Ru,Rh,Ru supramolecules containing 4,7-diphenyl-1,10-phenanthroline." *Angewandte Chemie-International Edition* **2011,** *50*, 12209-12213.
68. Stoll, T.; Gennari, M.; Fortage, J.; Castillo, C. E.; Rebarz, M.; Sliwa, M.; Poizat, O.; Odobel, F.; Deronzier, A.; Collomb, M.-N., "An Efficient Ru^{II}-Rh^{III}-Ru^{II} Polypyridyl Photocatalyst for Visible-Light-Driven Hydrogen Production in Aqueous Solution." *Angewandte Chemie-International Edition* **2014,** *53* (6), 1654-1658.
69. White, T. A.; Whitaker, B. N.; Brewer, K. J., "Discovering the balance of steric and electronic factors needed to provide a new structural motif for photocatalytic

hydrogen production from water." *Journal of the American Chemical Society* **2011,** *133* (39), 15332-15334.
70. Arachchige, S. M.; Brown, J.; Brewer, K. J., "Photochemical hydrogen production from water using the new photocatalyst [{$(bpy)_2Ru(dpp)$}$_2RhBr_2$]$(PF_6)_5$." *Journal of Photochemistry and Photobiology A: Chemistry* **2008,** *197* (1), 13-17.
71. Pfeffer, M. G.; Kowacs, T.; Wachtler, M.; Guthmuller, J.; Dietzek, B.; Vos, J. G.; Rau, S., "Optimization of Hydrogen-Evolving Photochemical Molecular Devices." *Angewandte Chemie-International Edition* **2015,** *54* (22), 6627-6631.

2. Mechanistic Insight into the Electronic Influences Imposed by Substituent Variation in Polyazine-Bridged Ruthenium(II)/Rhodium(III) Supramolecules

Reprinted with permission from "White, T. A.; Mallalieu, H. E.; Wang, J.; Brewer, K. J. *Chemistry – A European Journal* **2014**, *20*, 8265–8268." *Copyright 2015, John Wiley and Sons.*

2.1. Abstract

Unusual and unprecedented multipathway electrochemical mechanisms for a new class of supramolecular Ru,Rh bimetallic photocatalysts have been uncovered. The near isoenergetic Rh(dσ*) and bridging ligand(π*) molecular orbitals and a rate of halide loss that occurs on the cyclic voltammetry timescale provide a series of closely related complexes which display four different electrochemical mechanisms. A single complex displays two concurrent electrochemical pathways in marked contrast to all previously studied cis-$Rh(NN)_2X_2$ motifs.

2.2. Introduction

Converting solar energy into a viable, alternative fuel source is of considerable interest to minimize fossil fuel consumption.[1-2] Requirements for an artificial photosynthetic system are efficient light absorption, population of a highly oxidizing and reducing excited state, fast charge separation to generate a molecular potential gradient, electron and hole collecting reservoirs, and redox-active catalysts.[3-5] H_2O reduction to produce H_2 fuel requires electron collection for multielectron reduction.[6-8]

Catalytically active, Rh-containing complexes for electrochemical and photochemical water reduction are reported.[9-13] Often, the synthesized Rh^{III} acts as an

electron reservoir undergoing two successive, one-electron reductions to produce a coordinatively unsaturated Rh^{I} center that produces H_2 from H_2O.[11, 14-18]

The electrochemical properties of Rh systems provide insight into the chemical identity and stability of redox states. *cis*-$[Rh(NN)_2X_2]^+$ complexes (NN = bidentate polypyridyl ligand; X = halide) have been studied with ligand selection modulating redox properties and orbital energetics.[19-23] DeArmond *et al*. reported electrochemistry of *cis*-$[Rh^{III}(NN)_2Cl_2]^+$ complexes (NN = 2,2′-bipyridine (bpy) or 1,10-phenanthroline (phen)) where Rh undergoes two successive, one-electron reductions, appearing as a single $Rh^{III/II/I}$ couple in cyclic voltammetry (CV). The $Rh^{III/II}$ reduction promotes fast halide loss, followed by $Rh^{II/I}$ reduction and a second halide loss resulting in an ECEC mechanism (E = electrochemical or C = chemical step).[19-20]

The impact of halide and ligand variation was subsequently reported for $[Rh(NN)_2X_2]^+$ systems. The variation of X from Cl^- to Br^- to I^- provides a positive shift in the $Rh^{III/II/I}$ reduction consistent with weaker σ-donating character of I^- vs. Br^- vs. Cl^-.[23] Stabilization of Rh(dσ*) orbitals is achieved by variation of NN, 2,3-bis(2-pyridyl)pyrazine (dpp), 2,3-bis(2-pyridyl)quinoxaline (dpq), 2,3-bis(2-pyridyl)benzoquinoxaline (dpb), or 4,4′-Di-*tert*-butyl-2,2′-bipyridine (*t*Bu_2bpy).[21-22, 24] The ability of Rh to undergo two successive, one-electron reductions promoted its use as an electron collector for photocatalysis.[11, 25]

Coupling two Ru^{II} light absorbers to a Rh^{III} reactive metal affords Ru,Rh,Ru complexes, $[\{(TL)_2Ru(dpp)\}_2RhX_2]^{5+}$ (TL = terminal ligand = bpy, phen, Ph_2phen (4,7-diphenyl-1,10-phenanthroline); X = Cl^-, Br^-), that possess Rh(dσ*)-based LUMOs

(lowest unoccupied molecular orbitals), allowing photoinitiated electron collection (PEC) at Rh and their use as hydrogen photocatalysts.[11, 14-17] The mechanism proposes that a doubly reduced, coordinatively unsaturated Rh^{I} species, $[\{(TL)_2Ru(dpp)\}_2Rh^{I}]^{5+}$, is formed by excited state reductive quenching through an intermediate Rh^{II} species.

Coupling a single Ru^{II} light absorber to *cis*-$Rh^{III}Cl_2$ affords Ru^{II},Rh^{III} bimetallics, $[(TL)_2Ru(BL)RhCl_2(TL')]^{3+}$. The choice of bridging ligand (BL) and TL coordinated to Rh is critical to control orbital energetics.[18, 26-27] These bimetallic complexes display rich, unprecedented redox chemistry that is explored and described herein. The $[(TL)_2Ru(BL)RhX_2(TL')]^{3+}$ systems allow modulation of orbital energetics, providing systems that undergo PEC at Rh and closely related systems that do not due to BL-based LUMOs.[18, 27] In addition, systems that undergo PEC are not always photocatalysts as sterically accesible Rh^{I} sites dimerize, seen with $[(phen)_2Ru(dpp)Rh^{I}(bpy)]^{3+}$.[27]

Herein we report a detailed electrochemical study conducted to gain mechanistic insight into photocatalysis of H_2O reduction to H_2 employing a new series of bimetallic complexes, $[(Ph_2phen)_2Ru(dpp)RhCl_2(t\text{Bu}_2bpy)]^{3+}$, $[(Ph_2phen)_2Ru(dpp)RhCl_2(Ph_2phen)]^{3+}$, and $[(Ph_2phen)_2Ru(dpp)RhBr_2(Ph_2phen)]^{3+}$. The nearly isoenergetic dpp(π*) and Rh(dσ*) molecular orbitals are modulated by TL′ and X variation to better understand the redox properties of Ru,Rh systems which display the unusual phenomenon of orbital inversion upon minor structural variation. In marked contrast to the many reported systems containing *cis*-$[Rh^{III}(NN)_2X_2]^{+}$, the title Ru,Rh

bimetallics each display two simultaneous electrochemical pathways with a total of four mechanisms needed to describe the redox chemistry of this new series of complexes.

2.3. Results and Discussion

The Ru^{II},Rh^{III} bimetallic complexes were synthesized by using a building block approach and are efficient light absorbers, **Figure 2.1**.[18, 26-28]

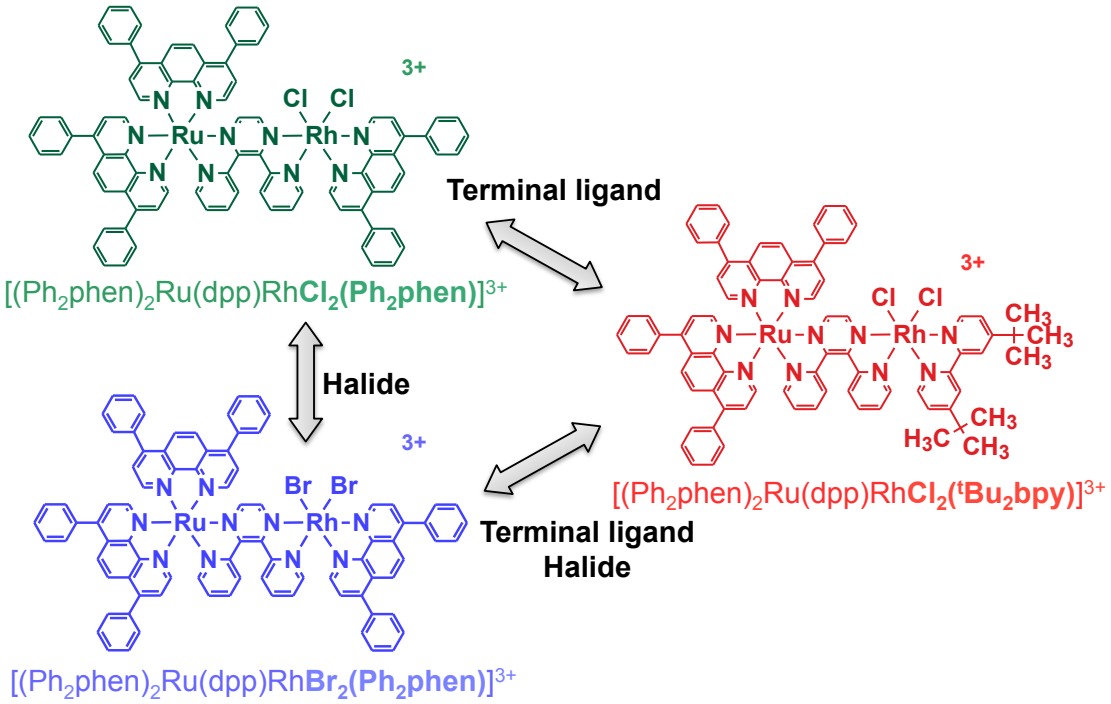

Figure 2.1. Structures of Ru(II),Rh(III) bimetallic supramolecular complexes.

The electronic absorption spectrum for $[(Ph_2phen)_2Ru(dpp)RhX_2(TL')]^{3+}$ is dominated by intense π→π* intraligand (IL) transitions in the UV and Ru(dπ)→ligand(π*) metal-to-ligand charge transfer (MLCT) transitions in the visible with the lowest energy absorption at 514 nm assigned to the Ru(dπ)→dpp(π*) ^{1}MLCT transition. Photoexcitation results in unity population of the weakly emissive ($\Phi^{em} \sim 10^{-4}$), low energy (λ^{em} = 770 nm) Ru(dπ)→dpp(π*) ^{3}MLCT excited state. Intramolecular electron transfer to populate a low-lying Ru(dπ)→Rh(dσ*) ^{3}MMCT excited state quenches the

observed emission and shortens the excited state lifetime (τ^{em} = 45 ns) when compared to the Ru^{II},Ru^{II} homobimetallic model, $[(Ph_2phen)_2Ru(dpp)Ru(Ph_2phen)_2]^{4+}$ ($\Phi^{em} = 1.7 \times 10^{-3}$; λ^{em} = 754 nm; τ^{em} = 192 ns).[17]

The unique and complicated electrochemistry of Ru^{II},Rh^{III} bimetallics provides insight into the frontier orbital energetics critical to understanding the photochemistry of these single-component, H_2O reduction photocatalysts. Anodic scans of $[(Ph_2phen)_2Ru(dpp)RhCl_2(tBu_2bpy)]^{3+}$, $[(Ph_2phen)_2Ru(dpp)RhCl_2(Ph_2phen)]^{3+}$, and $[(Ph_2phen)_2Ru(dpp)RhBr_2(Ph_2phen)]^{3+}$ exhibit a reversible, one-electron $Ru^{II/III}$ oxidation at +1.59 V vs. Ag/AgCl, **Table 2.S1**. Cathodic scans (25–1000 mVs^{-1}) reveal the complex nature of the reductive processes localized on (μ-dpp)$Rh^{III}X_2$(TL′). Current varies as a function of scan rate due to a chemical reaction occurring on the CV timescale, *n* = 1–2 for the first and *n* = 0–1 for the second reduction. This is further complicated by varied Rh(dσ*)- or dpp(π*)-based LUMOs. TL′ variation in $[(Ph_2phen)_2Ru(dpp)RhCl_2(TL')]^{3+}$ (where TL′ = tBu_2bpy or Ph_2phen) does not significantly affect the potential of the first reductive couple ($E_{½}$ = –0.37 V vs. Ag/AgCl for both TL′). Reversibility of the first couple is dependent on TL′ identity, **Figure 2.2**. For TL′ = tBu_2bpy, i_p^a/i_p^c (i_p^a = anodic peak current; i_p^c = cathodic peak current) for the first reduction is independent of scan rate, a largely reversible electrochemical step on the CV timescale. This is indicative of a $(dpp^{0/-})Rh^{III}Cl_2$ first reduction.

$[(Ph_2phen)_2Ru(dpp)RhCl_2(Ph_2phen)]^{3+}$ displays unique non-integer currents for the first and second reductions that result from a chemical reaction occurring on the CV timescale and a near coincident reduction potential of the $RhCl_2^{III/II}$ and $RhCl^{II/I}$ couples.

i_p^a/i_p^c for the first reduction of $[(Ph_2phen)_2Ru(dpp)RhCl_2(Ph_2phen)]^{3+}$ is scan rate dependent, ranging from 0.4–0.7 at 25–1000 mVs^{-1}. This is indicative of Rh reduction followed by halide loss occurring on the CV timescale.[15-17, 19-20, 22, 25] Changing TL′ from *t*Bu_2bpy to Ph_2phen provides orbital inversion with a dpp(π*) or Rh(dσ*)-based LUMO, respectively.

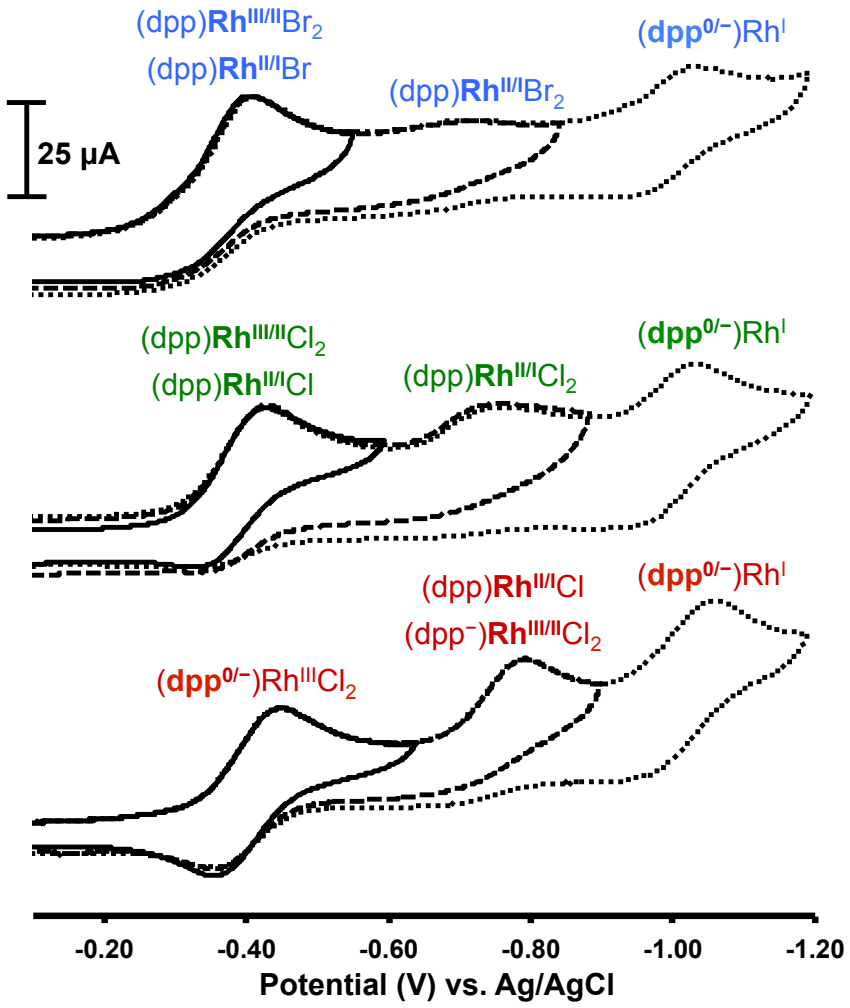

Figure 2.2. Cyclic voltammograms of 1 mM $[(Ph_2phen)_2Ru(dpp)RhBr_2(Ph_2phen)]^{3+}$ (top), $[(Ph_2phen)_2Ru(dpp)RhCl_2(Ph_2phen)]^{3+}$ (middle), and $[(Ph_2phen)_2Ru(dpp)RhCl_2(tBu_2bpy)]^{3+}$ (bottom) under Ar in 0.1 M Bu_4NPF_6 in CH_3CN at RT with a scan rate of 100 mVs^{-1}.

The second reduction (E_p^c = –0.76 V vs. Ag/AgCl (labeled $i_p^c{}_{(II)}$)) is irreversible for both TL′ = *t*Bu$_2$bpy and Ph$_2$phen, indicating a Rh-based reduction followed by a fast chemical reaction step on the CV timescale (EC). The peak current varies with scan rate and TL′ identity with $i_p^c{}_{(II)}/i_p^c{}_{(I)}$ ranging from 0.8–1.0 for *t*Bu$_2$bpy and 0.2–0.8 for Ph$_2$phen, **Figure 2.3B**. The third reductive couple ($E_{½}$ = –0.96 V vs. Ag/AgCl) has $i_p^a{}_{(III)}/i_p^c{}_{(III)}$ ~ 1 regardless of TL′, consistent with a dpp$^{0/-}$ reduction. Following three reductions, all complexes reach [(Ph$_2$phen)$_2$Ru(dpp$^-$)Rh^{I}(TL′)]$^{2+}$.

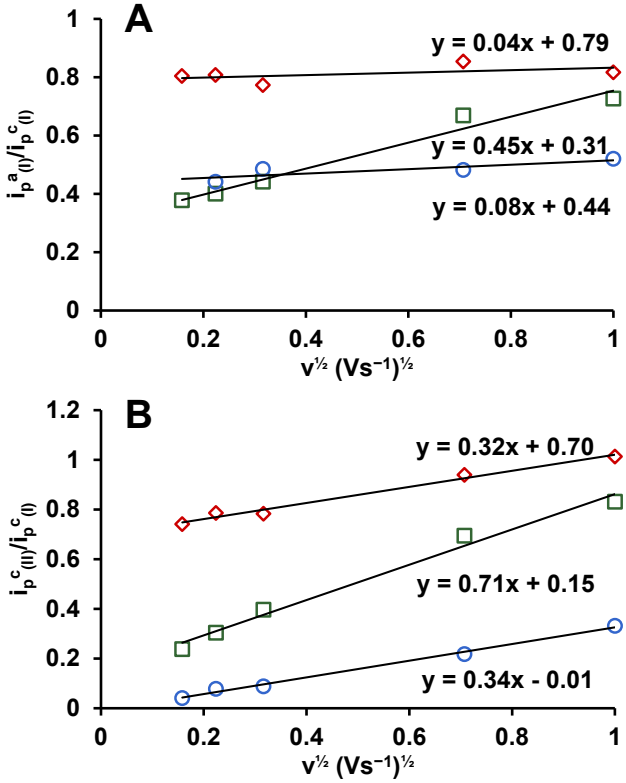

Figure 2.3. Plots displaying (**A**) $i_p^a{}_{(I)}/i_p^c{}_{(I)}$ vs. $v^{½}$ and (**B**) $i_p^c{}_{(II)}/i_p^c{}_{(I)}$ vs. $v^{½}$ for 1 mM [(Ph$_2$phen)$_2$Ru(dpp)RhBr$_2$(Ph$_2$phen)]$^{3+}$ (blue circles), [(Ph$_2$phen)$_2$Ru(dpp)RhCl$_2$(Ph$_2$phen)]$^{3+}$ (green squares), and [(Ph$_2$phen)$_2$Ru(dpp)RhCl$_2$(*t*Bu$_2$bpy)]$^{3+}$ (red diamonds) measured under an Ar atmosphere using 0.1 M Bu$_4$NPF$_6$ in CH$_3$CN at RT.

Four mechanisms are required to account for the electrochemical properties of the [(TL)$_2$Ru(dpp)RhX$_2$(TL′)]$^{3+}$ complexes, **Figure 2.4**.

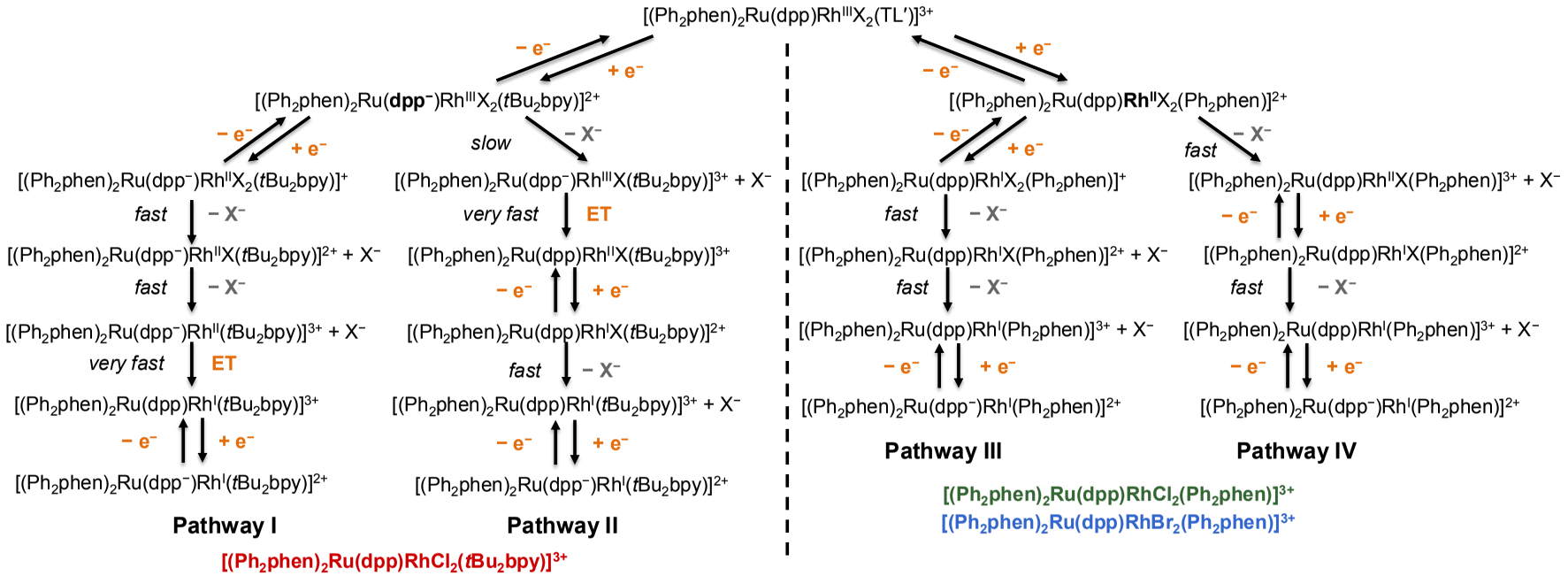

Figure 2.4. Proposed electrochemical mechanisms depicting various pathways possible upon reduction of the Ru^{II},Rh^{III} bimetallic complexes. $[(Ph_2phen)_2Ru(dpp)Rh^{III}X_2(TL')]^{3+}$ represents the synthesized state. Electrochemical steps are colored orange and chemical steps are colored gray.

This complicated electrochemistry is quite unusual and is unprecedented for such a series of closely related complexes and in distinct contrast to the ECEC mechanism of all other reported *cis*-$[Rh^{III}(NN)_2X_2]^+$ motifs. $[(Ph_2phen)_2Ru(dpp)RhX_2(TL')]^{3+}$ with TL′ = *t*Bu_2bpy or Ph_2phen and X = Cl^- or Br^- display first reductions that are $dpp^{0/-}$-based for *t*Bu_2bpy or $Rh^{III/II}$-based for Ph_2phen, differentiating Pathways I and II from III and IV. The TL′ = Ph_2phen systems display a chemical reaction, halide loss, that follows the $Rh^{III/II}$ couple. Fast halide loss leads to Pathway IV and slow halide loss allows $Rh^{II/I}$ reductions of the species with two halides bound, $Rh^{II/I}X_2$ (Pathway III). Intermediate rates of halide loss result in the observed electrochemistry simultaneously displaying Pathways III and IV.

The electrochemical mechanisms displayed by $[(Ph_2phen)_2Ru(dpp)RhX_2(tBu_2bpy)]^{3+}$ are Pathways I and II, unique mechanisms for Rh^{III} complexes, **Figure 2.4**. The first reduction is dpp(π*)-based. Interestingly, halide loss occurs upon dpp reduction due to the increased electron density at Rh, making the metal a weaker Lewis acid. Halide loss upon ligand reduction is unprecedented in Rh chemistry but reported by Kubiak *et al.* for $[Re^{I}(tBu_2bpy)(CO)_3Cl]$.[24] Halide loss promoted by dpp reduction is followed by electron transfer to the now more electron deficient $(dpp^-)Rh^{III}Cl$ site resulting in $(dpp)Rh^{II}Cl$ (Pathway II). Pathway II is coincident with Pathway I for the fraction of complex that does not undergo halide loss prior to the second reduction, which undergoes a $(dpp^-)Rh^{III/II}Cl_2$ reduction. The $(dpp^-)Rh^{II}X_2$ species undergoes rapid halide loss followed by intramolecular electron transfer and

dpp reduction to generate $[(Ph_2phen)_2Ru(dpp^-)Rh^I(tBu_2bpy)]^{3+}$, the same species formed through Pathway II.

Further exploration of this unusual redox chemistry is provided by variation of the halide coordinated to Rh. $[(Ph_2phen)_2Ru(dpp)RhBr_2(Ph_2phen)]^{3+}$ was postulated to display a faster chemical reaction following the first reductive couple than the chloride analogue. A study of $i_p{}^a{}_{(I)}/i_p{}^c{}_{(I)}$ showed a ratio of 0.4–0.5, consistent with the hypothesis that Br^- would be lost at a faster rate than Cl^-, **Figure 2.3A**, consistent with the weaker σ-donating ability of Br^- relative to Cl^-.

The observed electrochemistry for $[(Ph_2phen)_2Ru(dpp)RhX_2(TL')]^{3+}$ systems displays multiple electrochemical pathways, evidenced by peak currents consistent with n = 1–2 for the first reductive couple and n = 0–1 for the second couple as well as non-integer $i_p{}^c{}_{(II)}/i_p{}^c{}_{(I)}$ ratios for TL′ = tBu$_2$bpy or Ph$_2$phen, **Figure 2.4**. The electrochemical properties demonstrate that the one-electron reduced TL′ = tBu$_2$bpy complex possesses greater chemical stability than the analogous TL′ = Ph$_2$phen species, $(dpp^-)Rh^{III}Cl_2$ vs. $(dpp)Rh^{II}X_2$, **Figures 2.S2–S4**. Orbital energetics are modulated by component variation on *cis*-$Rh^{III}X_2(TL')$, one of the design properties of this bimetallic motif. The close proximity of the dpp(π*)- and Rh(dσ*)-based orbitals provides for complicated electrochemistry with two mechanistic pathways being simultaneously operative for any bimetallic studied and four mechanisms needed to describe the series of complexes. Complexes with Rh-based LUMOs are proposed as more active photocatalysts for the reduction of H_2O to H_2; therefore, the TL' = Ph$_2$phen bimetallics are predicted to outperform the TL' = tBu$_2$bpy bimetallic due to more efficient electron collection at Rh.

Gaining a greater understanding of the electrochemical pathways involved in the reduction of Rh^{III} to Rh^{I} allows deliberate design of suitable proton reduction photocatalysts. The unusual redox chemistry for Ru,Rh bimetallics highlights the complexity of possible pathways operative in the photochemical reduction of H_2O to H_2 by these Ru,Rh systems as in the presence of H_2O, additional species are possible for each Rh^{II} or Rh^{I} species observed herein due to protonation of the Rh center or possible oxidative addition of H_2O to the Rh^{I} center. Research in our laboratory is ongoing to better understand the intermediates and mechanisms involved throughout the photocatalytic cycle for reduction of H_2O to H_2 by these Ru(II),Rh(III) bimetallic supramolecules.

2.4. Acknowledgements

Acknowledgement is made to the Chemical Sciences, Geosciences and Biosciences Division, Office of Basic Energy Sciences, Office of Sciences, U.S. Department of Energy DE FG02-05ER15751 for the generous financial support of this research. Special thanks is given to Dr. Shamindri Arachchige for assistance with this manuscript.

2.5. Supplemental Information

2.5.1. Experimental Procedures

2.5.1.1. Materials

All chemicals were used as received unless otherwise stated. Electrochemical analysis grade (≥ 99.0%) tetrabutylammonium hexafluorophosphate (Bu_4NPF_6) was purchased from Fluka. Spectral grade acetonitrile was purchased from Burdick and

Jackson and distilled over calcium hydride. The bimetallic complexes $[(Ph_2phen)_2Ru(dpp)RhCl_2(Ph_2phen)](PF_6)_3$,[18] $[(Ph_2phen)_2Ru(dpp)RhBr_2(Ph_2phen)](PF_6)_3$,[28] and $[(Ph_2phen)_2Ru(dpp)RhCl_2(tBu_2bpy)](PF_6)_3$ [29] were synthesized as previously reported.

2.5.1.2. Synthesis of $[(Ph_2phen)_2Ru(dpp)RhCl_2(^tBu_2bpy)](PF_6)_3$

The Ru,Rh bimetallic was synthesized using a building block approach.[29] The Ru(II) monometallic $[(Ph_2phen)_2Ru(dpp)]^{2+}$ (0.20 g, 0.15 mmol) and Rh(III) monometallic $[RhCl_3(tBu_2bpy)(CH_3OH)]$ (0.12 g, 0.23 mmol) were dissolved separately in a 2:1 EtOH:H_2O (10 mL) solvent system. The dark orange Ru monometallic was added drop-wise to the Rh monometallic and heated at reflux for 1 h. The dark maroon solution was cooled to RT and added drop-wise to a NH_4PF_6 (aq) solution (1.0 g, 75 mL) to induce precipitation. The precipitate was filtered, washed with H_2O (60 mL), and washed with diethyl ether (150 mL). Purification was achieved using Sephadex® LH-20 size exclusion chromatography with a 2:1 EtOH:CH_3CN mobile phase. The dark maroon band was collected, rotary evaporated, and precipitated using CH_3CN and diethyl ether to yield a dark maroon product (0.075 g, 0.040 mmol, yield = 30%) (+)ESI-MS: $[M–PF_6]^+$, *m/z* = 1733.22.

2.5.1.3. Electrochemistry

Electrochemical studies were performed using a Bioanalytical System (BAS) Epsilon potentiostat with a single-cell, three-electrode configuration. For cyclic voltammetry, the system contained a glassy carbon disk working electrode, Pt wire auxiliary electrode, and Ag wire pseudo-reference electrode which was measured vs.

Ag/AgCl using ferrocene as an internal standard ($Fe(C_5H_5)_2^{0/+}$ = 0.46 V vs. Ag/AgCl 3 M NaCl).[30] The scan rate was varied between 25 and 1000 mVs^{-1} for cyclic voltammetric analyses.

2.5.2. Supplemental Figures and Tables

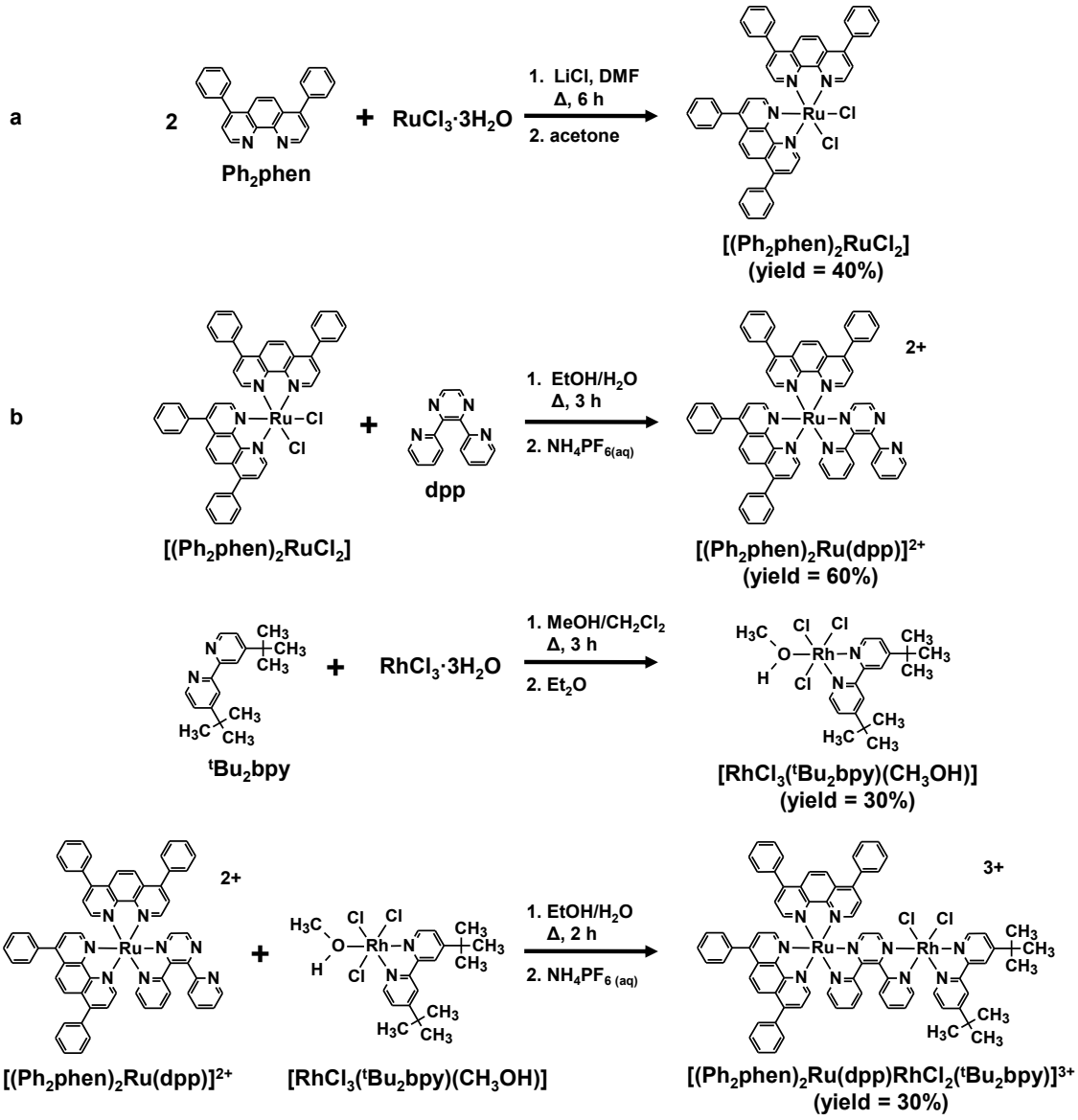

Figure 2.S1. Scheme showing the synthesis of $[(Ph_2phen)_2Ru(dpp)RhCl_2(tBu_2bpy)](PF_6)_3$ using the building block approach. [a] Reference 31. [b] Reference 32.

Table 2.S1. Electrochemical Properties of Ru,Rh Bimetallics and Related Complexes

complex [a]	$E_{½}$ (V)	ΔE_p (mV)	i_p^a/i_p^c	assignment
$[(Ph_2phen)_2Ru(dpp)]^{2+}$ [e]	+1.41	70	0.9	$Ru^{II/III}$
	–0.98	70	0.9	$dpp^{0/-}$
$[\{(Ph_2phen)_2Ru\}_2(dpp)]^{4+}$ [f]	+1.64	80	1.0	$Ru^{II/III}$
	+1.45	75	1.0	$Ru^{II/III}$
	–0.61	70	0.9	$dpp^{0/-}$
	–1.11	70	0.9	$dpp^{-/2-}$
$[\{(Ph_2phen)_2Ru(dpp)\}_2RhCl_2]^{5+}$ [f]	+1.59	130	0.9	2 $Ru^{II/III}$
	–0.35[b]	--	--	$Rh^{III/II/I}$
	–0.74	120	0.9	$dpp^{0/-}$
	–0.98	110	0.9	$dpp^{0/-}$
$[(Ph_2phen)_2Ru(dpp)RhCl_2(Ph_2phen)]^{3+}$	+1.59	85	0.8	$Ru^{II/III}$
	–0.37[c]	70	0.4	$Rh^{III/II}Cl_2$,$Rh^{II/I}Cl$
	–0.77[d]	--	--	$Rh^{II/I}Cl_2$
	–0.96	100	0.8	$dpp^{0/-}$
$[(Ph_2phen)_2Ru(dpp)RhBr_2(Ph_2phen)]^{3+}$	+1.59	90	0.9	$Ru^{II/III}$
	–0.38[c]	120	0.4	$Rh^{III/II}Br_2$,$Rh^{II/I}Br$
	–0.73[d]	--	--	$Rh^{II/I}Br_2$
	–0.98	100	0.8	$dpp^{0/-}$
$[(Ph_2phen)_2Ru(dpp)RhCl_2(t Bu_2bpy)]^{3+}$	+1.59	85	0.8	$Ru^{II/III}$
	–0.37	75	0.8	$dpp^{0/-}$
	–0.76[d]	--	--	$(dpp^-)Rh^{III/II}Cl_2$,$(dpp)Rh^{II/I}Cl$
	–0.96	110	0.8	$dpp^{0/-}$

[a] Measured using Ag wire pseudo-reference electrode and converted to Ag/AgCl using ferrocene as an internal standard ($Fe(C_5H_5)_2^{0/+}$ = 0.46 V vs. Ag/AgCl). Measurements were performed at a scan rate of 100 mVs^{-1} using deoxygenated 0.1 M Bu_4NPF_6 electrolyte in distilled CH_3CN at RT. Ph_2phen = 4,7-diphenyl-1,10-phenanthroline; $t Bu_2bpy$ = 4,4'-Di-*tert*-butyl-2,2'-bipyridine; dpp = 2,3-bis(2-pyridyl)pyrazine.

[b] E_p^c of two overlapping, one-electron irreversible processes.

[c] $E_{½}$ of quasi-reversible process.

[d] E_p^c of irreversible process.

[e] From reference 32-33.

[f] From reference 17.

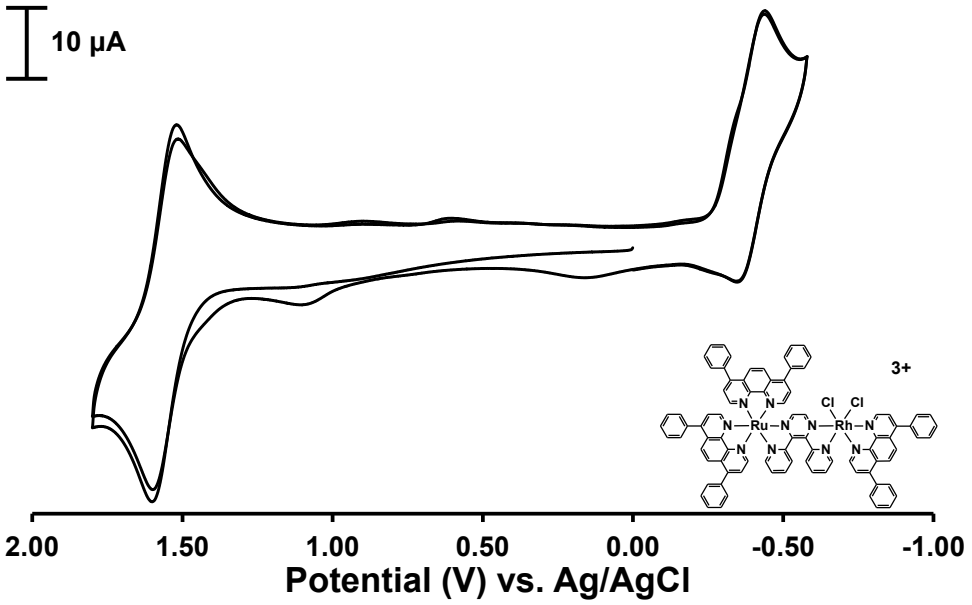

Figure 2.S2. Cyclic voltammogram of $[(Ph_2phen)_2Ru(dpp)RhCl_2(Ph_2phen)]^{3+}$ with a second oxidative scan following the first reduction under an Ar atmosphere in 0.1 M Bu_4NPF_6 acetonitrile solution at RT with a scan rate of 100 mV/s.

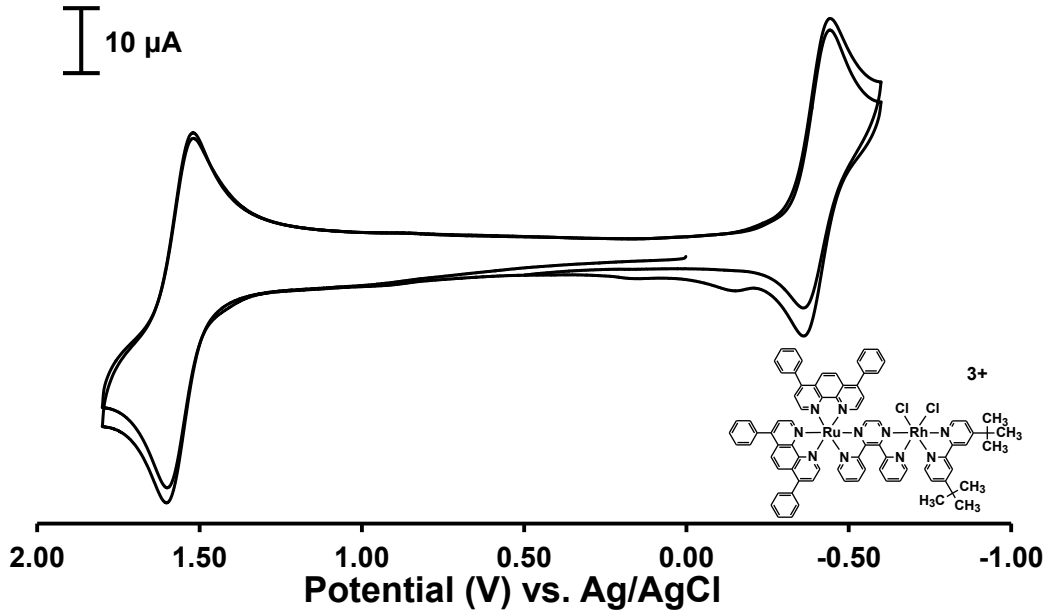

Figure 2.S3. Cyclic voltammogram of $[(Ph_2phen)_2Ru(dpp)RhCl_2(^tBu_2bpy)]^{3+}$ with a second oxidative scan following the first reduction under an Ar atmosphere in 0.1 M Bu_4NPF_6 acetonitrile solution at RT with a scan rate of 100 mV/s.

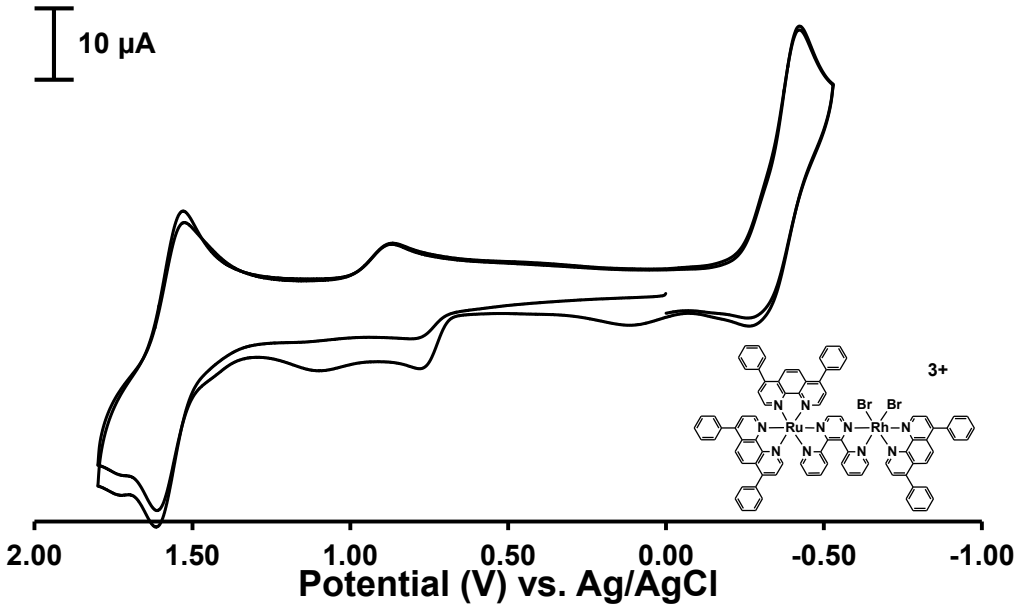

Figure 2.S4. Cyclic voltammogram of $[(Ph_2phen)_2Ru(dpp)RhBr_2(Ph_2phen)]^{3+}$ with an oxidative scan following the first reduction under an Ar atmosphere in 0.1 M Bu_4NPF_6 acetonitrile solution at RT with a scan rate of 100 mV/s.

2.6. References

1. Lewis, N. S.; Nocera, D. G., "Powering the planet: Chemical challenges in solar energy utilization." *Proceedings of the National Academy of Sciences of the United States of America* **2006,** *103* (43), 15729-15735.
2. Balzani, V.; Credi, A.; Venturi, M., "Photochemical conversion of solar energy." *ChemSusChem* **2008,** *1* (1-2), 26-58.
3. Kalyanasundaram, K., "Photophysics, Photochemistry and Solar Energy Conversion with Tris(bipyridyl)ruthenium(II) and its Analogs." *Coordination Chemistry Reviews* **1982,** *46* (OCT), 159-244.
4. Balzani, V.; Juris, A.; Venturi, M.; Campagna, S.; Serroni, S., "Luminescent and redox-active polynuclear transition metal complexes." *Chemical Reviews* **1996,** *96* (2), 759-833.
5. Indelli, M. T.; Chiorboli, C.; Scandola, F., Photochemistry and photophysics of coordination compounds: Rhodium. In *Photochemistry and Photophysics of Coordination Compounds I*, Springer-Verlag Berlin: Berlin, 2007; Vol. 280, pp 215-255.
6. Lehn, J. M.; Sauvage, J. P., "Chemical Storage Of Light Energy - Catalytic Generation Of Hydrogen By Visible-Light Or Sunlight - Irradiation Of Neutral Aqueous-Solutions." *Nouveau Journal De Chimie-New Journal of Chemistry* **1977,** *1* (6), 449-451.
7. Kirch, M.; Lehn, J. M.; Sauvage, J. P., "Hydrogen generation by visible-light irradiation of aqueous-solutions of metal-complexes - approach to the photo-chemical

conversion and storage of solar-energy " *Helvetica Chimica Acta* **1979,** *62* (4), 1345-1384.
8. Bard, A. J.; Fox, M. A., "Artificial Photosynthesis - Solar Splitting Of Water To Hydrogen And Oxygen." *Accounts of Chemical Research* **1995,** *28* (3), 141-145.
9. Chan, S. F.; Chou, M.; Creutz, C.; Matsubara, T.; Sutin, N., "Mechanism of the formation of dihydrogen from the photoinduced reactions of poly(pyridine)ruthenium(II) and poly(pyridine)rhodium(III) complexes " *Journal of the American Chemical Society* **1981,** *103* (2), 369-379.
10. Heyduk, A. F.; Nocera, D. G., "Hydrogen produced from hydrohalic acid solutions by a two-electron mixed-valence photocatalyst." *Science* **2001,** *293* (5535), 1639-1641.
11. Elvington, M.; Brown, J.; Arachchige, S. M.; Brewer, K. J., "Photocatalytic hydrogen production from water employing a Ru, Rh, Ru molecular device for photoinitiated electron collection." *Journal of the American Chemical Society* **2007,** *129* (35), 10644-10645.
12. Fukuzumi, S.; Kobayashi, T.; Suenobu, T., "Photocatalytic production of hydrogen by disproportionation of one-electron-reduced rhodium and iridium-ruthenium complexes in water." *Angewandte Chemie-International Edition* **2011,** *50* (3), 728-731.
13. Stoll, T.; Gennari, M.; Serrano, I.; Fortage, J.; Chauvin, J.; Odobel, F.; Rebarz, M.; Poizat, O.; Sliwa, M.; Deronzier, A.; Collomb, M. N., "$Rh^{III}(dmbpy)_2Cl_2^+$ as a Highly Efficient Catalyst for Visible-Light-Driven Hydrogen Production in Pure Water: Comparison with Other Rhodium Catalysts." *Chemistry-a European Journal* **2013,** *19* (2), 781-791.
14. Arachchige, S. M.; Brown, J.; Brewer, K. J., "Photochemical hydrogen production from water using the new photocatalyst $[\{(bpy)_2Ru(dpp)\}_2RhBr_2](PF_6)_5$." *Journal of Photochemistry and Photobiology A: Chemistry* **2008,** *197* (1), 13-17.
15. Arachchige, S. M.; Brown, J. R.; Chang, E.; Jain, A.; Zigler, D. F.; Rangan, K.; Brewer, K. J., "Design considerations for a system for photocatalytic hydrogen production from water employing mixed-metal photochemical molecular devices for photoinitiated electron collection." *Inorganic Chemistry* **2009,** *48* (5), 1989-2000.
16. White, T. A.; Rangan, K.; Brewer, K. J., "Synthesis, characterization, and study of the photophysics and photocatalytic properties of the photoinitiated electron collector $[\{(phen)_2Ru(dpp)\}_2RhBr_2](PF_6)_5$." *Journal of Photochemistry and Photobiology A: Chemistry* **2010,** *209* (2-3), 203-209.
17. White, T. A.; Higgins, S. L. H.; Arachchige, S. M.; Brewer, K. J., "Efficient photocatalytic hydrogen production in a single-component system using Ru,Rh,Ru supramolecules containing 4,7-diphenyl-1,10-phenanthroline." *Angewandte Chemie-International Edition* **2011,** *50*, 12209-12213.
18. White, T. A.; Whitaker, B. N.; Brewer, K. J., "Discovering the balance of steric and electronic factors needed to provide a new structural motif for photocatalytic hydrogen production from water." *Journal of the American Chemical Society* **2011,** *133* (39), 15332-15334.
19. Kew, G.; DeArmond, K.; Hanck, K., "Electrochemistry of rhodium-dipyridyl complexes." *Journal of Physical Chemistry* **1974,** *78* (7), 727-734.

20. Kew, G.; Hanck, K.; DeArmond, K., "Voltammetry of rhodium-1,10-phenanthroline complexes." *Journal of Physical Chemistry* **1975,** *79* (17), 1828-1835.
21. Bolinger, C. M.; Story, N.; Sullivan, B. P.; Meyer, T. J., "Electrocatalytic reduction of carbon dioxide by 2,2'-bipyridine complexes of rhodium and iridium." *Inorganic Chemistry* **1988,** *27* (25), 4582-4587.
22. Rasmussen, S. C.; Richter, M. M.; Yi, E.; Place, H.; Brewer, K. J., "Synthesis and characterization of a series of novel rhodium and iridium complexes containing polypyridyl bridging ligands: potential uses in the development of multimetal catalysts for carbon dioxide reduction." *Inorganic Chemistry* **1990,** *29* (20), 3926-3932.
23. Amarante, D.; Cherian, C.; Ernmel, C.; Chen, H. Y.; Dayal, S.; Koshy, M.; Megehee, E. G., "Improved synthetic routes to rhodium bipyridine complexes: Comparison of microwave vs. conventional synthesis." *Inorganica Chimica Acta* **2005,** *358* (7), 2231-2238.
24. Smieja, J. M.; Kubiak, C. P., "Re(bipy-tBu)$(CO)_3$Cl-improved Catalytic Activity for Reduction of Carbon Dioxide: IR-Spectroelectrochemical and Mechanistic Studies." *Inorganic Chemistry* **2010,** *49* (20), 9283-9289.
25. Elvington, M.; Brewer, K. J., "Photoinitiated electron collection at a metal in a rhodium-centered mixed-metal supramolecular complex." *Inorganic Chemistry* **2006,** *45* (14), 5242-5244.
26. Zigler, D. F.; Wang, J.; Brewer, K. J., "Ruthenium(II)-polyazine light absorbers bridged to reactive *cis*-dichlororhodium(III) centers in a bimetallic molecular architecture." *Inorganic Chemistry* **2008,** *47* (23), 11342-11350.
27. Wang, J.; White, T. A.; Arachchige, S. M.; Brewer, K. J., "A new structural motif for photoinitiated electron collection: Ru,Rh bimetallics providing insight into H_2 production via photocatalysis of water reduction by Ru,Rh,Ru supramolecules." *Chemical Communications* **2011,** *47* (15), 4451-4453.
28. Rogers, H. M.; White, T. A.; Stone, B. N.; Arachchige, S. M.; Brewer, K. J., "Nonchromophoric Halide Ligand Variation in Polyazine-Bridged Ru(II),Rh(III) Bimetallic Supramolecules Offering New Insight into Photocatalytic Hydrogen Production from Water." *Inorganic Chemistry* **2015,** *54* (7), 3545-3551.
29. White, T. A. Design and Modification of Polyazine-Bridged Ru(II),Rh(III) Bimetallic and Trimetallic Supramolecular Complexes Applicable in Solar Energy Harvesting for the Photocatalytic Reduction of Water to Hydrogen. Virginia Tech, Blacksburg, 2012.
30. Gennett, T.; Milner, D. F.; Weaver, M. J., "Role of solvent reorganization dynamics in electron-transfer processes. Theory-experiment comparisons for electrochemical and homogeneous electron exchange involving metallocene redox couples." *Journal of Physical Chemistry* **1985,** *89* (13), 2787-2794.
31. Basile, L. A.; Barton, J. K., "Design of a double-stranded DNA cleaving agent with two polyamine metal-binding arms: Ru$(DIP)_2$Macro^{n+}." *Journal of the American Chemical Society* **1987,** *109* (24), 7548-7550.
32. Mongelli, M. T.; Brewer, K. J., "Synthesis and study of the light absorbing, redox and photophysical properties of Ru(II) and Os(II) complexes of 4,7-diphenyl-1,10-

phenanthroline containing the polyazine bridging ligand 2,3-bis(2-pyridyl)pyrazine." *Inorganic Chemistry Communications* **2006,** *9* (9), 877-881.
33. Higgins, S. L. H.; White, T. A.; Winkel, B. S. J.; Brewer, K. J., "Redox, spectroscopic, and photophysical properties of Ru-Pt mixed-metal complexes incorporating 4,7-diphenyl-1,10-phenanthroline as efficient DNA binding and photocleaving agents." *Inorganic Chemistry* **2011,** *50* (2), 463-470.

3. Nonchromophoric Halide Ligand Variation in Polyazine-Bridged Ru(II),Rh(III) Bimetallic Supramolecules Offering New Insight into Photocatalytic Hydrogen Production from Water

Reprinted with permission from "Rogers, H. M.; White, T. A.; Stone, B. N.; Arachchige, S. M.; Brewer, K. J. *Inorganic Chemistry* **2015**, *54*, 3545–3551." *Copyright 2015, American Chemical Society*.

3.1. Abstract

The new bimetallic complex $[(Ph_2phen)_2Ru(dpp)RhBr_2(Ph_2phen)](PF_6)_3$ (**1**) (Ph_2phen = 4,7-diphenyl-1,10-phenanthroline; dpp = 2,3-bis(2-pyridyl)pyrazine) was synthesized and characterized to compare with the Cl^- analogue $[(Ph_2phen)_2Ru(dpp)RhCl_2(Ph_2phen)](PF_6)_3$ (**2**) in an effort to better understand the role of halide coordination at the Rh metal center in solar H_2 production schemes. Electrochemical properties of complex **1** display a reversible $Ru^{II/III}$ oxidation and cathodic scans indicate multiple electrochemical mechanisms exist to reduce Rh(III) by two electrons to Rh(I) followed by a quasi-reversible $dpp^{0/-}$ ligand reduction. The weaker σ-donating ability of Br^- vs. Cl^- impacts the cathodic electrochemistry and provides insight into photocatalytic function by these bimetallic supramolecules. Complexes **1** and **2** exhibit identical light absorbing properties with UV absorption dominated by intraligand (IL) π→π* transitions and visible absorption by metal-to-ligand charge transfer (MLCT) transitions to include a lowest energy Ru(dπ)→dpp(π*) ^{1}MLCT transition (λ^{abs} = 514 nm; ε = 16,000 $M^{-1}cm^{-1}$). The relatively short-lived, weakly emissive Ru(dπ)→dpp(π*) ^{3}MLCT excited-state (τ = 46 ns) for both bimetallic complexes is attributed to intramolecular electron transfer from the ^{3}MLCT excited-state to populate

a low energy Ru(dπ)→Rh(dσ*) triplet metal-to-metal charge transfer (^{3}MMCT) excited state that allows photoinitiated electron collection. Complex **1** outperforms the related Cl^- bimetallic analogue **2** as a H_2 photocatalyst despite identical light absorbing and excited-state properties. Additional H_2 experiments with added halide suggest ion pairing plays a role in catalyst deactivation and provides new insight into observed differences in H_2 production upon halide variation in Ru(II),Rh(III) supramolecular architectures.

3.2. Introduction

Hydrogen gas is a highly desired alternative to carbon-based fuels and can be formed *via* water splitting through solar energy conversion schemes.[1-3] To achieve artificial photosynthetic processes such as water splitting, the field of inorganic supramolecular chemistry shows promise with the design of molecules capable of performing complex tasks.[4-5] Supramolecular complexes, as described by Balzani, are intricate molecules comprised of subunits that each contribute to the overall task performed by the complex.[6] Photochemical molecular devices (PMDs) are a subclass of supramolecular complexes that carry out demanding photoinitiated processes made possible by judicious choice of molecular subunits. Transition metal complexes that absorb light and participate in excited-state reactions are ideal PMD candidates.[7-9] A prototypical light absorber, $[Ru(bpy)_3]^{2+}$ (bpy = 2,2′-bipyridine) is extensively studied in solar energy conversion schemes due to desirable redox activity and stability, intense UV and visible light absorption, a long-lived charge transfer excited state, and rapid oxidative or reductive quenching capabilities to afford electron transfer.[10-13] Substituting

one or more polypyridyl terminal ligands (TL) (e.g., bpy in $[Ru(bpy)_3]^{2+}$) with a polypyridyl bridging ligand (BL) (e.g., dpp; bpm = 2,2′-bipyrimidine) allows the construction of supramolecular architectures assembled through coordinate covalent linkage of molecular subunits.[14-18]

Supramolecular complexes that collect two or more reducing equivalents *via* photochemical processes are termed photoinitiated electron collectors (PECs). Complexes exist that function as PECs but are not catalytically active due to collection of reducing equivalents at a noncatalytic site.[19-23] The first use of a PEC to photocatalytically reduce H_2O to H_2 was reported for $[\{(bpy)_2Ru(dpp)\}_2RhCl_2]^{5+}$, possessing Ru light absorber subunits linked through dpp BLs to a Rh center.[24] The trimetallic photocatalyst functions through successive visible light excitations, reductive quenching by a sacrificial electron donor, and electron collection at a reactive metal permitted by low-lying Rh(dσ*)-based acceptor orbitals to produce H_2 by reduction of H_2O.[24]

Component modification *via* terminal ligand and/or halide variation was studied in architectures of the form $[\{(TL)_2Ru(dpp)\}_2RhX_2]^{5+}$ (where TL = bpy, phen (1,10-phenanthroline), or Ph_2phen; X = Cl^- or Br^-).[25-27] Within this motif, the TL = Ph_2phen and X = Br^- trimetallic complex is the highest performing H_2 photocatalyst.[27] Ph_2phen is a superior TL due to increased visible light absorption, increased lifetime of the ^{3}MLCT excited state, and enhanced driving force for H_2 production relative to TL = bpy and phen analogues. The weaker σ-donating ability of X = Br^- vs. Cl^- is thought to contribute to more efficient generation of the Rh(I) active catalyst following photoinitiated

electron collection. However, after one turnover of the catalyst, the same Ru(II),Rh(I),Ru(II) photocatalyst predominates regardless of halide identity, thus not identifying the disparity in long-term catalyst stability when the halide coordinated to Rh is varied. For each set of TLs in the previously studied Ru(II),Rh(III),Ru(II) trimetallic series, the light absorbing properties do not change upon halide variation, while the X = Cl^- analogues have larger quantum yields of emission (Φ^{em}) and longer excited-state lifetimes (τ). Smaller Φ^{em} and shorter τ in the X = Br^- analogues suggest more efficient population of a low-lying metal-to-metal charge transfer (^{3}MMCT) excited state, an important parameter for H_2O reduction by these photocatalysts that leads to more efficient H_2 photocatalysis.[25-27]

When the number of light absorbing units is decreased from two to one within Ru(II),Rh(III) supramolecules, a bimetallic motif results. A balance of proper steric and electronic components is required to achieve catalysis as demonstrated with component modification in the Ru(II),Rh(III) bimetallic architecture. The complex $[(phen)_2Ru(dpp)RhCl_2(bpy)]^{3+}$ undergoes PEC but does not serve as a photocatalyst for H_2 production due to the lack of steric bulk at Rh permitting Rh(I)-Rh(I) dimerization which prevents species coordination necessary to further the catalytic cycle.[28] Complex $[(Ph_2phen)_2Ru(dpp)RhCl_2(Ph_2phen)]^{3+}$ (**2**) containing a bulky, weakly electron donating Ph_2phen TL on Rh serves as a photocatalyst for H_2 production while $[(bpy)_2Ru(dpp)RhCl_2(^tBu_2bpy)]^{3+}$ with a bulky, more strongly electron donating $^tBu_2bpy$ TL on Rh does not produce H_2 under identical conditions.[29] The disparity in photocatalytic activity is attributed to the bulky TLs electronically modulating the lowest

unoccupied molecular orbital (LUMO) which is BL-based with TL = $^{t}Bu_2$bpy and Rh-based when TL = Ph_2phen, giving evidence for the necessity of a lowest-lying Rh-based acceptor orbital to achieve H_2 photocatalysis.[30] The Ru(II),Rh(I) bimetallic complexes [$(TL)_2$Ru(dpp)Rh^{I}(COD)] (TL = bpy or Me_2bpy (4,4'-dimethyl-2,2'-bipyridine); COD = 1,5-cyclooctadiene) serve as H_2 photocatalysts with steric protection about the Rh(I) center provided by the COD ligand,[31] further demonstrating the importance of steric effects to produce H_2O reduction photocatalysts.

With knowledge of the relative orbital energetics and steric requirements to achieve H_2 production photocatalysts, complex **1** was characterized and studied to better understand the role of the non-chomophoric halide ligand in H_2 photocatalysis. The synthesis, photophysical characterization, and H_2 production studies are reported herein for this Ru(II),Rh(III) bimetallic with comparison to the Cl^- analogue **2**. The excited-state properties will be explored to determine the impact of halide ligand variation on Φ^{em} and τ values for the bimetallic system. On the basis of halide variation studies within related Ru(II),Rh(III),Ru(II) trimetallic architectures,[25-27] complex **1** is predicted to outperform **2** as a photocatalyst for H_2 production, and insight on the influence of halide identity on catalytic function with regard to ion pairing will be discussed.

3.3. Experimental Section

3.3.1. Materials

All chemicals were used as received unless otherwise noted. The reagents $RuCl_3 \cdot 3H_2O$, $RhCl_3 \cdot 3H_2O$, $RhBr_3 \cdot 3H_2O$, trifluoromethanesulfonic acid (CF_3SO_3H), 4,7-

diphenyl-1,10-phenanthroline (Ph_2phen), and tetra-*n*-butylammonium chloride (Bu_4NCl) were purchased from Alfa Aesar. 2,3-Bis(2-pyridyl)pyrazine (dpp), tetra-*n*-butylammonium bromide (Bu_4NBr), *N,N*-dimethylaniline (DMA), and Sephadex® LH-20 were purchased from Sigma-Aldrich Corporation. Ammonium hexafluorophosphate (NH_4PF_6) was purchased from Strem Chemicals, Inc. Tetra-*n*-butylammonium hexafluorophosphate (Bu_4NPF_6) was purchased from Fluka. Spectral grade acetonitrile and *N,N*-dimethylformamide (DMF) were purchased from Burdick and Jackson. Ethanol was purchased from Decon Labs, Inc. Toluene, diethyl ether, methanol, and 80-200 mesh adsorption alumina were purchased from Fischer Scientific. Complexes $[(Ph_2phen)_2RuCl_2]$ (**1a**),[32] $[(Ph_2phen)_2Ru(dpp)](PF_6)_2$ (**1b**),[17, 33] and $[(Ph_2phen)_2Ru(dpp)RhCl_2(Ph_2phen)](PF_6)_3$ (**2**) [29] were prepared as previously reported.

3.3.2. Synthesis

Complex $[(Ph_2phen)RhBr_3(DMF)]$ (**1c**) was synthesized similar to a previously reported method.[34] The starting materials $RhBr_3{\cdot}3H_2O$ (0.10 g, 0.26 mmol) and Ph_2phen (0.09 g, 0.26 mmol) were combined with 2 mL of DMF and heated in a 60 °C oil bath for 2 h. Upon cooling to RT, an orange solid was precipitated in diethyl ether, dried under vacuum, and washed with water and diethyl ether (0.15 g, 0.21 mmol, yield = 77%). ESI-MS: $[M + NH_4^+]$, *m/z* = 766.86. The chloride Rh monometallic, $[(Ph_2phen)RhCl_3(DMF)]$, was synthesized using the above method using $RhCl_3{\cdot}3H_2O$ (0.10 g, 0.38 mmol) and Ph_2phen (0.13 g, 0.38 mmol). Upon synthesis and purification, a yellow solid was collected (0.16 g, 0.26 mmol, yield = 70%). ESI-MS: $[M + H^+]$, *m/z* = 614.00.

Complex $[(Ph_2phen)_2Ru(dpp)RhBr_2(Ph_2phen)](PF_6)_3$ (**1**) was synthesized similar to a previously reported method.[29] Complex **1b** (0.078 g, 0.061 mmol) was reacted with **1c** (0.050 g, 0.067 mmol) in 15 mL of 2:1 (v/v) ethanol/water at reflux for 2 h. Upon cooling to RT, the sample was added dropwise to a 30 mL of an aqueous NH_4PF_6 solution to induce precipitation as a PF_6^- salt. A maroon precipitate was collected *via* vacuum filtration and washed with excess water and diethyl ether. The crude sample was purified using Sephadex® LH-20 size-exclusion chromatography with a 2:1 (v/v) ethanol/acetonitrile mobile phase. A maroon band eluted first and was collected, rotary evaporated, dissolved in a minimal amount of acetonitrile, and reprecipitated in diethyl ether. A maroon solid was collected *via* vacuum filtration and rinsed with excess diethyl ether (0.049 g, 0.024 mmol, yield = 48%). ESI-MS: $[M - 2PF_6^-]^{2+}$, *m/z* = 870.05.

3.3.3. Mass Spectrometry

Samples were analyzed using electrospray ionization time-of-flight mass spectrometry with an Agilent Technologies 6220 Accurate-Mass TOF LC-MS with a dual ESI (electrospray ionization) source to obtain high-resolution mass spectral data. The solvent used was HPLC-grade acetonitrile.

3.3.4. Electrochemistry

Cyclic voltammograms were obtained using a Bioanalytical Systems (BAS) Epsilon electrochemical analyzer. In a three electrode, one compartment cell, 0.1 M Bu_4NPF_6 in spectrophotometric-grade CH_3CN was the supporting electrolyte solution. The working electrode was a platinum disk, and the auxiliary electrode was a platinum wire. The Ag wire pseudoreference electrode was calibrated against the

ferrocene/ferrocenium ($FeCp_2/FeCp_2^+$) redox couple as an internal standard (0.46 V vs. Ag/AgCl) at the end of each set of scans.[35] Cyclic voltammograms were obtained at a scan rate of 100 mV s^{-1}.

3.3.5. Electronic Absorption Spectroscopy

Electronic absorption spectra were obtained using a Hewlett Packard 8453 diode array spectrophotometer. Using a sampling interval of 1 nm, measurements were obtained in a wavelength range of 190-1100 nm. Measurements were carried out in a 0.2 cm or 1 cm path length quartz cuvette (Starna Cells, Inc., Atascadero, CA) in RT spectral grade acetonitrile. Extinction coefficient measurements were performed in triplicate.

3.3.6. Steady-State and Time-Resolved Emission Spectroscopy

Steady-state emission spectra were measured using a QuantaMaster Model QM-200-45E fluorimeter from Photon Technologies International, Inc. Spectra were obtained using a 1 cm path length quartz cuvette and RT measurements were taken in deoxygenated spectral-grade CH_3CN. The excitation source was a water-cooled 150 W xenon arc lamp and the emission spectra were obtained at a 90° angle with a thermoelectrically cooled Hamamatsu R2658 photomultiplier tube operating in photon counting mode with 0.25 nm resolution. The quantum yields of emission were measured relative to $[Os(bpy)_3]^{2+}$ ($\Phi^{em} = 4.62 \times 10^{-3}$).[36] Low temperature emission spectra were collected in a 4:1 (v/v) ethanol/methanol solution cooled to 77 K using liquid N_2 in a finger Dewar to form the rigid glass matrix. Emission spectra were corrected for PMT response using the manufacturer-supplied correction file.

The excited-state lifetimes were measured using a Photon Technologies International, Inc. PL-2300 nitrogen laser with an attached PL-201 tunable dye laser. The excitation monochromator was set to 540 nm and emission from the sample was detected at a 90° angle from the excitation source by passing through an emission monochromator set to 780 nm with a Hamamatsu R928 photomultiplier tube operating in direct output mode. The signal was recorded using a LeCroy 9361 oscilloscope, averaging the results of 300 sweeps.

The rate constants for intramolecular electron transfer (k_{et}) for **1** and **2** were found by calculating the rate constants for radiative decay (k_r) and nonradiative decay (k_{nr}) utilizing $[\{(Ph_2phen)_2Ru\}_2(dpp)]^{4+}$, the model bimetallic complex that lacks a ^{3}MMCT excited state.[27, 31]

3.3.7. Photolysis Experiments

Experiments carried out to measure H_2 production employing photocatalysts **1** and **2** were performed similar to previously reported methods.[24] Stock catalyst solutions prepared in DMF were combined with water in the photolysis reaction cell that was sealed with a 10 mm airtight septum. The catalyst in the DMF/water mixture was deoxygenated with Ar for approximately 10 min prior to injecting the separately deoxygenated DMA electron donor. The final volume of the photocatalytic solution was 4.5 mL (130 μM photocatalyst, 0.62 M H_2O, 1.5 M DMA, 0.11 mM $[DMAH^+][CF_3SO_3^-]$) with a headspace volume of 16.0 mL. For designated experiments, a total concentration of 260 μM Bu_4NX (Bu_4N = tetrabutylammonium; X = Br^- or Cl^-) in DMF solution was present in the photolysis solution keeping other concentrations consistent

with previous experiments. The solution was photolyzed using a 470 nm LED array constructed in our laboratory (LED array light flux = 2.36 ± 0.05 × 10^{19} photons/min).[37] HY-OPTIMA™ 700 in-line process solid-state H_2 sensors from H_2scan (Valencia, CA) were connected using an airtight septum to the reaction cell to monitor H_2 production in real-time. The reported value for H_2 production is an average of three experiments.

3.4. Results and Discussion

3.4.1. Synthesis

Using a building block method, individual molecular components were prepared systematically to produce the target molecule **1** (**Figure 3.1**). Complex **1a** was prepared by reacting 2 equiv of the bidentate terminal ligand, Ph_2phen, with $RuCl_3 \cdot 3H_2O$.[32] The highly luminescent $[Ru(Ph_2phen)_3]^{2+}$ impurity was removed using alumina adsorption chromatography. Next, the labile Cl^- ligands were removed under reflux in the presence of a bis-bidentate BL to assemble **1b**.[33] The new Rh(III) monometallic **1c** was prepared in high yield by reacting $RhBr_3 \cdot 3H_2O$ with Ph_2phen in DMF and purification was achieved by washing with water.[34] The monometallic precursors **1b** and **1c** were reacted in a 2:1 (v/v) ethanol/water solution to produce the new bimetallic complex **1** which was precipitated by metathesis in an aqueous NH_4PF_6 solution.

Compared to related trimetallic complexes of the form $[\{(TL)_2Ru(dpp)\}_2RhX_2]^{5+}$ (TL = terminal ligand; X = Cl^- or Br^-),[25-27] Ru(II),Rh(III) bimetallic complexes discussed herein are more synthetically challenging to prepare because of the need for a Rh(III) precursor containing only one bidentate ligand, Ph_2phen in this system. Rh(III) prefers to form bis-chelated species, as with *cis*-$[(NN)_2RhX_2]^+$ complexes (NN = bidentate

polypyridyl ligand; X = Cl^- or Br^-);[38-40] thus, mild conditions were necessary to prepare precursor **1c** for the target bimetallic species. The new complex **1** was characterized using ESI-MS, electrochemical analysis, electronic absorption spectroscopy, and time-resolved and steady-state emission spectroscopy.

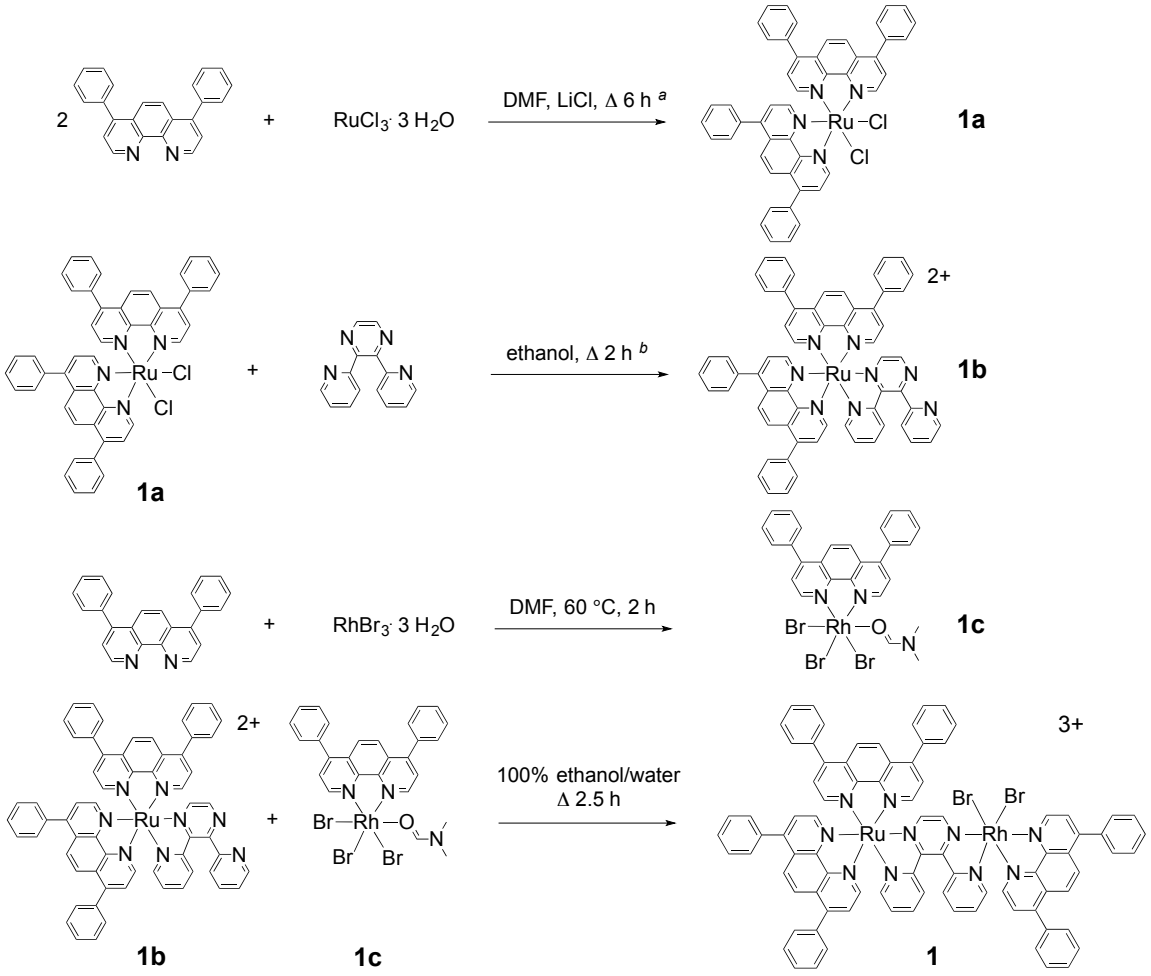

Figure 3.1. Building block synthetic scheme for the preparation of 1. [a] Reference 32; [b] Reference 33.

3.4.2. Electrochemistry

Complex **1** was analyzed using cyclic voltammetry to provide insight into the frontier orbital energetics and redox-active nature of the supramolecule and related precursors (**Figure 3.2**).

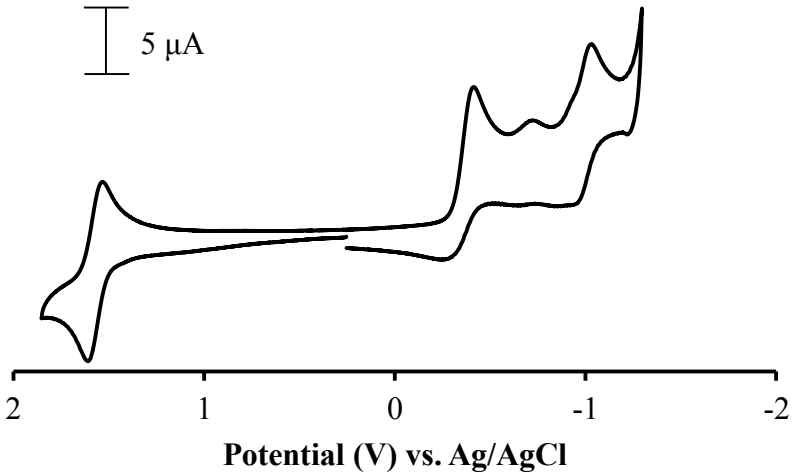

Figure 3.2. Cyclic voltammogram of **1** measured at RT under Ar in 0.1 M Bu_4NPF_6 in CH_3CN performed at 100 mV s^{-1} using a Pt disc working electrode, a Pt wire auxiliary electrode, and a Ag wire pseudoreference electrode with ferrocene internal standard and referenced to Ag/AgCl.

Table 3.1 lists electrochemical data for bimetallic complexes **1** and **2** and the monometallic synthon **1b**. Anodically, a reversible, one-electron couple ($E_{1/2}$ = +1.59 V vs. Ag/AgCl) is assigned as $Ru^{II/III}$. Coordination of the electropositive Rh(III) subunit to **1b** perturbs the electrochemical properties, evidenced with a more positive potential for the $Ru^{II/III}$ couple in the bimetallic complex resulting from Ru(dπ) orbital stabilization to make oxidation of the system more difficult.[33]

Table 3.1. Summary of Electrochemical Data

complex [a]	$E_{1/2}$ (V)	assignment
1	+1.59 [d]	$Ru^{II/III}$
	–0.38 [e]	$Rh^{III/II}Br_2$, $Rh^{II/I}Br$
	–0.73 [f]	$Rh^{II/I}Br_2$
	–0.98	$dpp^{0/-}$
2 [b]	+1.59 [d]	$Ru^{II/III}$
	–0.37 [e]	$Rh^{III/II}Cl_2$, $Rh^{II/I}Cl$
	–0.77 [f]	$Rh^{II/I}Cl_2$
	–0.96	$dpp^{0/-}$
1b [c]	+1.40 [d]	$Ru^{II/III}$
	–1.02	$dpp^{0/-}$
	–1.37	$Ph_2phen^{0/-}$
	–1.56	$Ph_2phen^{0/-}$

[a] Measured at RT under Ar in 0.1 M Bu_4NPF_6 in CH_3CN performed at 100 mV s^{-1} using Pt disc working electrode, Pt wire auxiliary electrode, and Ag wire pseudoreference electrode with ferrocene internal standard and referenced to Ag/AgCl.
[b] Reference 30.
[c] Reference 33.
[d] $E_{1/2} = E^o$ for reversible process.
[e] $E_{1/2}$ of quasi-reversible process.
[f] E_p^c of irreversible process.

Cathodically, electrochemical assignment is complicated by the nearly isoenergetic Rh(dσ*)- and dpp(π*)-based molecular orbitals. The electrochemical mechanism for complex **1** is best described using multiple pathways and is explained in detail in a separate, recent publication by our group.[30] The first cathodic wave (E_p^c = –0.38 V) is assigned as overlapping $Rh^{III/II}Br_2$ and $Rh^{II/I}Br$ reductions. The second cathodic wave (E_p^c = –0.73 V) is assigned as $Rh^{II/I}Br_2$ and exists for the fraction of complex that does not undergo halide loss prior to the second Rh-based reduction. A third, quasi-reversible reduction ($E_{1/2}$ = –0.98 V) is assigned as $dpp^{0/-}$ and provides evidence for higher lying BL-based orbitals relative to Rh-based orbitals. A similar electrochemical mechanism exists for the Cl^- bimetallic analogue **2** with the rate of halide loss modulating cathodic differences due to the increased σ-donating ability of Cl^-

vs. Br^-.[30] Ph_2phen terminal ligand and second dpp reductions are overlapping and occur beyond the first dpp reduction. Cyclic voltammetry establishes a Ru-based HOMO (highest occupied molecular orbital) and Rh-based LUMO for both bimetallic systems, important features for photoinitiated electron collection at Rh.

3.4.3. Electronic Absorption Spectroscopy

Complex **1** is an efficient light absorber in the UV and visible regions of the electromagnetic spectrum. **Figure 3.3** shows the electronic absorption spectra of the new Ru(II),Rh(III) bimetallic complex **1** overlaid with **2** and the monometallic precursor **1b** to illustrate the influence halide variation at Rh as well as coordination of an electropositive metal to the Ru(II) light absorber have on the light-absorbing properties, with tabulated data in **Table 3.2**.

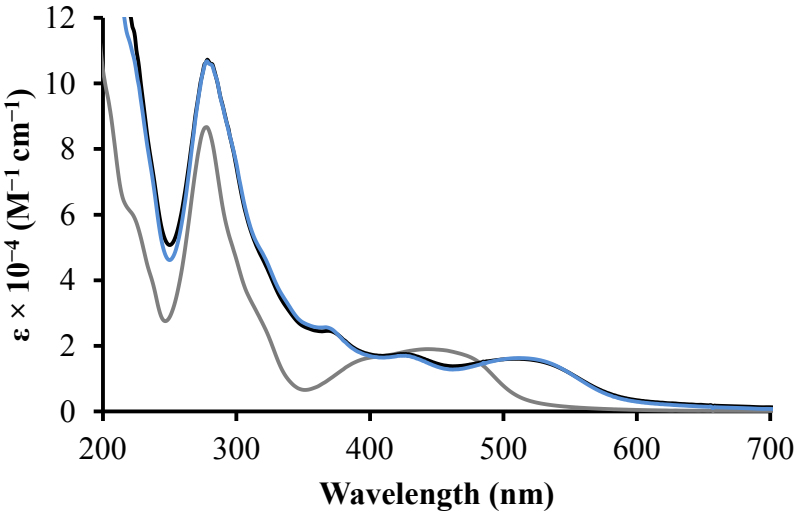

Figure 3.3. Electronic absorption spectra of **1** (black line), **2** (blue line), and **1b** (gray line), displaying the difference in light absorption upon coordination of a $Rh^{III}Br_2(Ph_2phen)$ moiety. Spectra were obtained in RT CH_3CN in a 1 cm quartz cuvette.

The UV is dominated by intraligand (^{1}IL) π→π* transitions, with λ^{abs} = 278 nm (107,000 $M^{-1}cm^{-1}$) for Ph_2phen π→π* transitions and λ^{abs} = 365 nm (24,000 $M^{-1}cm^{-1}$) for dpp π→π* transitions. In the visible, singlet metal-to-ligand charge transfer (^{1}MLCT) transitions dominate with Ru(dπ)→Ph_2phen(π*) CT transitions occurring at higher energy (λ^{abs} = 414 nm; 17,000 $M^{-1}cm^{-1}$) than Ru(dπ)→dpp(π*) CT transitions (λ^{abs} = 514 nm; 16,000 $M^{-1}cm^{-1}$).

Table 3.2. Summary of Light-Absorbing Properties

complex [a]	λ^{abs} (nm)	ε × 10^{-4} ($M^{-1}cm^{-1}$)	assignment
1	278	10.7	Ph_2phen π→π*
	365	2.4	dpp π→π*
	414	1.7	Ru(dπ)→Ph_2phen(π*) CT
	514	1.6	Ru(dπ)→dpp(π*) CT
2 [b]	278	10.7	Ph_2phen π→π*
	365	2.6	dpp π→π*
	414	1.7	Ru(dπ)→Ph_2phen(π*) CT
	514	1.6	Ru(dπ)→dpp(π*) CT
1b [c]	274	8.4	Ph_2phen π→π*
	309	3.4	dpp π→π*
	424	1.8	Ru(dπ)→Ph_2phen(π*) CT
	474	1.7	Ru(dπ)→dpp(π*) CT

[a] Measured at RT in CH_3CN in a 1 cm quartz cuvette.
[b] Values consistent with those in Reference 29.
[c] Values consistent with those in Reference 33.

When compared to precursor **1b**, complex **1** possesses a red-shifted Ru(dπ)→dpp(π*) CT transition due to stabilization of the dpp(π*)-based molecular orbitals upon coordination to a second electropositive metal center.[33] The energy of Ph_2phen IL transitions is unaffected by coordination of the Rh(III) subunit; however, the extinction coefficient increases due to an additional chromophoric Ph_2phen ligand.

Complex **1** displays nearly identical light absorbing properties to **2**.[29] This trend is expected because the component varied is a nonchromophoric ligand.

3.4.4 Steady-State and Time-Resolved Emission Spectroscopy

The emissive nature of the lowest-lying Ru(dπ)→dpp(π*) ^{3}MLCT excited state of complex **1** provides a probe into the excited-state dynamics of this complex. Variation of the halide coordinated to Rh in complexes **1** and **2** from Br^- to Cl^- does not impact the excited-state properties (**Figure 3.4**), tabulated in **Table 3.3** with comparison to the monometallic precursor **1b**.

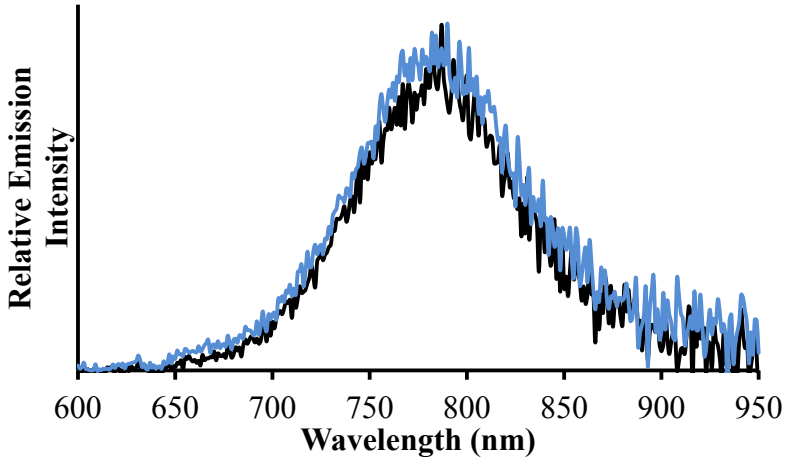

Figure 3.4. Emission spectra of **1** (black line) and **2** (blue line). Spectra were obtained in RT CH_3CN in a 1 cm quartz cuvette and were corrected for PMT response.

Table 3.3. Summary of Photophysical Data

	RT [a]						77 K [b]	
complex	λ^{em} (nm)	Φ^{em} (10^{-4})	τ (ns)	k_r (10^3 s^{-1})	k_{nr} (10^6 s^{-1})	k_{et} (10^7 s^{-1})	λ^{em} (nm)	τ (μs)
1	780	1.3	46	2.8	5.2	1.6	706	1.6
2	780	1.3	46	2.8	5.2	1.6	706	1.8
1b [c]	664	350	820	43	1.2	--	607	5.4

[a] Measured at RT in CH_3CN deoxygenated with Ar in a 1 cm quartz cuvette.
[b] Measured in 4:1 ethanol/methanol at 77 K.
[c] Reference 33.

Complexes **1**, **2**, and **1b** undergo excitation to a ^{1}MLCT excited state followed by intersystem crossing to populate a ^{3}MLCT excited state with unity efficiency. Upon coordination of a second electropositive metal in the Ru(II),Rh(III) bimetallic architectures, Rh(dσ*)-based acceptor orbitals become accessible to facilitate population of a low energy ^{3}MMCT excited state. Deactivation from the ^{3}MMCT excited state can occur through nonradiative decay (k_{nr}') back to the ^{1}GS or through a photochemical reaction (k_{rxn}) (**Figure 3.5**).

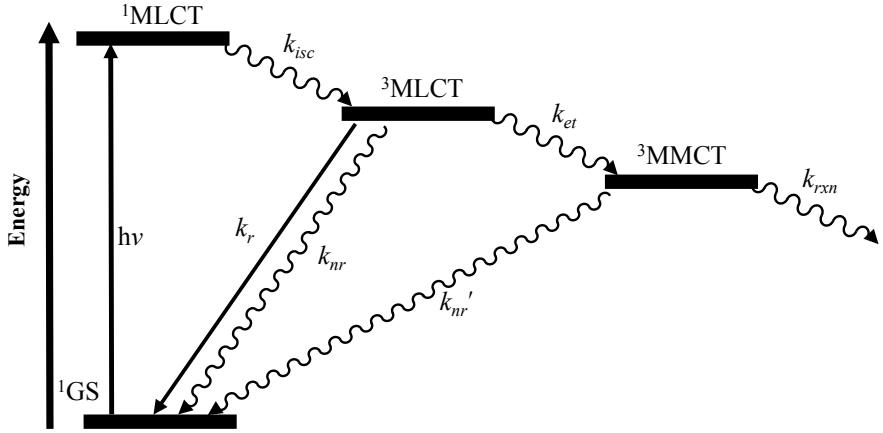

Figure 3.5. Simplified Jablonski-type state diagram for **1** and **2**. ^{1}GS = singlet ground state; k_{isc} = rate of intersystem crossing; k_r = rate of radiative decay; k_{nr} = rate of nonradiative decay; k_{et} = rate of intramolecular electron transfer; k_{rxn} = rate of photochemical reaction.

Variation of the halide coordinated to Rh in complexes **1** and **2** from Br^- to Cl^- produces identical steady-state and time-resolved emission properties in RT acetonitrile (λ^{em} = 780 nm, $\Phi^{em} = 1.3 \times 10^{-4}$, τ = 46 ns, $k_r = 2.8 \times 10^3$ s^{-1}, $k_{nr} = 5.2 \times 10^6$ s^{-1}), indicating equivalent rates of population of the low-lying ^{3}MMCT excited state ($k_{et} = 1.6 \times 10^7$ s^{-1}) when the halide coordinated to Rh is Br^- or Cl^-. Compared to the bimetallic model complex $[\{(Ph_2phen)_2Ru\}_2(dpp)]^{4+}$ that lacks a ^{3}MMCT excited state,[27] complexes **1** and **2** display quenched emission of the ^{3}MLCT excited state to validate ^{3}MMCT

excited state population required for photocatalysis. At 77 K in a rigid glass matrix, intramolecular electron transfer is impeded, providing further validation for RT ^{3}MLCT excited state quenching in these Ru(II),Rh(III) bimetallic systems.

In analogous motifs, quantum yield and excited-state lifetime values are influenced by halide identity.[25-27] Smaller Φ^{em} and shorter τ in such systems with Br^- ligands coordiated to Rh suggest more efficient population of a low-lying ^{3}MMCT excited state (faster k_{et}) that contributes to enhanced photocatalytic activity in the Br^- trimetallic system. Despite identical excited-state properties and k_{et} values for the Br^- and Cl^- bimetallic supramolecules, complex **1** is still photocatalytically superior. Thus, complexes **1** and **2** provide an ideal forum to study the impact of halide identity on photocatalytic H_2 generation when excited state-properties are identical.

3.4.5 Photocatalytic H_2 Production

H_2 production experiments were carried out to determine the role of halide variation in the Ru(II),Rh(III) supramolecular photocatalyst system. The Cl^- bimetallic analogue **2** is a photocatalyst for H_2O reduction.[29] The bimetallic complex undergoes light-assisted collection of reducing equivalents at Rh to produce an intact Ru(II),Rh(I) species that is the proposed active photocatalyst. With the substitution of Br^- for Cl^- halides shown herein to not greatly perturb spectroscopic and electrochemical properties, it is not surprising that **1** also serves as a photocatalyst for H_2 production (**Figure 3.6A**).

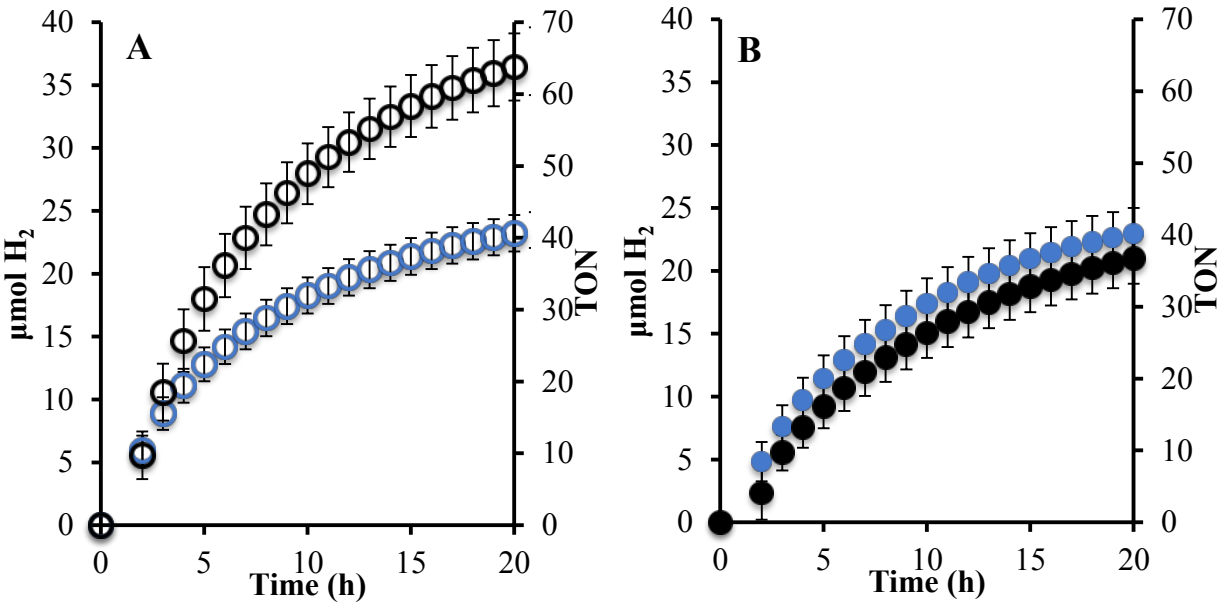

Figure 3.6. Hydrogen production profiles for **1** and **2** in Ar deoxygenated DMF solvent. (**A**) Black open circles: **1**; blue open circles: **2**. (**B**) Black filled circles: **1** with 260 μM Bu_4NCl; blue filled circles: **2** with 260 μM Bu_4NBr. Systems contained 130 μM photocatalyst, 0.62 M H_2O, 1.5 M DMA electron donor, and 110 μM $[DMAH^+][CF_3SO_3^-]$.

When photolyzed for 20 h with λ = 470 nm light in DMF (*N,N*-dimethylformamide) solvent in the presence of H_2O and DMA (*N,N*-dimethylaniline) electron donor, complex **1** produces 36±3 μmol of H_2 (62±5 TON = turnover number = mol H_2 produced/mol catalyst), an increase in H_2 production compared to **2**, 23±1 μmol of H_2 (40±2 TON). DMF was chosen as the solvent for these photocatalytic studies because its weaker ligating ability leads to enhanced photocatalysis.[29] The improved photocatalytic abilities of **1** relative to **2** is a unique result considering that the two complexes have identical excited-state properties (Φ^{em} and τ), values that are different in analogous Ru(II),Rh(III),Ru(II) trimetallic supramolecules.[25-27] Therefore, the discrepancy in H_2 production between the Ru(II),Rh(III) bimetallic systems described herein cannot be ascribed to differences in excited-state properties.

With knowledge that H_2 production is impacted by halide variation in Ru(II),Rh(III) bimetallic supramolecules possessing identical light absorbing and excited-state properties, the influence of halide was further investigated. Upon reduction of Rh by two equivalents, two halide ligands are lost to produce the square planar Rh(I)-containing supramolecule, yet these halides still seem to play an important role in photocatalysis. The close proximity of halide ion to the metal complex, made possible by ion pairing in low dielectric solvents such as DMF, may alter catalyst function by providing a high local concentration of halide ion to hinder interaction of the Rh(I) center with H_2O due to halide re-coordination.

Interestingly, when H_2 experiments were carried out adding two equivalents (260 μM) of the opposite halide to the photolysis solutions for each photocatalyst, accounting for two equivalents of halide lost, both systems demonstrated identical photocatalytic activity (**Figure 3.6B**). Using photocatalyst **1**, 260 μM Bu_4NCl (tetra-*n*-butylammonium chloride) was added to the photolysis solution, producing 21±2 μmol of H_2 (36±3 TON) after 20 h photolysis. Conversely, 260 μM Bu_4NBr (tetra-*n*-butylammonium bromide) was added to the photolysis solution utilizing photocatalyst **2** and produced 23±2 μmol of H_2 (39±4 TON) after 20 h. These experimental conditions allow for equal concentrations of Br^- and Cl^- in solution following generation of the active Ru(II),Rh(I) catalyst.

Complex **1** showed a decrease of 20 TONs with added Cl^- relative to the H_2 experiment with no added halide, while complex **2** only showed a decrease of ~1 TON upon added Br^-. A local high concentration of halide ion promotes halide recoordination

to the catalytically active Rh(I), impeding its interactions with H_2O and affording lower H_2 yields. Recoordination of the halide *via* formation of an ion paired complex between the halide and the photocatalyst is probable and has been shown as a deactivation pathway for other homogeneous transition metal catalysts.[41] The added Cl^- more negatively affects catalysis relative to added Br^-, demonstrating that the more σ-donating Cl^- ligands can ion pair more strongly with the photocatalyst and inhibit catalyst function. By contrast, bulkier and less strongly σ-donating Br^- addition does not impact catalysis as significantly, consistent with a comparatively weaker ion pair formed between Br^- and the photocatalyst and supporting increased H_2 production in Br^- analogues of Ru(II),Rh(III) photocatalysts.

3.5. Conclusions

The new complex **1** was synthesized and characterized to explore the impact of halide variation on spectroscopic and electrochemical properties as well as on photocatalytic H_2 production capabilities relative to the previously reported Cl^- bimetallic supramolecule. Cyclic voltammetry of complex **1** provides evidence for a Ru-based HOMO and a Rh-based LUMO which are requirements for H_2O reduction photocatalysis *via* photoinitiated electron collection at Rh. The complex absorbs light in the UV with ligand π→π* transitions and in the visible with Ru(dπ)→ligand(π*) ^{1}MLCT transitions (ligand = Ph_2phen or dpp). Radiative decay from a ^{3}MLCT excited state shows a relatively low quantum yield of emission and short excited-state lifetime due to population of a low energy ^{3}MMCT excited state, necessary behavior for electron collection at the Rh site to achieve active H_2 photocatalysts. With light absorption in the

visible and collection of reducing equivalents on a Rh-based LUMO, complex **1** is a photocatalyst for H_2O reduction and displays enhanced activity compared to the Cl^- analogue **2**. Added halide experiments indicate that ion pairing deactivates the catalyst due to the local concentration of halide ion in proximity to the photocatalyst, with the more σ-donating Cl^- ligands more negatively influencing photocatalysis relative to Br^-. These results are significant because they provide remarkable evidence showing that halide identity impacts catalysis even after halides are dissociated to form the Rh(I)-containing photocatalyst. Studies are ongoing in our laboratory to examine potential catalytic intermediates that involve ligand variation at the Rh center as the complex cycles from Rh(III) to Rh(I) to produce H_2 from H_2O.

3.6. Acknowledgement

Acknowledgement is made to the Chemical Sciences, Geosciences and Biosciences Division, Office of Basic Energy Sciences, Office of Sciences, U.S. Department of Energy (DE FG02-05ER15751) for their generous financial support of the work described herein. Special thanks are given to Dr. James Tanko and Ms. Kristen Felice for assistance with this manuscript. Mr. William Bebout of the Virginia Tech Department of Chemistry Analytical Services Laboratory is acknowledged for assistance with mass spectral data.

3.7. References

1. Bard, A. J.; Fox, M. A., "Artificial photosynthesis: Solar splitting of water to hydrogen and oxygen." *Accounts of Chemical Research* **1995,** *28* (3), 141-145.
2. Lewis, N. S.; Nocera, D. G., "Powering the planet: Chemical challenges in solar energy utilization." *Proceedings of the National Academy of Sciences of the United States of America* **2006,** *103* (43), 15729-15735.

3. Kirch, M.; Lehn, J. M.; Sauvage, J. P., "Hydrogen generation by visible-light irradiation of aqueous-solutions of metal-complexes - approach to the photo-chemical conversion and storage of solar-energy " *Helvetica Chimica Acta* **1979,** *62* (4), 1345-1384.
4. Balzani, V.; Bergamini, G.; Campagna, S.; Puntoriero, F., Photochemistry and photophysics of coordination compounds: Overview and general concepts. In *Photochemistry and Photophysics of Coordination Compounds I*, Balzani, V.; Campagna, S., Eds. 2007; Vol. 280, pp 1-36.
5. Denti, G.; Campagna, S.; Sabatino, L.; Serrni, S.; Ciano, M.; Balzani, V., "Luminescent and redox-reactive building blocks for the design of photochemical molecular devices: Mono-, di-, tri-, and tetranuclear ruthenium(II) polypyridine complexes." *Inorganic Chemistry* **1990,** *29* (23), 4750-4758.
6. Balzani, V.; Moggi, L.; Scandola, F., Towards a Supramolecular Photochemistry: Assembly of Molecular Components to Obtain Photochemical Molecular Devices. In *Supramolecular Photochemistry*, Balzani, V., Ed. NATO ASI Series 214, Reidel, Dordrecht: The Netherlands: 1987; pp 1-28.
7. Holliday, B. J.; Mirkin, C. A., "Strategies for the construction of supramolecular compounds through coordination chemistry." *Angewandte Chemie-International Edition* **2001,** *40* (11), 2022-2043.
8. Kalyanasundaram, K.; Gratzel, M.; Nazeeruddin, M. K., "Excited-State Interactions In Ligand-Bridged Chromophore Quencher Complexes Containing Rhodium(Iii) And Ruthenium(Ii) Polypyridyl Units." *Journal of Physical Chemistry* **1992,** *96* (14), 5865-5872.
9. Kalyanasundaram, K., *Photochemistry of Polypyridine and Porphyrin Complexes*. Academic Press Inc.: San Diego, 1992.
10. Kalyanasundaram, K., "Photophysics, Photochemistry and Solar Energy Conversion with Tris(bipyridyl)ruthenium(II) and its Analogs." *Coordination Chemistry Reviews* **1982,** *46* (OCT), 159-244.
11. Vanhouten, J.; Watts, R. J., "Temperature Dependence of the Photophysical and Photochemical Properties of Tris(2,2'-bipyridyl)ruthenium(II) Ion in Aqueous Solution." *Journal of the American Chemical Society* **1976,** *98* (16), 4853-4858.
12. Vanhouten, J.; Watts, R. J., "Photochemistry of Tris(2,2'-bipyridyl)ruthenium(II) in Aqueous Solutions." *Inorganic Chemistry* **1978,** *17* (12), 3381-3385.
13. Meyer, T. J., "Photochemistry of metal coordination complexes: metal to ligand charge transfer excited states." *Pure and Applied Chemistry* **1986,** *58* (9), 1193-1206.
14. Brewer, K. J.; Murphy, W. R.; Spurlin, S. R.; Petersen, J. D., "The next generation of (polyazine)ruthenium(II) complexes." *Inorganic Chemistry* **1986,** *25* (6), 882-884.
15. Wallace, A. W.; Murphy, W. R.; Petersen, J. D., "Electrochemical and photophysical properties of monometallic and bimetallic ruthenium(II) complexes " *Inorganica Chimica Acta* **1989,** *166* (1), 47-54.
16. Schulz, M.; Karnahl, M.; Schwalbe, M.; Vos, J. G., "The role of the bridging ligand in photocatalytic supramolecular assemblies for the reduction of protons and carbon dioxide." *Coordination Chemistry Reviews* **2012,** *256* (15-16), 1682-1705.

17. Mongelli, M. T.; Brewer, K. J., "Synthesis and study of the light absorbing, redox and photophysical properties of Ru(II) and Os(II) complexes of 4,7-diphenyl-1,10-phenanthroline containing the polyazine bridging ligand 2,3-bis(2-pyridyl)pyrazine." *Inorganic Chemistry Communications* **2006,** *9* (9), 877-881.
18. Zigler, D. F.; Wang, J.; Brewer, K. J., "Ruthenium(II)-Polyazine Light Absorbers Bridged to Reactive cis-Dichlororhodium(III) Centers in a Bimetallic Molecular Architecture." *Inorganic Chemistry* **2008,** *47* (23), 11342-11350.
19. Konduri, R.; Ye, H. W.; MacDonnell, F. M.; Serroni, S.; Campagna, S.; Rajeshwar, K., "Ruthenium photocatalysts capable of reversibly storing up to four electrons in a single acceptor ligand: A step closer to artificial photosynthesis." *Angewandte Chemie-International Edition* **2002,** *41* (17), 3185-3187.
20. Molnar, S. M.; Nallas, G.; Bridgewater, J. S.; Brewer, K. J., "Photoinitiated electron collection in a mixed-metal trimetallic complex of the form $[\{(bpy)_2Ru(dpb)\}_2IrCl_2](PF_6)_5$ (bpy = 2,2'-bipyridine and dpb = 2,3-bis(2-pyridyl)benzoquinoxaline)." *Journal of the American Chemical Society* **1994,** *116* (12), 5206-5210.
21. Rangan, K.; Arachchige, S. M.; Brown, J. R.; Brewer, K. J., "Solar energy conversion using photochemical molecular devices: photocatalytic hydrogen production from water using mixed-metal supramolecular complexes." *Energy & Environmental Science* **2009,** *2* (4), 410-419.
22. Polyansky, D. E.; Cabelli, D.; Muckerman, J. T.; Fukushima, T.; Tanaka, K.; Fujita, E., "Mechanism of hydride donor generation using a Ru(II) complex containing an NAD(+) model ligand: Pulse and steady-state radiolysis studies." *Inorganic Chemistry* **2008,** *47* (10), 3958-3968.
23. Polyansky, D.; Cabelli, D.; Muckerman, J. T.; Fujita, E.; Koizumi, T.; Fukushima, T.; Wada, T.; Tanaka, K., "Photochemical and radiolytic production of an organic hydride donor with a Ru-II complex containing an NAD(+) model ligand." *Angewandte Chemie-International Edition* **2007,** *46* (22), 4169-4172.
24. Elvington, M.; Brown, J.; Arachchige, S. M.; Brewer, K. J., "Photocatalytic hydrogen production from water employing a Ru, Rh, Ru molecular device for photoinitiated electron collection." *Journal of the American Chemical Society* **2007,** *129* (35), 10644-10645.
25. Arachchige, S. M.; Brown, J.; Brewer, K. J., "Photochemical hydrogen production from water using the new photocatalyst $[\{(bpy)_2Ru(dpp)\}_2RhBr_2](PF_6)_5$." *Journal of Photochemistry and Photobiology A: Chemistry* **2008,** *197* (1), 13-17.
26. White, T. A.; Rangan, K.; Brewer, K. J., "Synthesis, characterization, and study of the photophysics and photocatalytic properties of the photoinitiated electron collector $[\{(phen)_2Ru(dpp)\}_2RhBr_2](PF_6)_5$." *Journal of Photochemistry and Photobiology A: Chemistry* **2010,** *209* (2-3), 203-209.
27. White, T. A.; Higgins, S. L. H.; Arachchige, S. M.; Brewer, K. J., "Efficient photocatalytic hydrogen production in a single-component system using Ru,Rh,Ru supramolecules containing 4,7-diphenyl-1,10-phenanthroline." *Angewandte Chemie-International Edition* **2011,** *50*, 12209-12213.

28. Wang, J.; White, T. A.; Arachchige, S. M.; Brewer, K. J., "A new structural motif for photoinitiated electron collection: Ru,Rh bimetallics providing insight into H_2 production via photocatalysis of water reduction by Ru,Rh,Ru supramolecules." *Chemical Communications* **2011,** *47* (15), 4451-4453.
29. White, T. A.; Whitaker, B. N.; Brewer, K. J., "Discovering the balance of steric and electronic factors needed to provide a new structural motif for photocatalytic hydrogen production from water." *Journal of the American Chemical Society* **2011,** *133* (39), 15332-15334.
30. White, T. A.; Mallalieu, H. E.; Wang, J.; Brewer, K. J., "Mechanistic Insight into the Electronic Influences Imposed by Substituent Variation in Polyazine-Bridged Ruthenium(II)/ Rhodium(III) Supramolecules." *Chemistry - A European Journal* **2014,** *20*, 8265 - 8268.
31. Crabtree, R. H., "Deactivation in Homogeneous Transition Metal Catalysis: Causes, Avoidance, and Cure." *Chemical Reviews* **2015,** *115* (1), 127-150.
32. Basile, L. A.; Barton, J. K., "Design of a double-stranded DNA cleaving agent with two polyamine metal-binding arms: $Ru(DIP)_2Macro^{n+}$." *Journal of the American Chemical Society* **1987,** *109* (24), 7548-7550.
33. Higgins, S. L. H.; White, T. A.; Winkel, B. S. J.; Brewer, K. J., "Redox, spectroscopic, and photophysical properties of Ru-Pt mixed-metal complexes incorporating 4,7-diphenyl-1,10-phenanthroline as efficient DNA binding and photocleaving agents." *Inorganic Chemistry* **2011,** *50* (2), 463-470.
34. Sau, Y.-K.; Chan, K.-W.; Zhang, Q.-F.; Williams, I. D.; Leung, W.-H., "Alkyl and Aryl Compounds of Rhodium(III) and Iridium(III) Supported by 4,4'-Di-*tert*-butyl-2,2'-bipyridyl." *Organometallics* **2007,** *26*, 6338-6345.
35. Gennett, T.; Milner, D. F.; Weaver, M. J., "Role Of Solvent Reorganization Dynamics In Electron-Transfer Processes - Theory Experiment Comparisons For Electrochemical And Homogeneous Electron Exchange Involving Metallocene Redox Couples." *Journal of Physical Chemistry* **1985,** *89* (13), 2787-2794.
36. Caspar, J. V.; Kober, E. M.; Sullivan, B. P.; Meyer, T. J., "Application Of The Energy-Gap Law To The Decay Of Charge-Transfer Excited-States." *Journal of the American Chemical Society* **1982,** *104* (2), 630-632.
37. Brown, J. R.; Elvington, M.; Mongelli, M. T.; Zigler, D. F.; Brewer, K. J., "Analytical methods development for supramolecular design in solar hydrogen production." *Proc. SPIE-Opt. Photo. Sol. Hydrogen Nanotechnology* **2006,** *6340*, 634007W1-13.
38. Rasmussen, S. C.; Richter, M. M.; Yi, E.; Place, H.; Brewer, K. J., "Synthesis and characterization of a series of novel rhodium and iridium complexes containing polypyridyl bridging ligands: potential uses in the development of multimetal catalysts for carbon dioxide reduction." *Inorganic Chemistry* **1990,** *29* (20), 3926-3932.
39. Bolinger, C. M.; Story, N.; Sullivan, B. P.; Meyer, T. J., "Electrocatalytic reduction of carbon dioxide by 2,2'-bipyridine complexes of rhodium and iridium." *Inorganic Chemistry* **1988,** *27* (25), 4582-4587.
40. Kew, G.; DeArmond, K.; Hanck, K., "Electrochemistry of rhodium-dipyridyl complexes." *Journal of Physical Chemistry* **1974,** *78* (7), 727-734.

41. McCormick, T. M.; Han, Z.; Weinberg, D. J.; Brennessel, W. W.; Holland, P. L.; Eisenberg, R., "Impact of Ligand Exchange in Hydrogen Production from Cobaloxime-Containing Photocatalytic Systems." *Inorganic Chemistry* **2011,** *50* (21), 10660-10666.

4. Enhancement of Solar Fuel Production Schemes by Using a Supramolecular Photocatalyst Containing Hydroxide Labile Ligands

Reprinted with permission from "Rogers, H. M.; Arachchige, S. M.; Brewer, K. J. *Chemistry – A European Journal* **2015**, *21*, 16948–16954." *Copyright 2015, John Wiley and Sons.*

4.1. Abstract

Polyazine-bridged $Ru^{II}Rh^{III}Ru^{II}$ complexes with two halide ligands, Cl^- or Br^-, bound to the catalytically active Rh center are efficient single-component photocatalysts for H_2O reduction to H_2 fuel, with the coordination environment on Rh impacting photocatalysis. Herein reported is a new, halide-free $Ru^{II}Rh^{III}Ru^{II}$ photocatalyst with OH^- ligands bound to Rh, further enhancing the photocatalytic reactivity of the structural motif. H_2 production experiments using the photocatalyst bearing OH^- ligands at Rh relative to the analogues bearing halides at Rh in solvents of varying polarity (DMF, CH_3CN, and H_2O) suggest that ion pairing with halides deactivates photocatalyst function, representing an exciting phenomenon to exploit in the development of catalysts for solar H_2 production schemes.

4.2. Introduction

Solar-to-chemical energy conversion via water splitting is a promising approach to alleviate the global dependence on carbon-based fuels.[1-4] To harness solar energy in the form of chemical bonds, one method employs photosensitizers to absorb light and funnel energy through electron transfer to an appropriate substrate such as H_2O for reduction to H_2 fuel,[5-9] and multi-component systems exist that undergo this light-assisted electron collection to produce H_2 fuel.[10-13] To better understand molecular

processes required for solar H_2 production schemes, supramolecular complexes that function as photochemical molecular devices (PMDs) are prepared by covalent linkage of molecular subunits.[14-16] PMDs maintain the properties of individual molecular components while each constituent collaborates to achieve an overall goal such as H_2O reduction.[17]

PMDs that collect reducing equivalents at an unoccupied, energetically low-lying site are known as photoinitiated electron collectors (PECs). Complex $[\{(bpy)_2Ru(dpb)\}_2IrCl_2]^{5+}$ (bpy = 2,2′-bipyridine; dpb = 2,3-bis(2-pyridyl)benzoquinoxaline) served as a PEC with electron collection occurring at dpb bridging ligand (BL) π* orbitals,[18] and related PECs exist that also undergo ligand-centered electron collection.[19-22] These early models are important for the design of systems that collect electrons at a catalytically active metal center, established with photocatalyst $[\{(bpy)_2Ru(dpp)\}_2RhCl_2]^{5+}$ (dpp = 2,3-bis(2-pyridyl)pyrazine).[23] The trimetallic supramolecule served as a PEC to photocatalyze H_2O reduction in an organic solvent/water mixture with *N,N*-dimethylaniline (DMA) as a sacrificial reductant. When irradiated with visible light in the presence of DMA, $[\{(bpy)_2Ru(dpp)\}_2RhCl_2]^{5+}$ converts from six-coodinate Rh^{III} to four-coordinate Rh^{I}, accompanied by the loss of both halides, to form $[\{(bpy)_2Ru(dpp)\}_2Rh^{I}]^{5+}$ that photochemically reduces H_2O to H_2 fuel.[23-24]

Component variation within trimetallic architectures $[\{(TL)_2Ru(BL)\}_2RhX_2]^{5+}$ (TL = terminal ligand; X = Cl^- or Br^-) provides valuable insight about requirements for the molecular photocatalysis of H_2 evolution from H_2O.[25-28] Pertinent to the work discussed herein is variation of the halides coordinated to Rh from X = Cl^- to Br^-, ligands that

dissociate to form the intact $Ru^{II}Rh^{I}Ru^{II}$ active photocatalyst. Regardless of TL, the X = Br^- complexes are more photocatalytically active, with greater H_2 production attributed to more efficient population of the low-lying triplet metal-to-metal charge transfer (^{3}MMCT) excited state from where H_2 photocatalysis was proposed to occur.[25-28] Recently, $Ru^{II}Pt^{II}$ bimetallic photocatalysts for H_2 evolution were reported where the halides coordinated to Pt were varied from Cl^- to I^-.[29] Enhanced solar H_2 production was observed for the species bearing I^- ligands at Pt, producing 40 times more H_2 than the Cl^- analogue and further demonstrating the large impact subtle structural changes can have on photocatalysis.

$Ru^{II}Rh^{III}$ bimetallic complexes $[(Ph_2phen)_2Ru(dpp)RhX_2(Ph_2phen)]^{3+}$ (Ph_2phen = 4,7-diphenyl-1,10-phenanthroline; X = Cl^- or Br^-) are active H_2 photocatalysts, with halide identity again shown to impact H_2 evolution.[30-31] The X = Br^- complex was a superior H_2 evolution photocatalyst relative to the X = Cl^- analogue, even with identical light absorbing and excited state properties upon halide variation in this series. H_2 production experiments with added halide revealed that halides negatively impacted photocatalysis as they could ion pair with the coordinatively unsaturated supramolecule, impeding interaction with the H_2O substrate as the complex cycled from $Rh^{III/II/I}$ during photocatalysis.[30] In a separate study with a $Ru^{II}Pd^{II}$ bimetallic complex bearing two Cl^- ligands at Pd, added Cl^- also hindered H_2 production.[32] Ion pairing with coordinating counter ions suppressed activity by an ethylene polymerization transition metal catalyst, with high functioning achieved only in the presence of non-coordinating counter ions.[33] Coordinating anions in close proximity to active metal catalysts bearing open

coordination sites often inhibit catalysis by preventing coordination of the desired substrate, with solvent selection playing an important role.[34] These studies demonstrate that ion pairing is an important consideration when developing catalytic schemes.

H_2 production studies for single-component photocatalysts are typically carried out in organic solvents with added H_2O substrate and a sacrificial reductant.[35-38] However, the development of photocatalytic systems that produce H_2 fuel in purely aqueous media is an attractive, environmentally desirable approach. Few examples of aqueous H_2 production catalyzed by single-component photocatalysts are reported, with a $Ru^{II}Rh^{III}Ru^{II}$ complex linked by non-conjugated BLs the highest yielding to date.[39-43]

Herein we report the synthesis, characterization, and photocatalysis studies of a new photocatalyst for solar-driven H_2 evolution, $[\{(bpy)_2Ru(dpp)\}_2Rh(OH)_2](PF_6)_5$ (**1-OH**). This complex bears OH^- ligands at the Rh center and is photocatalytically active in both aqueous and organic solvents. The halide-free **1-OH** affords an ideal system to study the influence of the monodentate ligands bound to the catalytically active metal center in H_2 production schemes. Comparing the photochemistry and photophysics of **1-OH** with the halide analogues $[\{(bpy)_2Ru(dpp)\}_2RhX_2](PF_6)_5$ (X = Cl^- (**1-Cl**) or Br^- (**1-Br**)) provides new and important mechanistic insight about the H_2 production scheme by this series and related photocatalysts.

4.3. Results and Discussion

4.3.1. Synthesis and Characterization

A building block approach was used to prepare the new supramolecule **1-OH** (**Figure 4.1**).

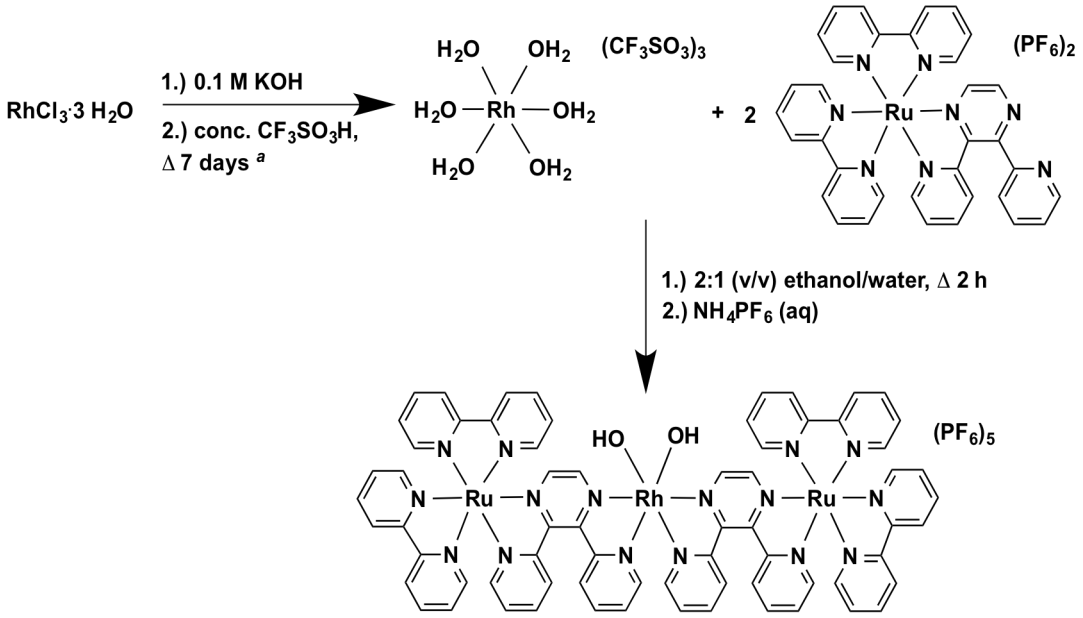

Figure 4.1. Building block synthetic route for the preparation of new complex $[\{(bpy)_2Ru(dpp)\}_2Rh(OH)_2](PF_6)_5$ (**1-OH**). [a] from Reference 44.

Starting material $[(bpy)_2RuCl_2]\cdot 2H_2O$ was reacted with an excess of the dpp BL to prepare $[(bpy)_2Ru(dpp)](PF_6)_2$,[45] the Ru^{II} monometallic precursor with open coordination sites to further the supramolecular architecture. To synthesize the Rh^{III} monometallic precursor, $RhCl_3\cdot 3H_2O$ was reacted with KOH (aq), forming a pale yellow solid as the pH of the solution was raised to 13. The solid was centrifuged several times and the supernatant was removed after each run, washing the remaining solid with H_2O to ensure the removal of halide. The yellow solid was then suspended in H_2O and reacted with neat CF_3SO_3H at reflux for 7 days to prepare $[Rh(H_2O)_6](CF_3SO_3)_3$.[44] Finally, the

target trimetallic complex **1-OH** was prepared by the reaction of two equivalents of $[(bpy)_2Ru(dpp)](PF_6)_2$ with one equivalent of $[Rh(H_2O)_6](CF_3SO_3)_3$ in a 2:1 (v/v) ethanol/H_2O solvent mixture for 1 h, achieving purification by reprecipitation from CH_3CN/diethyl ether. ESI-MS (electrospray ionization mass spectrometry) experiments are consistent with theoretical calculations and confirm the charge of **1-OH** as 5+ (**Figure 4.S1**).

Cyclic voltammetry (CV) experiments provide insight about the relative orbital energetics of **1-OH** (**Figure 4.S2**). Similar to **1-Cl** and **1-Br** (**Table 4.1**)[23, 28], a reversible $Ru^{II/III}$ couple assigned to two, overlapping oxidations of the largely electronically uncoupled Ru centers occurs at +1.62 V vs Ag/AgCl in CH_3CN. An irreversible $Rh^{III/II/I}$ reduction occurs at –0.38 V followed by two ligand-based $dpp^{0/-}$ reductions at –0.71 and –1.03 V. The CV results provide evidence for a Ru-based highest occupied molecular orbital (HOMO) and Rh-based lowest unoccupied molecular orbital (LUMO), requirements for PEC and active molecular photocatalysis of H_2 production. The $Rh^{III/II/I}$ reduction occurs more negatively in **1-OH** than in **1-Cl** (–0.34 V) or **1-Br** (–0.32 V). The stronger field OH^- ligands make the Rh center more difficult to reduce in **1-OH** than in the complexes bearing halides, therefore shifting the Rh-based reduction to a more negative potential.[28, 46]

Table 4.1. Summary of Electrochemical Properties

Complex [a]	$E_{1/2}$ (V)	Assignment
1-OH	+1.62	2 $Ru^{II/III}$
	–0.38 [d]	$Rh^{III/II/I}$
	–0.71	dpp,dpp/dpp,dpp^-
	–1.03	dpp,dpp^-/dpp^-,dpp^-
1-Cl [b]	+1.60	2 $Ru^{II/III}$
	–0.34 [d]	$Rh^{III/II/I}$
	–0.75	dpp,dpp/dpp,dpp^-
	–1.02	dpp,dpp^-/dpp^-,dpp^-
1-Br [c]	+1.60	2 $Ru^{II/III}$
	–0.32 [d]	$Rh^{III/II/I}$
	–0.73	dpp,dpp/dpp,dpp^-
	–1.04	dpp,dpp^-/dpp^-,dpp^-

[a] Measurements were performed at a scan rate of 100 mVs^{-1} using deoxygenated 0.1 M Bu_4NPF_6 electrolyte in CH_3CN at RT with a glassy carbon working electrode, platinum wire auxiliary electrode, and Ag/AgCl reference electrode. [b] Values consistent with those in [23]. [c] Values consistent with those in Reference 28. [d] E_p^c of reversible process.

Complex **1-OH** is an efficient light absorber in the UV and visible regions, an important feature for carrying out H_2O reduction photocatalysis (**Figure 4.2**).

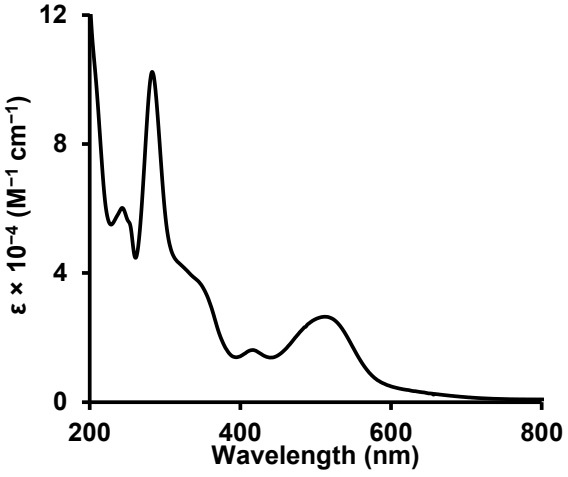

Figure 4.2. Electronic absorption spectrum for complex **1-OH** in RT CH_3CN.

The UV absorption is dominated by intraligand (IL) π→π* transitions, with bpy π→π* transitions at λ^{abs} = 283 nm (ε = 10.2×10^4 $M^{-1}cm^{-1}$) and dpp π→π* transitions at λ^{abs} =

342 nm (ε = 3.8×10^4 $M^{-1}cm^{-1}$). The visible absorption is dominated by Ru(dπ)→ligand(π*) metal-to-ligand charge transfer (^{1}MLCT) transitions, with Ru(dπ)→bpy(π*) CT transitions at λ^{abs} = 417 nm (ε = 1.6×10^4 $M^{-1}cm^{-1}$) and lowest-energy Ru(dπ)→dpp(π*) CT transitions at λ^{abs} = 512 nm (ε = 2.7×10^4 $M^{-1}cm^{-1}$). Nearly identical light absorbing properties among **1-OH**, **1-Cl**, and **1-Br** (**Table 4.2**) demonstrate that the ground state optical properties of the trimetallic complexes are not greatly perturbed by substitution of the nonchromophoric ligands at Rh.

Table 4.2. Summary of Light Absorbing Properties

Complex [a]	λ^{abs} (nm)	ε (10^4 $M^{-1}cm^{-1}$)	Assignment
1-OH	283	10.2	bpy(π)→(π*)
	342	3.8	dpp(π)→(π*)
	417	1.6	Ru(dπ)→bpy(π*)
	512	2.7	Ru(dπ)→dpp(π*)
1-Cl [b]	283	10.4	bpy(π)→(π*)
	342	3.9	dpp(π)→(π*)
	416	1.7	Ru(dπ)→bpy(π*)
	510	2.7	Ru(dπ)→dpp(π*)
1-Br [b]	284	10.4	bpy(π)→(π*)
	342	3.8	dpp(π)→(π*)
	417	1.8	Ru(dπ)→bpy(π*)
	511	2.7	Ru(dπ)→dpp(π*)

[a] Spectra obtained in CH_3CN at RT in a 1 cm quartz cuvette. [b] Values consistent with those in Reference 23. [c] Values consistent with those in References 28 and 47.

Photoexcitation into the lowest-energy ^{1}MLCT excited state results in unity population of the ^{3}MLCT excited state from where radiative decay occurs and provides a probe to study the excited state dynamics (**Figure 4.3**). In the Rh-centered complexes, intramolecular electron transfer to produce the Ru(dπ)→Rh(dσ*) ^{3}MMCT excited state is accomplished due to the Rh(dσ*)-based LUMO. Complex **1-OH** displays a weak, low-energy emission (λ^{em} = 785 nm, Φ^{em} = 3.2×10^{-4}, τ = 41 ns) (**Figure 4.S3**) that is

quenched 70% relative to the model complex $[\{(bpy)_2Ru\}_2(dpp)]^{4+}$ (λ^{em} = 790 nm, Φ^{em} = 9.7×10^{-4}, τ = 140 ns)[26] that lacks a low-energy Ru(dπ)→Rh(dσ*) ^{3}MMCT excited state.

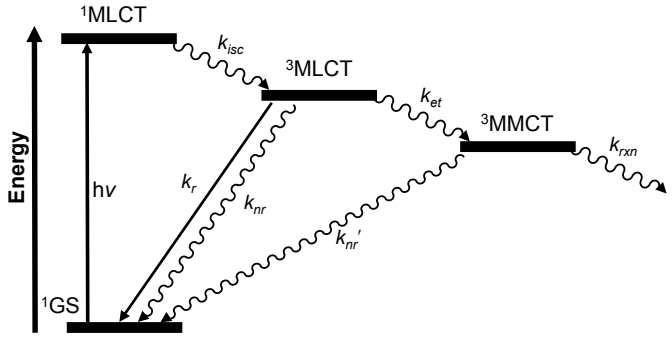

Figure 4.3. Simplified Jablonski-type state diagram for **1-OH**, **1-Cl**, and **1-Br**. ^{1}GS = singlet ground state; k_{isc} = rate of intersystem crossing; k_r = rate of radiative decay; k_{nr} = rate of nonradiative decay; k_{et} = rate of intramolecular electron transfer; k_{rxn} = rate of photochemical reaction.

Compared to **1-Cl** and **1-Br**,[26, 47] the larger Φ^{em} and decreased electron transfer rate to populate the ^{3}MMCT excited state (k_{et}) in **1-OH** is consistent with the stronger field OH^- ligands providing greater destabilization of the Rh-based acceptor orbitals. The small Φ^{em} and short τ for **1-Br** is consistent with the heavy atom effect playing a role in excited state deactivation.[48] Differences in excited state properties among **1-OH**, **1-Cl**, and **1-Br** (**Table 4.3**) imply different rates of population of the lowest lying ^{3}MMCT excited state ($k_{et}\times10^7$ (s^{-1}) **1-OH** = 1.7; **1-Cl** = 1.9; **1-Br** = 2.3), a factor postulated to influence photocatalytic H_2 production efficiency.

Table 4.3. Summary of Excited State Properties

Complex [a]	λ^{em} (nm)	Φ^{em} (10^{-4})	τ (ns)	k_{et} (10^7 s^{-1})
1-OH	785	3.2	41	1.7
1-Cl [b]	776	2.6	38	1.9
1-Br [b]	776	1.4	34	2.3

[a] Spectra obtained in deoxygenated CH_3CN at RT in a 1 quartz cm cuvette. [b] Values from References 26 and 47.

An enhanced rate of population of the ^{3}MMCT excited state (k_{et}) in **1-Br** was previously proposed to account for greater photocatalytic H_2 production relative to photocatalyst **1-Cl**,[27-28] and the halide-free **1-OH** allows further exploration of this complex phenomenon. Among **1-OH**, **1-Cl**, and **1-Br**, **1-OH** has the lowest k_{et} value, indicating a decreased rate of population of the ^{3}MMCT excited state from the ^{3}MLCT excited state. Greater H_2 production in organic solvent by **1-OH** relative to **1-Cl** or **1-Br** (*vide infra*) suggests alternative pathways exist to enhance photoinitiated electron collection at Rh. The excited state reduction potentials for the ^{3}MLCT and ^{3}MMCT excited states for **1-OH** are estimated using our reported method[27] to be 1.40 and 1.07 V vs. NHE (normal hydrogen electrode), respectively. The DMA sacrificial reductant is therefore thermodynamically capable of quenching both the ^{3}MLCT and ^{3}MMCT excited states ($E_{1/2}^{oxd}$ = 1.05 V vs. NHE) with similar driving forces for reductive quenching for **1-OH**, **1-Cl**, and **1-Br**.[27] Earlier studies indicated that the ^{3}MLCT excited state provides a catalytically important pathway for photoreduction to produce H_2. Enhanced photocatalytic activity for **1-OH** despite the lower k_{et} of population of the ^{3}MMCT excited state further supports this idea that reductive quenching of the ^{3}MLCT excited state is important in H_2 production schemes for this structural motif. Additional factors capable of influencing H_2 production by **1-OH**, **1-Cl**, and **1-Br** will be later discussed.

4.3.2. Photocatalytic H_2 Production Studies

Complex **1-OH** was investigated as a solar H_2 evolution photocatalyst due to its ability to efficiently absorb light and collect electrons at Rh. Photocatalytic H_2 production experiments by **1-OH** compared to **1-Cl** and **1-Br** were carried out to gain an

understanding about the role of the labile ligands at Rh during photocatalysis. When photolyzed for 20 h at 470 nm with DMA electron donor (1.5 M) in *N,N*-dimethylformamide (DMF) solvent containing H_2O (0.62 M), **1-OH** (65 μM) produces 24±2 μmol of H_2 (83±6 TON = turnover number = mol H_2 produced/mol catalyst) (**Figure 4.4**), a nearly 3-fold increase in H_2 production relative to photocatalyst **1-Cl**, producing 9±1 μmol of H_2 (30±4 TON) under the same conditions. Photocatalyst **1-Br** is more active than **1-Cl** and less active than **1-OH**, producing 13±1 μmol of H_2 (45±4 TON). Switching to CH_3CN as the photocatalytic solvent, **1-OH** remains the most active photocatalyst in the series, producing 8±0.7 μmol of H_2 (28±2 TON), followed by **1-Br** with 4±0.1 μmol of H_2 (15±1 TON), and lastly **1-Cl** with 3±0.4 μmol of H_2 (10±1 TON). While H_2 yields are lower overall in CH_3CN solvent due to its stronger ligating ability relative to DMF,[31, 49] the trend in photocatalytic activity is consistent in both solvents of similar polarity.

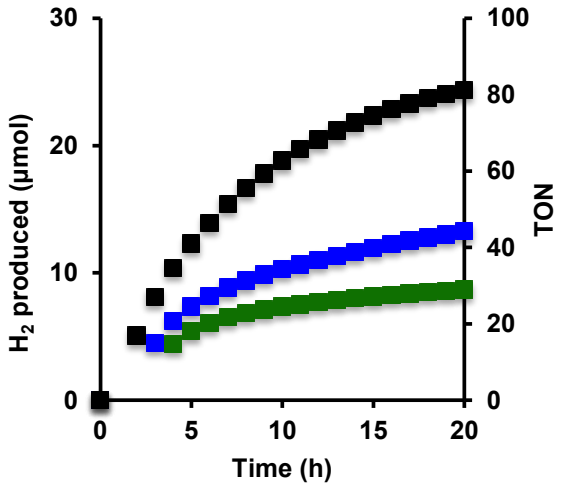

Figure 4.4. H_2 production by photocatalysts **1-OH** (black squares), **1-Cl** (green squares), and **1-Br** (blue squares) in Ar-purged DMF solvent. [photocatalyst] = 65 μM; [H_2O] = 0.62 M; [DMA] = 1.5 M; [$DMAH^+$][$CF_3SO_3^-$] = 110 μM; λ^{irr} = 470 nm.

With the goal of accomplishing solar H_2 evolution in a more environmentally conscious solvent, photolysis experiments were performed in purely aqueous solution (**Figure 4.5**).

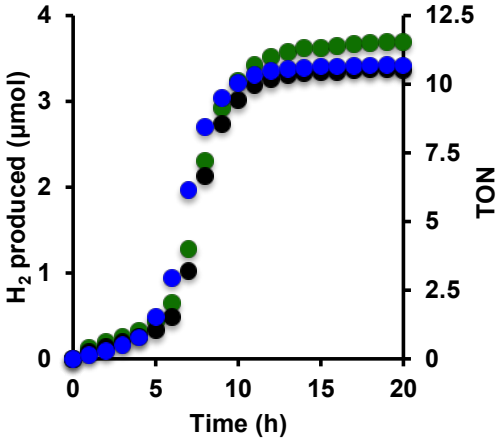

Figure 4.5. H_2 production by photocatalysts **1-OH** (black circles), **1-Cl** (green circles), and **1-Br** (blue circles) in Ar-purged aqueous solvent. [photocatalyst] = 65 μM; [ascorbate buffer] = 1.1 M; λ^{irr} = 470 nm.

DMA electron donor is poorly miscible with H_2O; therefore, ascorbate buffer was used as the sacrificial reductant. When 65 μM of photocatalyst is irradiated at 470 nm for 20 h in aqueous medium with pH 4 ascorbate buffer (0.55 M sodium ascorbate; 0.55 M ascorbic acid), relatively lower H_2 yields are obtained in H_2O solvent as expected;[41] yet interestingly, **1-OH**, **1-Cl**, and **1-Br** produce nearly identical amounts of H_2 (**1-OH** produces 3.4±0.1 μmol of H_2 (11±1 TON), **1-Cl** produces 3.7±0.1 μmol of H_2 (11±1 TON), and **1-Br** produces 3.4±0.3 μmol of H_2 (11±1 TON)). The electronic absorption spectra of **1-OH**, **1-Cl**, and **1-Br** after photocatalysis in H_2O are identical (**Figure 4.6**), indicating that the same photoreduced species are present in solution after photolysis.

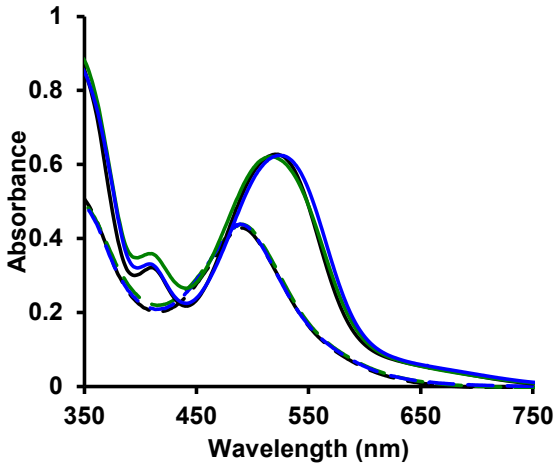

Figure 4.6. Electronic absorption spectrum for complexes **1-OH**: black line, **1-Cl**: green line, and **1-Br**: blue line in Ar-purged water (———) and following 20 h photolysis in the presence of pH 4 ascorbate buffer electron donor (- - - -).

The shift to higher energy of the Ru→dpp ^{1}MLCT transition following photolysis in the presence of an electron donor is consistent with the formation of the two-electron-reduced photoproduct, $[\{(bpy)_2Ru(dpp)\}_2Rh^{I}]^{5+}$.[23-24, 49] H_2 photocatalysis by **1-OH**, **1-Cl**, and **1-Br** operating through PEC with a readily available electron donor in aqueous solution is a promising direction for this series and related homogeneous, single-component photocatalysts.

Many factors exist that must be considered when examining the H_2 production abilities of photocatalysts **1-OH**, **1-Cl**, and **1-Br**. In relatively low polarity solvents such as DMF and CH_3CN, the identity of the labile ligands coordinated to Rh impacts the observed photocatalytic H_2 production. The influence of the ligands at Rh on photocatalysis is an interesting result considering these ligands must dissociate from the six-coordinate Rh^{III} to form the four-coordinate Rh^{I} catalyst capable of reducing H_2O to H_2 fuel (**Figure 4.7**).[24]

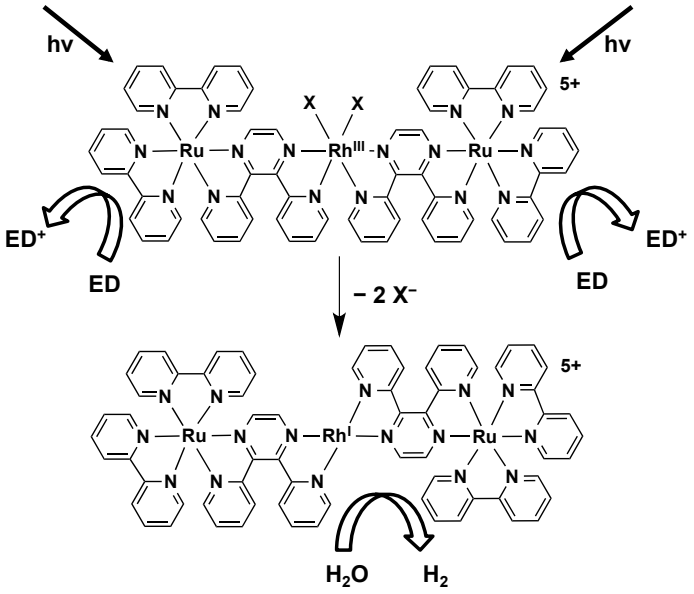

Figure 4.7. Scheme representing photoinitiated electron collection leading to photocatalytic H_2 production from H_2O by complexes **1-OH**, **1-Cl**, or **1-Br** (X^- = OH^-, Cl^-, or Br^-). hv = photoexcitation; ED = sacrificial electron donor.

Recently, we provided evidence for ion pairing with halides as a photocatalyst deactivator in a $Ru^{II}Rh^{III}$ bimetallic motif bearing either Cl^- or Br^- halides at Rh.[30] Solvent variation affords a medium to study ion pairing in the $Ru^{II}Rh^{III}Ru^{II}$ architecture as the force for ion pairing is inversely related to solvent polarity, represented by the solvent's dielectric constant (ε). Consequently, in relatively low dielectric solvents of similar polarity like DMF (ε = 38) and CH_3CN (ε = 37), ion pairing between the photocatalyst and the anions formerly coordinated to Rh is probable, providing an explanation for the observed differences in H_2 production among **1-OH**, **1-Cl**, and **1-Br**. However, in aqueous solvent, the identity of the labile ligands bound to Rh does not alter the observed H_2 evolution. Water, a more polar solvent (ε = 80) than DMF and CH_3CN, provides an environment where ion pairing is minimized, thus the influence of the dissociated halides and OH^- ligands is indistinguishable.

When H_2 photocatalysis experiments are carried out in solvents of lower polarity such as DMF or CH_3CN, an apparent photocatalyst solution pH of ~9 exists based on the pKa of $DMAH^+$ (5.07).[27] When **1-Cl** or **1-Br** are employed for solar H_2 photocatalysis, the halide ligands are dissociated upon formation of the active Rh^I catalyst. Yet, the identity of the halides alters H_2 evolution. Because of the low pKa of both HCl (–7) and HBr (–8), the halides will not be protonated in the bulk solution (pH ~ 9) and will remain negatively charged and in close proximity to the positively charged photocatalyst. With electrostatic attraction dominating through ion pairing between the halides and the photocatalyst as it cycles from $Rh^{III/II/I}$, halides may hinder interaction of the photocatalyst with the H_2O substrate and negatively impact observed H_2 production yields. However, with photocatalyst **1-OH**, the OH^- ligands dissociated upon formation of the Rh^I active catalyst are likely protonated in the bulk solution (pKa of H_2O = 14)[50] as photocatalysis proceeds. The H_2O generated in the bulk solution furthers the catalytic cycle for H_2 production from this substrate. H_2 evolution by **1-OH** is not impeded by ion pairing between the photocatalyst and negatively charged ions capable of hindering substrate interaction as observed for the halide analogues.

4.4. Conclusions

A new $Ru^{II}Rh^{III}Ru^{II}$ photocatalyst **1-OH** was synthesized with OH^- ligands bound to the catalytically active Rh center. The complex was characterized and studied for H_2O reduction photocatalysis relative to halide analogues **1-Cl** and **1-Br**. CV results for **1-OH** establish a Ru-based HOMO and Rh-based LUMO that provide evidence for multi-electron collection at Rh. **1-OH** is an effective UV and visible light absorber, possessing

a lowest energy Ru(dπ)→dpp(π*) ^{1}MLCT transition. The ground state electronic properties of the complex are not perturbed by substitution of the OH^- ligands at Rh for Cl^- or Br^- halides. Quenched emission and a short excited state lifetime from the ^{3}MLCT excited state for **1-OH** relative to the $Ru^{II}Ru^{II}$ model complex support photoinitiated electron collection at Rh via population of the low energy Ru(dπ)→Rh(dσ*) ^{3}MMCT excited state.

H_2 photocatalytic experiments provide further insight on the impact of the ligands bound to Rh in solar fuel production schemes by single-component photocatalysts. **1-OH** is a superior H_2 photocatalyst in organic solvents DMF and CH_3CN relative to **1-Cl** and **1-Br**, suggesting that halides are detrimental to photocatalysis and that ion pairing between the halides and the photocatalyst may be important. Furthermore, differences in photocatalytic H_2 evolution and excited state properties among **1-OH**, **1-Cl**, and **1-Br** suggest intramolecular electron transfer within the supramolecule may impact rates of photoinitiated electron collection at Rh, thereby affecting observed photocatalytic activity. The mechanism for solar H_2 production using these molecular architectures is quite complicated and evidently many factors contribute to the functioning of the photosystem. Notable differences in photocatalysis with seemingly small structural variation emphasize the importance of judicious molecular component choice to achieve superior H_2 yields. **1-OH**, **1-Cl**, and **1-Br** are photocatalytically active toward H_2 evolution in aqueous solution, a desirable solvent system with positive environmental implications. Interestingly, similar H_2 production activity is shown for all three photocatalysts in the high dielectric aqueous solvent where ion pairing is minimized, indicating that ion pairing

is an important consideration in the development of molecular architectures for photocatalytic H_2 production schemes. Studies are ongoing in our laboratory to better understand the factors that impact photocatalytic function by these and related photocatalysts.

4.5. Experimental Section

4.5.1. Materials

All chemicals unless otherwise noted were used as received. The reagents ruthenium trichloride trihydrate ($RuCl_3 \cdot 3H_2O$), rhodium trichloride trihydrate ($RhCl_3 \cdot 3H_2O$), potassium hydroxide (KOH), and trifluoromethanesulfonic acid (CF_3SO_3H) were purchased from Alfa Aesar. 2,3-Bis(2-pyridyl)pyrazine (dpp) was purchased from Sigma-Aldrich Corporation. Ammonium hexafluorophosphate (NH_4PF_6) and cis-dichlorobis(2,2'-bipyridine)ruthenium(II) hydrate $[(bpy)_2RuCl_2] \cdot 2H_2O$ were purchased from Strem Chemicals, Inc. Tetra-n-butylammonium hexafluorophosphate (Bu_4NPF_6) was purchased from Fluka. Spectrophotometric grade acetonitrile (CH_3CN) was purchased from Burdick and Jackson. 100% Ethanol was purchased from Decon Labs, Inc. Toluene, diethyl ether, and 80-200 mesh adsorption alumina were purchased from Fischer Scientific. $[(bpy)_2Ru(dpp)](PF_6)_2$,[45] $[\{(bpy)_2Ru(dpp)\}_2RhCl_2](PF_6)_5$ (**1-Cl**),[51] and $[\{(bpy)_2Ru(dpp)\}_2RhBr_2](PF_6)_5$ (**1-Br**)[28] were prepared as previously reported.

4.5.2. Synthesis of $[Rh(H_2O)_6](CF_3SO_3)_3$

The complex $[Rh(H_2O)_6](CF_3SO_3)_3$ was prepared similar to a reported method.[44] The starting material $RhCl_3 \cdot 3H_2O$ (0.50 g, 1.90 mmol) was dissolved at RT with stirring in 15 mL water. To the deep red solution, a 0.1 M KOH solution was added drop wise

until pH 13 was reached. As the pH of the solution increased, a cloudy yellow precipitate formed. The suspension was transferred to a centrifuge tube and centrifuged multiple times, removing the supernatant and washing with copious amounts water each time to ensure removal of all Cl^-. The remaining yellow solid was suspended in a minimal amount of water in a two-neck round bottom flask. Neat CF_3SO_3H (~2 mL) was added drop wise until the solid fully dissolved. The yellow solution was heated at reflux for 7 d. Upon completion of heating, the yellow solution was syringe filtered prior to analysis. Electronic absorption spectroscopy in CF_3SO_3H acidified water, λ (ε): 311 nm (64.7 $M^{-1}cm^{-1}$) and 396 nm (62 $M^{-1}cm^{-1}$).[52]

*4.5.3. Synthesis of [{(bpy)$_2$Ru(dpp)}$_2$Rh(OH)$_2$](PF$_6$)$_5$ (**1-OH**)*

The new complex [{(bpy)$_2$Ru(dpp)}$_2$Rh(OH)$_2$](PF$_6$)$_5$ was prepared with adaptation of a similar method.[51] The starting materials [(bpy)$_2$Ru(dpp)](PF$_6$)$_2$ (0.30 g, 0.32 mmol) and [Rh(H$_2$O)$_6$](CF$_3$SO$_3$)$_3$ (0.16 mmol, prepared spectrophotometrically) were combined in 2:1 (v/v) ethanol/water and heated at reflux for 1 h. Upon cooling to RT, the sample was added drop wise to a 2 M aqueous NH_4PF_6 solution to induce precipitation as a PF_6^- salt. A deep red/purple solid was collected via vacuum filtration. Typical size-exclusion purification for multimetallic $Ru^{II}Rh^{III}$ complexes was not performed with the synthesized complex due to the strong likelihood of the cis-Rh(OH)$_2$ subunit interacting with the stationary phase of the chromatography column. Therefore, the complex was purified by 3× reprecipitation from CH_3CN/diethyl ether. A deep red/purple solid was collected via vacuum filtration and rinsed with excess diethyl ether (0.31 g, 0.14 mmol, yield = 89%). ESI-MS: $[M - PF_6^-]^+$, *m/z* = 2013.03.

4.6. Acknowledgements

The Chemical Sciences, Geosciences and Biosciences Division, Office of Basic Energy Sciences, Office of Sciences, U.S. Department of Energy (DE FG02-05ER15751) is acknowledged for generous financial support of this work. Prof. J. M. Tanko, Dr. Travis A. White, Mr. Theodore R. Canterbury, and Dr. Alec T. Wagner are acknowledged for assistance with the preparation of this manuscript. Mr. William Bebout of the Virginia Tech Department of Chemistry Analytical Services Laboratory is acknowledged for assistance with mass spectral data.

4.7. Supplemental Information

4.7.1. Methods

4.7.1.1. Mass Spectrometry

Samples were analyzed using electrospray ionization time-of-flight mass spectrometry (ESI-MS) with an Agilent Technologies 6220 Accurate-Mass TOF LC-MS with a dual ESI source to obtain high-resolution mass spectral data. The solvent used was HPLC grade methanol.

4.7.1.2. Electrochemistry

Cyclic voltammograms were obtained using a Bioanalytical Systems (BAS) Epsilon electrochemical analyzer. In a three electrode, one compartment cell, 0.1 M Bu_4NPF_6 in spectrophotometric grade CH_3CN was the supporting electrolyte solution. The working electrode was glassy carbon, the auxiliary electrode was a platinum wire, and the reference electrode was Ag/AgCl calibrated against the ferrocene/ferrocenium

($FeCp_2/FeCp_2^+$) redox couple.[53] Cyclic voltammograms were obtained at a scan rate of 100 mVs^{-1}.

4.7.1.3. Electronic Absorption Spectroscopy

Electronic absorption spectra were obtained using a Hewlett Packard 8453 diode array spectrophotometer. Using a sampling interval of 1 nm, measurements were obtained in a wavelength range of 190-1100 nm. Measurements were carried out in a 0.4 cm or 1 cm path length quartz cuvette (Starna Cells, Inc., Atascadero, CA) in room temperature spectrophotometric grade CH_3CN. Extinction coefficient measurements were performed in triplicate.

4.7.1.4. Steady-State Luminescence Spectroscopy

Steady-state emission spectra were measured using a QuantaMaster Model QM-200-45E fluorimeter from Photon Technologies Internation, Inc. Spectra were obtained using a 1 cm path length quartz cuvette and room temperature deoxygenated spectrophotometric grade CH_3CN. The excitation source was a water-cooled 150 W xenon arc lamp and the emission spectra were obtained at a 90° angle with a thermoelectrically cooled Hamamatsu 2658 photomultiplier tube operating in photon counting mode with 0.25 nm resolution. The quantum yields of emission were measured relative to $[Os(bpy)_3]^{2+}$ ($\Phi^{em} = 4.62 \times 10^{-3}$).[54] Emission spectra were corrected for PMT response using the manufactured-supplied correction file.

4.7.1.5. Time-Resolved Luminescence Spectroscopy

The excited state lifetimes were measured using a Photon Technologies International, Inc. PL-2300 nitrogen laser with an attached PL-201 tunable dye laser

using Coumarin 500 dye. The excitation monochromator was set to 540 nm and emission from the sample was detected at a 90° angle from the excitation source by passing through an emission monochromator set to 780 nm with a Hamamatsu R928 photomultiplier tube operating in direct output mode. The signal was recorded using a Techronix TDX 3052C oscilloscope, averaging the results of 300 sweeps.

4.7.1.6. H_2 Photolysis Experiments

To measure photocatalytic H_2 production by photocatalysts **1-OH**, **1-Cl**, and **1-Br**, experiments were carried out using a similar method as reported by our group.[24] For those reactions involving organic solvent (CH_3CN or DMF), stock solutions were spectrophotometrically prepared in the appropriate solvent and then combined with water in the airtight photolysis reaction cell sealed with a 10 mm septum. The catalyst in the organic solvent/water mixture was deoxygenated using Ar gas for 10 min before injection of the separately deoxygenated DMA electron donor. The 4.5 mL total solution volume was comprised of 65 μM (0.29 μmol) photocatalyst, 0.62 M H_2O, 1.5 M DMA, 0.11 mM $[DMAH^+][CF_3SO_3^-]$, and the cell had a headspace of 16.0 mL. For those reactions involving aqueous solvent, stock solutions were spectrophotometrically prepared in water and combined with the ascorbate buffer solution prior to degassing for 15 min. The 5.0 mL total solution was comprised of 65 μM photocatalyst (0.29 μmol) and 1.1 M pH 4 ascorbate buffer solution (0.55 M sodium ascorbate; 0.55 M ascorbic acid), and the cell had a headspace of 15.5 mL. The solution was irradiated with a 470 nm LED array constructed in-house (LED array light flux = $2.36\pm0.05 \times 10^{19}$ photons/min).[55] H_2 gas production was monitored in real time using HY-OPTIMA 700 in-

line process solid-state H_2 sensors from H_2scan (Valencia, CA) that was connected to the photolysis cell using an o-ring for an airtight seal. The value reported for H_2 production is an average of three trials run simultaneously.

4.7.2. Supplemental Figures

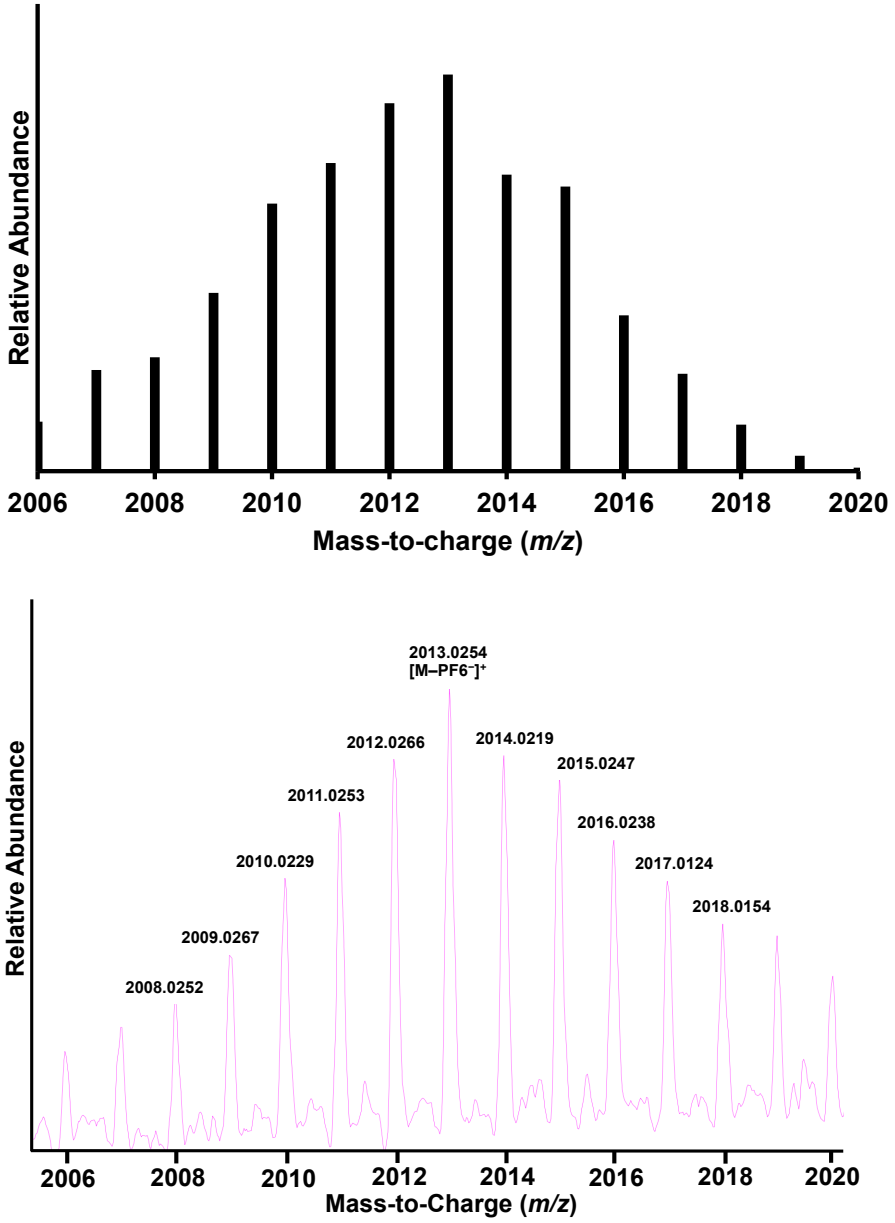

Figure 4.S1. Calculated (top) and experimental (bottom) mass spectrum for complex $[\{(bpy)_2Ru(dpp)\}_2Rh(OH)_2](PF_6)_5$ (**1-OH**). The molecular ion peak corresponds to $[M–PF_6^-]^+$.

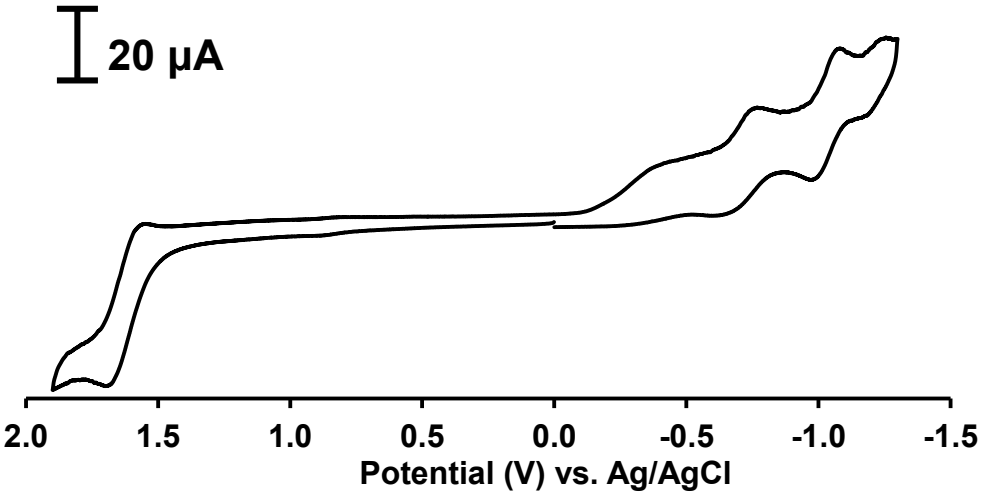

Figure 4.S2. Cyclic voltammogram for complex $[\{(bpy)_2Ru(dpp)\}_2Rh(OH)_2](PF_6)_5$ (**1-OH**) under an Ar atmosphere in 0.1 M Bu_4NPF_6/CH_3CN solution at RT with a glassy carbon working electrode (v = 100 mVs^{-1}).

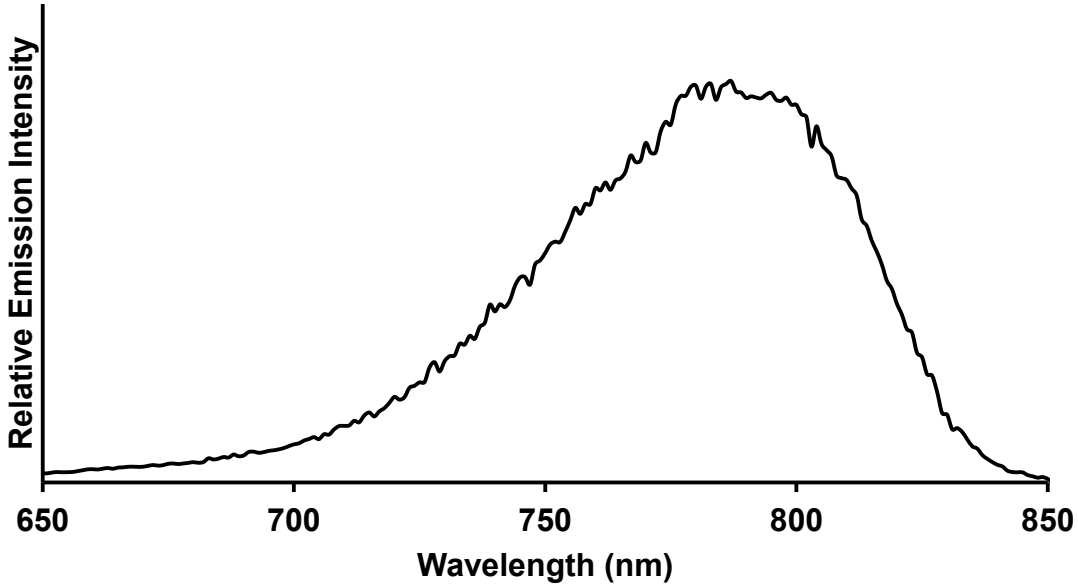

Figure 4.S3. Steady-state emission spectrum for complex $[\{(bpy)_2Ru(dpp)\}_2Rh(OH)_2](PF_6)_5$ (**1-OH**) obtained in RT deoxygenated CH_3CN in a 1 cm quartz cuvette cell.

4.8. References

1. Hammarstrom, L., "Accumulative Charge Separation for Solar Fuels Production: Coupling Light-Induced Single Electron Transfer to Multielectron Catalysis." *Accounts of Chemical Research* **2015,** *48* (3), 840-850.
2. Berardi, S.; Drouet, S.; Francas, L.; Gimbert-Surinach, C.; Guttentag, M.; Richmond, C.; Stoll, T.; Llobet, A., "Molecular artificial photosynthesis." *Chemical Society Reviews* **2014,** *43* (22), 7501-7519.
3. Walter, M. G.; Warren, E. L.; McKone, J. R.; Boettcher, S. W.; Mi, Q. X.; Santori, E. A.; Lewis, N. S., "Solar water splitting cells." *Chemical Reviews* **2010,** *110* (11), 6446-6473.
4. McDaniel, N. D.; Bernhard, S., "Solar fuels: thermodynamics, candidates, tactics, and figures of merit." *Dalton Transactions* **2010,** *39* (42), 10021-10030.
5. Khnayzer, R. S.; Thoi, V. S.; Nippe, M.; King, A. E.; Jurss, J. W.; El Roz, K. A.; Long, J. R.; Chang, C. J.; Castellano, F. N., "Towards a comprehensive understanding of visible-light photogeneration of hydrogen from water using cobalt(II) polypyridyl catalysts." *Energy & Environmental Science* **2014,** *7* (4), 1477-1488.
6. Han, Z.; Eisenberg, R., "Fuel from Water: The Photochemical Generation of Hydrogen from Water." *Accounts of Chemical Research* **2014,** *47* (8), 2537-2544.
7. Frischmann, P. D.; Mahata, K.; Wurthner, F., "Powering the future of molecular artificial photosynthesis with light-harvesting metallosupramolecular dye assemblies." *Chemical Society Reviews* **2013,** *42* (4), 1847-1870.
8. Eckenhoff, W. T.; Eisenberg, R., "Molecular systems for light driven hydrogen production." *Dalton Transactions* **2012,** *41* (42), 13004-13021.
9. Esswein, M. J.; Nocera, D. G., "Hydrogen production by molecular photocatalysis." *Chemical Reviews* **2007,** *107* (10), 4022-4047.
10. Deponti, E.; Luisa, A.; Natali, M.; Iengo, E.; Scandola, F., "Photoinduced hydrogen evolution by a pentapyridine cobalt complex: elucidating some mechanistic aspects." *Dalton Transactions* **2014,** *43* (43), 16345-16353.
11. Shan, B.; Baine, T.; Ma, X. A. N.; Zhao, X.; Schmehl, R. H., "Mechanistic Details for Cobalt Catalyzed Photochemical Hydrogen Production in Aqueous Solution: Efficiencies of the Photochemical and Non-Photochemical Steps." *Inorganic Chemistry* **2013,** *52* (9), 4853-4859.
12. Chan, S. F.; Chou, M.; Creutz, C.; Matsubara, T.; Sutin, N., "Mechanism of the formation of dihydrogen from the photoinduced reactions of poly(pyridine)ruthenium(II) and poly(pyridine)rhodium(III) complexes " *Journal of the American Chemical Society* **1981,** *103* (2), 369-379.
13. Kirch, M.; Lehn, J. M.; Sauvage, J. P., "Hydrogen generation by visible-light irradiation of aqueous-solutions of metal-complexes - approach to the photo-chemical conversion and storage of solar-energy " *Helvetica Chimica Acta* **1979,** *62* (4), 1345-1384.
14. Schulz, M.; Karnahl, M.; Schwalbe, M.; Vos, J. G., "The role of the bridging ligand in photocatalytic supramolecular assemblies for the reduction of protons and carbon dioxide." *Coordination Chemistry Reviews* **2012,** *256* (15-16), 1682-1705.

15. Ozawa, H.; Sakai, K., "Photo-hydrogen-evolving molecular devices driving visible-light-induced water reduction into molecular hydrogen: structure-activity relationship and reaction mechanism." *Chemical Communications* **2011,** *47* (8), 2227-2242.
16. Balzani, V.; Moggi, L.; Scandola, F., Towards a Supramolecular Photochemistry: Assembly of Molecular Components to Obtain Photochemical Molecular Devices. In *Supramolecular Photochemistry*, Balzani, V., Ed. NATO ASI Series 214, Reidel, Dordrecht: The Netherlands: 1987; pp 1-28.
17. Balzani, V.; Juris, A.; Venturi, M.; Campagna, S.; Serroni, S., "Luminescent and redox-active polynuclear transition metal complexes." *Chemical Reviews* **1996,** *96* (2), 759-833.
18. Molnar, S. M.; Nallas, G.; Bridgewater, J. S.; Brewer, K. J., "Photoinitiated electron collection in a mixed-metal trimetallic complex of the form $[\{(bpy)_2Ru(dpb)]_2IrCl_2\}(PF_6)_5$ (bpy = 2,2'-bipyridine and dpb = 2,3-bis(2-pyridyl)benzoquinoxaline)." *Journal of the American Chemical Society* **1994,** *116* (12), 5206-5210.
19. Fukushima, T.; Fujita, E.; Muckerman, J. T.; Polyansky, D. E.; Wada, T.; Tanaka, K., "Photochemical Stereospecific Hydrogenation of a Ru Complex with an NAD(+)/NADH-Type Ligand." *Inorganic Chemistry* **2009,** *48* (24), 11510-11512.
20. Polyansky, D. E.; Cabelli, D.; Muckerman, J. T.; Fukushima, T.; Tanaka, K.; Fujita, E., "Mechanism of hydride donor generation using a Ru(II) complex containing an NAD(+) model ligand: Pulse and steady-state radiolysis studies." *Inorganic Chemistry* **2008,** *47* (10), 3958-3968.
21. Konduri, R.; Ye, H. W.; MacDonnell, F. M.; Serroni, S.; Campagna, S.; Rajeshwar, K., "Ruthenium photocatalysts capable of reversibly storing up to four electrons in a single acceptor ligand: A step closer to artificial photosynthesis." *Angewandte Chemie-International Edition* **2002,** *41* (17), 3185-3187.
22. Kim, M. J.; Konduri, R.; Ye, H. W.; MacDonnell, F. M.; Puntoriero, F.; Serroni, S.; Campagna, S.; Holder, T.; Kinsel, G.; Rajeshwar, K., "Dinuclear ruthenium(II) polypyridyl complexes containing large, redox-active, aromatic bridging ligands: Synthesis, characterization, and intramolecular quenching of MLCT excited states." *Inorganic Chemistry* **2002,** *41* (9), 2471-2476.
23. Elvington, M.; Brewer, K. J., "Photoinitiated electron collection at a metal in a rhodium-centered mixed-metal supramolecular complex." *Inorganic Chemistry* **2006,** *45* (14), 5242-5244.
24. Elvington, M.; Brown, J.; Arachchige, S. M.; Brewer, K. J., "Photocatalytic hydrogen production from water employing a Ru, Rh, Ru molecular device for photoinitiated electron collection." *Journal of the American Chemical Society* **2007,** *129* (35), 10644-10645.
25. White, T. A.; Higgins, S. L. H.; Arachchige, S. M.; Brewer, K. J., "Efficient photocatalytic hydrogen production in a single-component system using Ru,Rh,Ru supramolecules containing 4,7-diphenyl-1,10-phenanthroline." *Angewandte Chemie-International Edition* **2011,** *50*, 12209-12213.

26. White, T. A.; Rangan, K.; Brewer, K. J., "Synthesis, characterization, and study of the photophysics and photocatalytic properties of the photoinitiated electron collector [{(phen)$_2$Ru(dpp)}$_2$RhBr$_2$](PF$_6$)$_5$." *Journal of Photochemistry and Photobiology A: Chemistry* **2010,** *209* (2-3), 203-209.
27. Arachchige, S. M.; Brown, J. R.; Chang, E.; Jain, A.; Zigler, D. F.; Rangan, K.; Brewer, K. J., "Design considerations for a system for photocatalytic hydrogen production from water employing mixed-metal photochemical molecular devices for photoinitiated electron collection." *Inorganic Chemistry* **2009,** *48* (5), 1989-2000.
28. Arachchige, S. M.; Brown, J.; Brewer, K. J., "Photochemical hydrogen production from water using the new photocatalyst [{(bpy)$_2$Ru(dpp)}$_2$RhBr$_2$](PF$_6$)$_5$." *Journal of Photochemistry and Photobiology A: Chemistry* **2008,** *197* (1), 13-17.
29. Pfeffer, M. G.; Kowacs, T.; Wachtler, M.; Guthmuller, J.; Dietzek, B.; Vos, J. G.; Rau, S., "Optimization of Hydrogen-Evolving Photochemical Molecular Devices." *Angewandte Chemie-International Edition* **2015,** *54* (22), 6627-6631.
30. Rogers, H. M.; White, T. A.; Stone, B. N.; Arachchige, S. M.; Brewer, K. J., "Nonchromophoric Halide Ligand Variation in Polyazine-Bridged Ru(II),Rh(III) Bimetallic Supramolecules Offering New Insight into Photocatalytic Hydrogen Production from Water." *Inorganic Chemistry* **2015,** *54* (7), 3545-3551.
31. White, T. A.; Whitaker, B. N.; Brewer, K. J., "Discovering the balance of steric and electronic factors needed to provide a new structural motif for photocatalytic hydrogen production from water." *Journal of the American Chemical Society* **2011,** *133* (39), 15332-15334.
32. Rau, S.; Schafer, B.; Gleich, D.; Anders, E.; Rudolph, M.; Friedrich, M.; Gorls, H.; Henry, W.; Vos, J. G., "A supramolecular photocatalyst for the production of hydrogen and the selective hydrogenation of tolane." *Angewandte Chemie-International Edition* **2006,** *45* (37), 6215-6218.
33. Macchioni, A., "Ion pairing in transition-metal organometallic chemistry." *Chemical Reviews* **2005,** *105* (6), 2039-2073.
34. Crabtree, R. H., "Deactivation in Homogeneous Transition Metal Catalysis: Causes, Avoidance, and Cure." *Chemical Reviews* **2015,** *115* (1), 127-150.
35. Peuntinger, K.; Pilz, T. D.; Staehle, R.; Schaub, M.; Kaufhold, S.; Petermann, L.; Wunderlin, M.; Gorls, H.; Heinemann, F. W.; Li, J.; Drewello, T.; Vos, J. G.; Guldi, D. M.; Rau, S., "Carbene based photochemical molecular assemblies for solar driven hydrogen generation." *Dalton Transactions* **2014,** *43* (36), 13683-13695.
36. Knoll, J. D.; Higgins, S. H.; White, T. A.; Brewer, K. J., "Subunit Variation to Uncover Properties of Polyazine-Bridged Ru(II), Pt(II) Supramolecules with Low Lying Charge Separated States Providing Insight into the Functioning as H2O Reduction Photocatalysts to Produce H-2." *Inorganic Chemistry* **2013,** *52* (17), 9749-9760.
37. Wang, M.; Na, Y.; Gorlov, M.; Sun, L. C., "Light-driven hydrogen production catalysed by transition metal complexes in homogeneous systems." *Dalton Transactions* **2009,** (33), 6458-6467.
38. Fihri, A.; Artero, V.; Razavet, M.; Baffert, C.; Leibl, W.; Fontecave, M., "Cobaloxime-based photocatalytic devices for hydrogen production." *Angewandte Chemie-International Edition* **2008,** *47* (3), 564-567.

39. Stoll, T.; Gennari, M.; Fortage, J.; Castillo, C. E.; Rebarz, M.; Sliwa, M.; Poizat, O.; Odobel, F.; Deronzier, A.; Collomb, M.-N., "An Efficient Ru^{II}-Rh^{III}-Ru^{II} Polypyridyl Photocatalyst for Visible-Light-Driven Hydrogen Production in Aqueous Solution." *Angewandte Chemie-International Edition* **2014,** *53* (6), 1654-1658.
40. McCormick, T. M.; Han, Z.; Weinberg, D. J.; Brennessel, W. W.; Holland, P. L.; Eisenberg, R., "Impact of Ligand Exchange in Hydrogen Production from Cobaloxime-Containing Photocatalytic Systems." *Inorganic Chemistry* **2011,** *50* (21), 10660-10666.
41. Rangan, K.; Arachchige, S. M.; Brown, J. R.; Brewer, K. J., "Solar energy conversion using photochemical molecular devices: photocatalytic hydrogen production from water using mixed-metal supramolecular complexes." *Energy & Environmental Science* **2009,** *2* (4), 410-419.
42. Ozawa, H.; Yokoyama, Y.; Haga, M.-a.; Sakai, K., "Syntheses, characterization, and photo-hydrogen-evolving properties of tris(2,2 '-bipyridine) ruthenium(II) derivatives tethered to a cis-Pt(II)Cl-2 unit: insights into the structure-activity relationship." *Dalton Transactions* **2007,** (12), 1197-1206.
43. Ozawa, H.; Haga, M. A.; Sakai, K., "A photo-hydrogen-evolving molecular device driving visible-light-induced EDTA-reduction of water into molecular hydrogen." *Journal of the American Chemical Society* **2006,** *128* (15), 4926-4927.
44. Abbasi, A.; Skripkin, M. Y.; Eriksson, L.; Torapava, N., "Ambidentate coordination of dimethyl sulfoxide in rhodium(III) complexes." *Dalton Transactions* **2011,** *40* (5), 1111-1118.
45. Braunstein, C. H.; Baker, A. D.; Strekas, T. C.; Gafney, H. D., "Spectroscopic and electrochemical properties of the dimer tetrakis(2,2'-bipyridine)(μ-2,3-bis(2-pyridyl)pyrazine)diruthenium(II) and its monomeric analog." *Inorganic Chemistry* **1984,** *23* (7), 857-864.
46. Amarante, D.; Cherian, C.; Ernmel, C.; Chen, H. Y.; Dayal, S.; Koshy, M.; Megehee, E. G., "Improved synthetic routes to rhodium bipyridine complexes: Comparison of microwave vs. conventional synthesis." *Inorganica Chimica Acta* **2005,** *358* (7), 2231-2238.
47. Manbeck, G. F.; Brewer, K. J., "Photoinitiated electron collection in polyazine chromophores coupled to water reduction catalysts for solar H2 production." *Coordination Chemistry Reviews* **2013,** *257* (9–10), 1660-1675.
48. Koziar, J. C.; Cowan, D. O., "Photochemical heavy-atom effects." *Accounts of Chemical Research* **1978,** *11* (9), 334-341.
49. Arachchige, S. M.; Shaw, R.; White, T. A.; Shenoy, V.; Tsui, H.-M.; Brewer, K. J., "High turnover in a photocatalytic system for water reduction to produce hydrogen using a Ru,Rh,Ru photoinitiated electron collector." *ChemSusChem* **2011,** *4* (4), 514-518.
50. Harris, D. C., *Quantitative Chemical Analysis*. 7th ed.; New York, 2007.
51. Molnar, S. M.; Jensen, G. E.; Vogler, L. M.; Jones, S. W.; Laverman, L.; Bridgewater, J. S.; Richter, M. M.; Brewer, K. J., "Photochemical properties of mixed-metal supramolecular complexes." *Journal of Photochemistry and Photobiology A: Chemistry* **1994,** *80* (1-3), 315-322.

52. Hills, E. F.; Moszner, M.; Sykes, A. G., "Kinetics and mechanism of the reduction of rhodium(III) complexes $Rh(H_2O)_5X^{2+}$ By Cr^{2+}." *Inorganic Chemistry* **1986,** *25* (3), 339-341.
53. Gennett, T.; Milner, D. F.; Weaver, M. J., "Role of solvent reorganization dynamics in electron-transfer processes. Theory-experiment comparisons for electrochemical and homogeneous electron exchange involving metallocene redox couples." *Journal of Physical Chemistry* **1985,** *89* (13), 2787-2794.
54. Caspar, J. V.; Kober, E. M.; Sullivan, B. P.; Meyer, T. J., "Application Of The Energy-Gap Law To The Decay Of Charge-Transfer Excited-States." *Journal of the American Chemical Society* **1982,** *104* (2), 630-632.
55. Brown, J. R.; Elvington, M.; Mongelli, M. T.; Zigler, D. F.; Brewer, K. J., "Analytical methods development for supramolecular design in solar hydrogen production." *Proc. SPIE-Opt. Photo. Sol. Hydrogen Nanotechnology* **2006,** *6340*, 634007W1-13.

5. Conclusions

New $Ru^{II}Rh^{III}$ multimetallic supramolecular complexes were synthesized for use as photocatalysts for the photochemical reduction of H_2O to H_2 fuel. Bimetallic complex $[(Ph_2phen)_2Ru(dpp)RhBr_2(Ph_2phen)]^{3+}$ was prepared for comparison to reported analogue $[(Ph_2phen)_2Ru(dpp)RhCl_2(Ph_2phen)]^{3+}$, and the impact of halide variation on the electrochemical, light absorbing, and excited state properties was examined. The number of Ru light absorbing subunits in the bimetallic architecture was increased from one to two for the preparation of new trimetallic complex $[\{(bpy)_2Ru(dpp)\}_2Rh(OH)_2]^{5+}$. This halide-free complex containing OH^- ligands was studied in comparison to halide-containing complexes $[\{(bpy)_2Ru(dpp)\}_2RhX_2]^{5+}$ (X = Cl^- or Br^-). Previous studies reported that the identity of the ligands coordinated to Rh in $Ru^{II}Rh^{III}$ supramolecules impacted H_2 photocatalysis; however, no previous studies investigated the excited state properties or labile ligand variation for $Ru^{II}Rh^{III}$ bimetallic complexes. Furthermore, no $Ru^{II}Rh^{III}$ multimetallic complex has been synthesized containing OH^- ligands at the reactive metal center. Variation of the ligands coordinated to the catalytically active Rh center was carried out to gain insight about the impact of the nonchromophoric, monodentate ligands on photocatalytic H_2 evolution employing single-component photocatalysts.

A building block approach was used to prepare new complexes $[(Ph_2phen)_2Ru(dpp)RhBr_2(Ph_2phen)]^{3+}$ and $[\{(bpy)_2Ru(dpp)\}_2Rh(OH)_2]^{5+}$. Complex $[(Ph_2phen)_2Ru(dpp)RhBr_2(Ph_2phen)](PF_6)_3$ was prepared from a 1:1 molar ratio of $[(Ph_2phen)_2Ru(dpp)](PF_6)_2$ and new complex $[(Ph_2phen)RhBr_3(DMF)]$, coupling the Ru

LA subunit to the *cis*-$RhBr_2$ reactive metal center. The new Rh^{III} monometallic complex containing one bidentate polypyridyl Ph_2phen ligand was challenging to synthesize, and low heat over a shortened reaction time was required to prevent coordination of two Ph_2phen bidentate ligands. Complex $[\{(bpy)_2Ru(dpp)\}_2Rh(OH)_2](PF_6)_5$ was prepared from a 2:1 molar ratio of $[(bpy)_2Ru(dpp)](PF_6)_2$ and $[Rh(H_2O)_6](CF_3SO_3)_3$, coupling two Ru LAs to a halide-free *cis*-$Rh(OH)_2$ reactive metal center. Both bimetallic and trimetallic complexes were prepared using a step-wise synthetic approach that allowed for judicious choice of molecular components needed to explore the impacts of ligand variation.

Cyclic voltammetry provided a forum to study the relative orbital energetics of $Ru^{II}Rh^{III}$ supramolecular complexes. Complexes $[(Ph_2phen)_2Ru(dpp)RhX_2(Ph_2phen)]^{3+}$ (X = Cl^- or Br^-) possessed rich redox behavior, with unprecedented cathodic electrochemistry tuned by the halides coordinated to the Rh center. Near isoenergetic Rh(dσ*) and dpp(π*) molecular orbitals in the bimetallic motif provided for multiple electrochemical reduction pathways influenced by the scan rate of the experiment and the identity of the halide. Anodic scans revealed a reversible $Ru^{II/III}$ oxidation regardless of halide identity. Cathodic scans revealed two largely irreversible Rh-based reductions, with subsequent halide loss, that provided evidence for the collection of two redox equivalents at the reactive metal center. The first reductive couple corresponded to either $Rh^{III/II/I}$ (number of electrons transferred = n = 2) or $Rh^{III/II}$ (n = 1), with the former dominating when X = Br^- and at slower scan rate (< 0.1 V/s) and the latter dominating when X = Cl^- and at faster scan rates (> 0.1 V/s). The second reductive couple

corresponded to $Rh^{II/I}$ (n = 1) and existed for the fraction of complex that did not undergo a two-electron reduction in the first couple. Both pathways occurred simultaneously on the CV timescale, accounting for the observed non-integer current response. Despite complicated electrochemical pathways, CV results provided clear evidence for a Ru(dπ)-based HOMO and a Rh(dσ*)-based LUMO, which are requirements for photoinitiated electron collection and active H_2 photocatalysis. Complex $[\{(bpy)_2Ru(dpp)\}_2Rh(OH)_2]^{5+}$ also displayed rich cathodic and anodic electrochemistry. An overlapping, two-electron $Ru^{II/III}$ oxidation corresponded to oxidation of the predominantly electronically uncoupled Ru LA subunits. Cathodically, the complex displayed overlapping, two-electron $Rh^{III/II/I}$ reductions followed by two $dpp^{0/-}$ reductions, providing evidence for lowest lying Rh-based molecular orbitals. As with the electrochemistry of the bimetallic complexes, the electrochemistry of the trimetallic complex containing OH^- ligands provided evidence for a Ru(dπ)-based HOMO and a Rh(dσ*)-based LUMO that are crucial for the preparation of H_2O reduction photocatalysts.

The studied $Ru^{II}Rh^{III}$ multimetallic complexes were efficient light absorbers in the UV and visible regions, an important characteristic for visible-light induced H_2 photocatalysis. Both $[(Ph_2phen)_2Ru(dpp)RhBr_2(Ph_2phen)]^{3+}$ and $[\{(bpy)_2Ru(dpp)\}_2Rh(OH)_2]^{5+}$ possessed IL (π→π*) transitions in the visible region, corresponding to TL and dpp ligand-based transitions. The visible region was dominated by ^{1}MLCT transitions, with both multimetallic complexes possessing Ru(dπ)→TL(π*) transitions and lowest energy Ru(dπ)→dpp(π*) transitions (λ^{abs} = 512 – 514 nm; ε ~ 10^4 M^{-1} cm^{-1}). For the both multimetallic architectures, variation of the ligands bound to Rh

did not greatly impact the energies (λ) or intensities (ε) of the electronic transitions associated with light absorption. Thus, the monodentate ligands bound to Rh were nonchromophoric, and their identity did not perturb the ground state optical properties of the supramolecular photocatalysts.

An emissive ^{3}MLCT excited state in both the bimetallic and trimetallic Ru,Rh architectures provided a probe to study the excited state dynamics. Upon excitation into the lowest-energy Ru(dπ)→dpp(π*) ^{1}MLCT excited state, intersystem crossing occurred to populate the ^{3}MLCT excited state from where radiative decay occurred. However, relatively low quantum yields and short excited state lifetimes for $[(Ph_2phen)_2Ru(dpp)RhBr_2(Ph_2phen)]^{3+}$ ($\Phi_{em} = 1.4\times10^{-4}$; $\tau = 46$ ns) and $[\{(bpy)_2Ru(dpp)\}_2Rh(OH)_2]^{5+}$ ($\Phi_{em} = 3.2\times10^{-4}$; $\tau = 41$ ns) provided evidence for population of a low-lying ^{3}MMCT excited state from where active H_2 photocatalysis was postulated to occur. Complexes $[(Ph_2phen)_2Ru(dpp)RhX_2(Ph_2phen)]^{3+}$ (X = Cl^- or Br^-) possessed similar excited state properties, providing an ideal forum to examine the impact of halide identity on photocatalytic H_2 evolution where light absorbing and excited state properties are the same. Conversely, trimetallic complexes $[\{(bpy)_2Ru(dpp)\}_2RhX_2]^{5+}$ (X = OH^-, Cl^-, or Br^-) possessed different excited state properties upon variation of the ligands coordinated to Rh that suggested the rate of population of the ^{3}MLCT excited state, not only the ^{3}MMCT excited state as previously proposed, influenced photochemical H_2 production. Undoubtedly, the excited state dynamics are important to understand for the design of supramolecular architectures applicable to H_2 evolution from H_2O.

With evidence for the appropriate orbital energetics needed to achieve photoinitiated electron collection at the Rh reactive metal center, new complexes $[(Ph_2phen)_2Ru(dpp)RhBr_2(Ph_2phen)]^{3+}$ and $[\{(bpy)_2Ru(dpp)\}_2Rh(OH)_2]^{5+}$ were active H_2 production photocatalysts and displayed increased H_2 evolution in DMF solvent relative to their reported analogues. *N,N*-Dimethylaniline (DMA) served as an effective electron donor to quench the photogenerated Ru^{III} chromophoric subunit and allow photoinitiated electron collection at the Rh reactive metal center. Complex $[(Ph_2phen)_2Ru(dpp)RhBr_2(Ph_2phen)]^{3+}$ was more active (62±5 TON) than $[(Ph_2phen)_2Ru(dpp)RhCl_2(Ph_2phen)]^{3+}$ (40±2 TON), maintaining the trend observed for trimetallic complexes that Br^- analogues are more active than their Cl^- counterparts. However, with identical light absorbing and excited state properties, a new phenomenon was required to explain the discrepancies in photocatalytic efficiencies. With halide loss occurring to form the proposed active catalyst $[(Ph_2phen)_2Ru(dpp)Rh^{I}(Ph_2phen)]^{3+}$, halide-dependent H_2 photocatalysis is a surprising result. However, upon halide loss, the anionic ligands were thought to remain in close proximity to the positively charged multimetallic photocatalyst via ion pairing, which inhibited further interaction with the H_2O substrate required for H_2 photocatalysis. Br^-, a weaker σ-donor than Cl^-, was predicted to form comparatively weaker ion pairs with the metal complex, accounting for larger TONs relative to the Cl^- analogue. H_2 production experiments with added halide confirmed that halides were detrimental to photocatalysis and that Cl^- poisoned the photocatalytic system to a greater extent than Br^-. Trimetallic complex $[\{(bpy)_2Ru(dpp)\}_2Rh(OH)_2]^{5+}$ (83±6 TON) was more active as a photocatalyst for H_2

production in DMF solvent than $[\{(bpy)_2Ru(dpp)\}_2RhCl_2]^{5+}$ (30±4 TON) or $[\{(bpy)_2Ru(dpp)\}_2RhBr_2]^{5+}$ (45±4 TON). Upon consideration of the pKa of the respective monodentate ligands, the OH^- complex was a superior photocatalyst by comparison to the halide analogues because the dissociated OH^- ligands were likely protonated in the bulk solution, unlike the halides that remained negatively charged upon dissociation and were capable of detrimental ion pairing. Interestingly, in aqueous solvent, the three trimetallic photocatalysts produced nearly identical amounts of H_2. Variation of the photocatalytic solvent and the ligands coordinated to Rh provided further evidence that ion pairing played a role in the deactivation of the supramolecular photocatalysts. In low dielectric solvents (DMF or CH_3CN), the identity of the ligands coordinated to Rh impacted observed photocatalytic H_2 yields through ion pairing between the dissociated anionic ligands and the positively charged multimetallic complex; however, in a high dielectric solvent (H_2O), ligand identity did not impact the observed H_2 evolution because the dissociated halides and hydroxides were indistinguishable in the aqueous bulk solution where ion pairing was minimized.

The experiments described in this dissertation provided evidence that minor structural variation at the catalytically active metal center in $Ru^{II}Rh^{III}$ supramolecular complexes impacted solar H_2 production schemes. By investigation of the electrochemical, light absorbing, and excited state properties, insight was gained to better understand the molecular features that dictate photochemical H_2 production abilities. In both the bimetallic and trimetallic architectures, halides coordinated to the Rh center limited photocatalytic H_2 production in organic solvents by ion pairing with the

photogenerated $Ru^{II}Rh^{I}$ supramolecule and inhibiting further interaction of the H_2O substrate with the photocatalyst. The negative impact of ion pairing on H_2 photocatalysis was further confirmed through the use of a high dielectric aqueous solvent where ion pairing was minimized; thus, no discrepancy in H_2 evolution was observed upon ligand variation at Rh. The knowledge gained about component and solvent selection for photocatalytic H_2 production employing supramolecular photocatalysts provided important insight to optimize architectures for solar H_2 production schemes.